CoA Memo Aero. No. 33

June, 1964

THE COLLEGE OF AERONAUTICS

DEPARTMENT OF AERODYNAMICS

Non-equilibrium flow in plane expansion waves

- by -

J.W. Cleaver, B.A., D.C.Ae.

SUMMARY

The non-equilibrium supersonic flow of a relaxing or reacting gas through a plane expansion has been studied from a numerical, analytical and experimental point of view.

The flow of an ideal dissociating gas in a two dimensional expansion has been solved numerically by writing the governing equations of motion in their characteristic form.

In conflict with linearised theory along the wall, the numerical solutions do not asymptote to the infinite rate equilibrium values. To estimate how far the asymptotic state deviates from the infinite rate equilibrium values, a formal second order solution has been developed with the aid of transform techniques. An example has been discussed for a simplified relaxing gas model, and estimates of the asymptotic state have been obtained. An exact solution over the whole field was not possible but by treating the parameter $\left(\frac{M_e^2-1}{M_f^2-1}-1\right)$ as small, an approximate answer has been found.

To understand in more detail the coupling effects of two relaxation processes, linearised theory has been extended to cope with the flow of a gas with more than one relaxing mode. An example has been discussed for Carbon Dioxide and the effect of possible coupling between the bending and stretching modes of the molecule in a plane expansion has been investigated.

The Mach-Zehnder interferometer and Schlieren method have been used in conjunction with a 2" - diameter shock tube to study the density and density gradients within, and following a sharp two-dimensional expansion for shock heated Carbon Dioxide. Measurement of the density gradient at the leading edge of the expansion by quantitative Schlieren methods have allowed relaxation times to be obtained. This method has the advantage that relaxation times can be obtained for specific values of the density and temperature for only small departures from an equilibrium state.

INDEX OF CONTENTS

INDEX OF FIGURES

Figure No.	Title
3.4 (2)	Interferograms of the flow of Carbon Dioxide through a plane 20° expansion
3.4 (3)	Measured density ratios through a 20° expansion

LIST OF SYMBOLS

a_f	frozen speed of sound
a_e	equilibrium speed of sound
a_1	speed of sound with mode 1 active
a_2	speed of sound with mode 2 active
a	$z\{B^2+z/1+z\}^{1/2}$
c_α	concentration by mass of α species
e	internal energy
h	enthalpy
k_F	specific reaction rate coefficient for dissociation
k_r	specific reaction rate coefficient for recombination
p	pressure
q	velocity
r	radial distance from the corner
(s,n)	natural co-ordinates
u	component of velocity in x direction
v	component of velocity in y direction
(x,y)	rectangular cartesian co-ordinates
z	transform variable
$\alpha,\beta,\gamma,\delta$	roots of equation 2·4 (12)
β_f	defined on Page 9
γ_f	frozen ratio of specific heats
ε	defined on Page 9
ζ	vorticity
(ξ,η)	semi-characteristic co-ordinates
θ	flow direction angle
θ_v	characteristic temperature for vibration
μ_α	chemical potential of α species

LIST OF SYMBOLS
(Continued.)

μ_f	$\mu_f = \sin^{-1} 1/M_f$ = characteristic direction
$\nu_\mp$	increments along characteristic directions
ρ	density
σ_α	defined on Page 9
$\tau, \tau', \tau'', \tau'''$	relaxation times
φ	defined in equation 2.5 (7)
ψ	" " " 2.5 (8)
Ω	" " " 2.5(10)
Λ	" " " 2.5(11)
ϑ	" " " 2.5(13)
B_f	frozen Ackeret Factor $\sqrt{M_f^2 - 1}$
B_e	equilibrium Ackeret Factor $\sqrt{M_e^2 - 1}$
B_1	Ackeret factor based on a_1
B_2	Ackeret factor based on a_2
B	$\{(M_e^2 - 1)/(M_f^2 - 1)\}^{1/2}$
$C_{\alpha\beta}$	specific heat of β^{th} mode of α species
C_{p_f}	frozen specific heat at constant pressure
C_{v_f}	frozen specific heat at constant volume
$(\omega_1, \omega_2, \cdot)$	specific heat of internal modes
E	total internal energy
F	defined in equation 2.5(14)
G	" " " 2.5(29)
H	" " " 2.5(30)
I	" " " 2.5(31)
J	" " " 2.5(36)
K	" " " 2.5(37)

LIST OF SYMBOLS
(Continued.)

K_α	net mass rate of production of α species
L	a characteristic length
M_f	frozen Mach number
M_e	equilibrium Mach number
$\bar{P}$	transform of p
$\bar{Q}$	transform of q
R	gas constant
S	entropy
T_D	dissociation temperature
T	temperature
$(T_v, T_1, T_2 \ldots)$	vibrational temperatures
$T(x)$	definition of boundary shape

Subscripts

e	equilibrium conditions
f	frozen conditions
$(1, 2, \text{etc})$	label associated with an internal mode
∞	initial conditions

$-$	signifies a transformed quantity

ACKNOWLEDGMENTS

To Dr. K.N.C. Bray, whose valued suggestions and criticisms have been a constant source of encouragement, and under whose supervision this work has been carried out.

To Mr. J.R. Busing for considerable help and advice during the course of the experiments.

To Dr. J.F. Clarke for many stimulating and fruitful discussions.

To Professor G.M. Lilley for his advice and many helpful suggestions.

Finally, thanks are due to Mr. S.H. Lilley and Mr. S. Clarke and the rest of the Aerodynamics Staff at The College of Aeronautics for their ever willing help in practical matters.

1.0 Introduction

Over the past decade the fluid dynamicist has become increasingly concerned with the flow of high temperature gases and this has resulted in the union of existing work in physics and chemistry to fluid dynamics. At sufficiently high temperatures the inert degrees of freedom of the molecules can absorb sufficient energy for considerable departures from ideal (structureless) gas theory to occur. This has meant that the overall equations describing the flow must be modified to allow for the re-distribution of energy among the internal degrees of freedom. Provided the reaction processes are known, and knowledge of the energy distribution within the molecules is available, the equations can be readily formulated. If, also, this energy re-distribution occurs infinitely quickly, the equations of motion are outwardly unchanged and only the equations of state are affected.

In practice, once a gas is disturbed from some initial equilibrium state, the reactions and relaxations of the molecules take a finite time before complete equilibrium among all the degrees of freedom is re-established. For example the translational degree of freedom is in equilibrium after about one or two collisions, the rotational modes usually require about 10 collisions whereas the vibrational modes of a molecule may take up to 10,000 collisions. Thus, while the translational and rotational modes may be considered to be in equilibrium for most situations encountered in fluid dynamics the vibrational modes and dissociation and recombination modes will take some finite time to readjust themselves. This time is generally inversely proportional to some power of the density and a function of temperature. Thus, in most gas dynamic problems it is possible to find conditions where the relaxation times are sufficiently long for portions of the flow to be carried large (measurable) distances before equilibrium is re-established. (For example such a situation can arise in the hypersonic flight regime of a re-entry vehicle at high altitude). Thus, if the relaxation or reaction times are long compared with the flow times pertinent to the problem, then local

departures from statistical equilibrium may occur. This can result in significant differences of the pressure, temperature and density from the values computed as if the fluid was at all times in equilibrium. These effects can be particularly important when large amounts of energy are tied up in the inert modes. For the class of problems in which viscosity, heat conduction and diffusion may be considered as negligible, and which are dealt with here, Kirkwood and Wood -(1957) conveniently formulated the basic equations for any number of reactions and relaxations, all of which may be locally out of equilibrium.

These 'real' gas effects introduce into the problems non-linearities, over and above those which already exist in ideal gases to such an extent that even the one dimensional steady flow in a nozzle which for an ideal gas can be solved exactly, becomes analytically impossible and numerical techniques must be used (cf Bray 1959). For complex reacting and relaxing systems, (Vincenti 1961), even the numerical solutions can become prohibitively long and, thus, when dealing with more complex flow situations the trend in recent years has been to develop more approximate but analytical techniques for preliminary exploration of the problem. These approaches have shed light on some of the underlying physics of the problem, but generally, if exact answers have been required, the field of non-equilibrium gas dynamics has been in the province of the numerical analysist.

Because of the difficulties encountered with the one dimensional problem of a real gas, in order to look at the two-dimension flow from a numerical, analytical and experimental point of view, the problem of the supersonic flow past a sharp expansion has been considered. Like the one dimensional problem this has an exact solution (Prandtl-Meyer solution) for the ideal gas and thus the extra non-linearities associated with giving the gas an internal structure can readily be appreciated. Fortunately this particular problem has already received some attention and thus provides a sound basis for the present study.

The problem was tackled simultaneously by Moore and Gibson (1960) and Clarke (1960) who both applied linearised theory to non-equilibrium flow and consequently obtained analytical solutions.

These authors following the basic work of Chu (1957) show, after linearising the equations, that the partial differential equation characterising the flow of a gas with one mode (either vibrational or dissociative) not in equilibrium is now of third order and is given by

$$\tau_\infty u_\infty \frac{\partial}{\partial x}\left\{(M_f^2-1)\frac{\partial^2 p'}{\partial x^2} - \frac{\partial^2 p'}{\partial y^2}\right\} + \left\{(M_e^2-1)\frac{\partial^2 p'}{\partial x^2} - \frac{\partial^2 p'}{\partial y^2}\right\} = 0$$

Where p' is the perturbation pressure, M_f are the Mach numbers based on the frozen and equilibrium sound speeds, and τ_∞ a relaxation time. Moore and Gibson (1960) approximate this equation by the telegraph equation and find solutions over the whole field whereas Clarke (1960) solves it exactly and compares the solution at the wall for a sharp expansion with numerical solutions obtained by Cleaver (1959) for an Ideal Dissociating gas. A more exhaustive numerical solution was then obtained by Appleton (1960) and more recently by Glass and Takano (1963). Another analytical approach to the problem was proposed by Napolitano (1960) who suggested a series solution in terms of the radial distance from the corner. This is only valid close to the corner and a comparison with the numerical solution is made in section (2.3:3).

One of the shortcomings of numerical solutions arises from the numerical approach used and this appears to be quite important in this problem. The work of Appleton (1960), and the present computations indicate that the pressure recovery downstream of the corner does not increase monotonically to the new equilibrium state far downstream of the corner but overshoots this value and approaches it asymptotically from above. Although plausible explanations for the phenomenon exist, there is always the possibility that such an occurance could be attributed solely to the numerics. More recent work by Glass and Takano (1963) suggest that downstream of the corner energy can be supplied to the gas at a sufficient rate for a weak upstream facing shock to be produced. This was not found by Appleton (1960) or in the present computation which suggests that once again great care must be taken in drawing too many physical

conclusions from the computations. To add to the difficulty, because entropy and vorticity is produced when a gas is out of equilibrium, it is impossible to predict 'a priori' the new equilibrium state that will be reached far downstream of the corner. Although as shown by Appleton (1963) momentum considerations indicate that the pressure at least, must return to the infinite rate equilibrium value, the rest of the variables are undetermined. Thus, the pressure is the only check on the entire solution.

Because of these inherent difficulties in the numerical approach to the problem it is desirable to have an analytical solution, even if approximate, to elucidate some of the above queries. A well established technique is to seek a series solution in some small parameter characteristic to the problem (in this case the expansion angle). Linearised or acoustic theory arises by neglecting terms of order two or greater in the small parameter. As mentioned above to this approximation a solution has already been obtained by Moore and Gibson (1960) and Clarke (1960).

Vorticity and Entropy production is an essential characteristic of non-equilibrium systems but in the process of linearisation it is considered to be zero. Nevertheless, despite this apparently severe approximation, the results of linear theory reveal most of the salient features pertinent to many non-equilibrium flow problems. In particular for the plane flow past a corner the linear theory describes surprisingly well the variation of the pressure, density, etc. in the relaxation zone downstream of the corner (cf section 2.3). However, to first order the theory is inadequate in that it does not predict, for example, how far the new equilibrium state, which is achieved far downstream of the corner, deviates from the conditions calculated as if the flow was at all times in equilibrium. Because, to the first order approximation the flow is isentropic, the linear theory automatically implies that the final asymptotic state is the one obtained using the infinite rate equilibrium solution, which from physical arguments must be incorrect. Thus, to make the approach more valid, a higher

approximation is needed which allows for finite entropy and vorticity production. Therefore it is logical to include some of the neglected terms in the original series solutions to see whether a 'better' answer can be obtained. (From the outset there is of course no guarantee that the proposed series solution is convergent and it is possible for higher order solutions to be worse). In consequence, a formal second order solution is attempted in section 2.5, and although an exact solution was not possible some of the queries raised about the numerical solutions can in some measure be answered. In particular it is possible to show that far downstream of the corner the pressure, to the second order approximation tends to the infinite rate equilibrium value. This agrees with momentum arguments and gives some confidence in the predictions of the asymptotic values at the wall of the other state variables.

Apart from some very preliminary experiments by Feldman (1957) no experimental evidence has been published relating to the plane supersonic expansion of a gas which is out of equilibrium. To rectify this, a series of experiments has been undertaken which uses the high temperature steady supersonic flow of gas following the primary shock in a shock tube as the test gas. By inserting a wedge shaped aerofoil section into the unexpanded part of the shock tube, a plane expansion has been generated. The flow field was investigated optically to measure the density and density gradients by means of the Mach-Zhender interferometer and by Schlieren techniques.

Since the theoretical studies suggest that experimental observation of a plane expansion could provide a further technique for measuring the rate at which a non-equilibrium process occurs, a feasibility study was made with Carbon Dioxide as the test gas. This was chosen because of the relative ease with which its vibrational modes are excited and because its relaxation time is small, (criteria determined by the performance of the shock tube) and most important, because the properties of this gas have been well studied by other techniques and thus a comparison of the results can readily be made.

The fact that Carbon Dioxide has more than one inert mode does to some degree complicate the issue but at the same time it has provided the incentive to look at the linearised problem of a gas with more than one inert mode (cf Section 2.4).

For expansive flows, temperature is the ideal measurement to make and density the worst if non-equilibrium effects are to be isolated, and from this point of view the density measurements obtained, especially within and downstream of the expansion have been inconclusive. However, along the leading edge of the expansion, it is possible to show, Appleton (1960), that the gradient of the flow variables decay in an exponential manner away from the corner when non-equilibrium effects are present. This decay has been detected by Schlieren and Interferometric techniques and has allowed relaxation times to be estimated. Although the technique cannot claim great accuracies (probably no better than ± 50%) it has the advantage that a relaxation time can be obtained for specific values of the density and temperature upstream of the corner for small departures from an equilibrium state. The results agree on the whole with those obtained by studying the relaxation zone after a normal shock as reported by Johannesen et al (1963). These preliminary results suggest the technique bodes well for the possible determination of recombination rate coefficients in oxygen and perhaps nitrogen.

2.0 Theoretical

2.1 The Basic Flow Equations

The derivation of the conservation equations for quite complex reacting and relaxing gas flows is well formulated even for systems in which local statistical equilibrium among the various degrees of freedom is not sustained. For completeness these equations are briefly stated and follow identically the formulation first given by Kirkwood and Wood (1957).

For the class of problem which is dealt with here the fluid is considered as non heat conducting, non-diffusive and inviscid. When an arbitrary number of chemical reactions coupled with relaxations of the internal modes of the molecular species can occur, the overall equations of continuity and the Eulerian equations of motion remain unaffected and take their familiar form

$$\frac{D\rho}{Dt} + \rho \operatorname{div} \underset{\sim}{q} = 0 \qquad 2.1(1)$$

and

$$\frac{D\underset{\sim}{q}}{Dt} + \frac{1}{\rho} \operatorname{grad} p = 0 \qquad 2.1(2)$$

the equation of energy is also outwardly unchanged and is given by

$$\rho \frac{Dh}{Dt} + \frac{Dp}{Dt} = 0 \qquad 2.1(3)$$

where $\frac{D}{Dt}$ is the convective operator $\frac{\partial}{\partial t} + \operatorname{grad}$, p is the pressure, $\underset{\sim}{q}$ the velocity vector, ρ the density and h is the specific enthalpy which is dependent on the structure of the gas.

For a chemically reacting gas there will exist a rate equation for each chemical species

$$\rho \frac{Dc_\alpha}{Dt} = K_\alpha \quad (\alpha = 1, \ldots, n) \qquad 2.1(4)$$

where K_α is the net mass rate of production of the α species per unit volume and c_α is the concentration by mass of the α species. If R

reactions are taking place then $K_\alpha = \sum_{j=1}^{R} K_{\alpha j}$ where $K_{\alpha j}$ is the mass rate of production of the j^{th} species arising from the j^{th} reaction.

At the same time as the chemical reactions are occuring adjustments of the internal degrees of freedom will also take place. The rate processes governing the approach to a common equilibrium temperature between the various degrees of freedom are given in the form

$$\frac{DT_{\alpha\beta}}{Dt} = Q_{\alpha\beta} \quad (\beta = 1, \ldots, m) \qquad 2.1(5)$$

where $Q_{\alpha\beta}$ are functions of the local thermodynamic state and the subscript β indicates the β^{th} mode of the molecular species α. Generally little is known about $Q_{\alpha\beta}$ but in the past it has been assumed that linear rate laws hold and that the rate at which equilibrium is re-established is proportional to the deviation of the vibrational temperature $T_{\alpha\beta}$ from the translational temperature T and hence

$$Q_{\alpha\beta} = \frac{T - T_{\alpha\beta}}{\tau_{\alpha\beta}}$$

$\tau_{\alpha\beta}$ has the dimensions of time and is defined as the relaxation time for the β^{th} mode of the α species, and is generally a function of the density and temperature. For polyatomic molecules the above rate equation may be inadequate to describe how the internal mode adjusts itself and other forms of $Q_{\alpha\beta}$ must be considered, see for example section 2.4.

To complete the system of equations the thermal and caloric equations of state must be specified, i.e.

$$\rho = \rho(T, p, c_\alpha) \qquad 2.1(6)$$

and

$$h = h(T, p, c_\alpha, T_{\alpha\beta}) \qquad 2.1(7)$$

These will depend on the thermal and chemical kinetics of the gas and have been tabulated for many gases.

From the practical point of view the set of independent state parameters are usually taken as T, p and c_α but in some

circumstances it is convenient to choose p, c_α, and S_t the translational entropy to describe the system. For example if the density is taken as $\rho = \rho(p, S_t, c_\alpha)$ then

$$\frac{D\rho}{Dt} = \left(\frac{\partial\rho}{\partial p}\right)_{S_t,c_\alpha}\frac{Dp}{Dt} + \left(\frac{\partial\rho}{\partial S_t}\right)_{p,c_\alpha}\frac{DS_t}{Dt} + \sum_\alpha\left(\frac{\partial\rho}{\partial c_\alpha}\right)_{p,S_t,c_\beta}\frac{Dc_\alpha}{Dt} \qquad 2.1(8)$$

From the original work of Kirkwood and Wood (1957) or the more recent publication of Clarke and McChesney (1964), where the associated analysis is concisely recorded, the rate of change of translational entropy along a streamline can be obtained, and after some lengthy algebra it can eventually be shown that equation 2.1(8) can be written

$$\left(\frac{\partial\rho}{\partial p}\right)_{S_t,c_\alpha}\frac{Dp}{Dt} - \frac{D\rho}{Dt} + \rho\sum_\alpha\sum_\beta \varepsilon_\alpha C_{\alpha\beta}\frac{DT_{\alpha\beta}}{Dt} + \rho\sum_\alpha \sigma_\alpha\frac{Dc_\alpha}{Dt}$$

The density derivative can then be eliminated by means of equation 2.1(1) to give

$$\frac{Dp}{Dt} + \rho a_f^2 \operatorname{div}\underline{q} + \rho a_f^2\sum_\alpha\sum_\beta \varepsilon_\alpha C_{\alpha\beta}\frac{DT_{\alpha\beta}}{Dt} + \rho a_f^2\sum_\alpha \sigma_\alpha\frac{Dc_\alpha}{Dt} = 0 \qquad 2.1(9)$$

where

$$\varepsilon_\alpha = \frac{\rho\beta_f c_\alpha}{C_{p_f}} \qquad C_{p_f} = \left\{\frac{\partial h}{\partial T}\right\}_{p,c_\alpha,T_{\alpha\beta}}$$

$$\beta_f = \left\{\frac{\partial(1/\rho)}{\partial T}\right\}_{p,c_\alpha} \qquad a_f^2 = \left\{\frac{\partial p}{\partial\rho}\right\}_{S_t,c_\alpha} = \left\{\frac{\partial p}{\partial\rho}\right\}_{s,c_\alpha,T_{\alpha\beta}}$$

$C_{\alpha\beta}$ = specific heat of mode of species

and

$$\sigma_\alpha = \frac{\rho\beta_f}{C_{p_f}}\left[\left\{\frac{\partial h}{\partial c_\alpha}\right\}_{p,T,T_{\alpha\beta},c_\beta} - \frac{C_{p_f}}{\beta_f}\left\{\frac{\partial(1/\rho)}{\partial c_\alpha}\right\}_{p,T,c_\beta}\right]$$

In addition one may note (cf Clarke, McChesney) that the total entropy production along streamlines is given by

$$\rho T\frac{Ds}{Dt} = -\sum_\alpha \mu_\alpha K_\alpha - \rho\sum_\alpha\sum_\beta \frac{T_{\alpha\beta}-T}{T_{\alpha\beta}} c_\alpha C_{\alpha\beta}\frac{DT_{\alpha\beta}}{Dt} \qquad 2.1(10)$$

where μ_α is effectively the chemical potential of the α species.

So far no particular significance has been attached to a_f and all that can be deduced from equation 2.1(9) is that it has the dimensions of a velocity. Chu (1957) was able to show that a_f is the speed at which wave fronts of infinitesimal strength propagate and since the analysis shows that a_f is evaluated by assuming all the inert modes to be inactive, it has in consequence been called the frozen speed of sound. However when the reactions and relaxations occur infinitely quickly the vibrational temperatures $T_{\alpha\beta}$ and the concentrations c_α are able to keep in equilibrium with the translational degree of freedom and in consequence $\frac{DT_{\alpha\beta}}{Dt} = \frac{Dc_\alpha}{Dt} = 0$, and then equation 2.1(9) is replaced by

$$\frac{Dp}{Dt} + \rho a_e^2 \operatorname{div} \underline{q} = 0.$$

a_e^2 is now defined as $\left(\frac{\partial p}{\partial \rho}\right)_{s, c_{\alpha e}, T_{\alpha\beta e}}$, the subscript e indicating that the inert modes are in equilibrium. For this condition the wave fronts are found to propagate at the speed a_e which is called the equilibrium sound speed. In the development of the subject there was some confusion about the role of a_e when the rate processes are fast but not infinitely fast. Chu (1957) clarified the situation and was able to demonstrate the a_e in near equilibrium flow is the phase velocity and a_f is the wave front velocity. Thus if a finite disturbance is propagated into a relaxing fluid, the head of the disturbance always propagates at a_f but the magnitude of the wave head decays and the bulk of the disturbance is found to follow behind the wave front at a speed a_e .

2.2 Method of Characteristics

For plane flow equations (2.1(1) - 2.1(7)) constitute $(5+mn)$ quasi-linear partial differential and algebraic equations in the $(5+nm)$ unknown dependent variables and the independent variables x, y. Solutions of these equations, except for particular cases, can only be obtained by numerical techniques and from this aspect it is practical to develop the governing equations into their characteristic form.

As the basic equations stand they contain derivatives with repect to both x and y. From the numerical point of view it would be preferable if each equation were total rather than partial in that it would contain derivatives with respect to only one variable. If a combination of the basic equations can be found such that the resulting equations contain derivatives which are in one direction only, then this direction is called a characteristic direction and the curve which they describe is the characteristic curve. Across these curves the dependent variables are continuous but the normal derivatives need not be so, in fact a property of characteristics is that they are loci of possible discontinuities in the partial derivatives of the first or higher order.

To find these derivatives (ref. Courant and Friedrich) a system of multipliers λ_j (say) dependent on (x , y) is specified such that in a linear combination of the original system of equations (formally of the form $a_{ij}\,\partial u_i/\partial x + b_{ij}\,\partial u_i/\partial y + c_j = 0$) all the dependent variables appear differentiated in the same direction given by $dy/dx = \alpha$ (say). If the curve specified by $dy/dx = \alpha$ is given by $x(\xi), y(\xi)$ where ξ is a parameter associated with the characteristic curve, the condition that all the variables be differentiated in the same direction is given by $\frac{dy}{d\xi} : \frac{dx}{d\xi} = (\lambda_j b_{ij}) : (\lambda_j a_{ij})$ If the $(5+nm)$ governing equations are compatible, i.e. if a characteristic direction exists, then the λ_j may be eliminated to yield a characteristic determinental rotation which defines the direction of the tangents to the characteristic curves at the point (x , y). In this case the directions are given by

$$\frac{dy}{dx} = \tan(\theta \pm \mu) \qquad 2.2(1)$$

where θ is the flow angle to x axis and $\mu = \sin^{-1} 1/M_f$ where is the Mach number based on the frozen speed of sound. Provided the flow is supersonic the characteristics are real.

The equations connecting the dependent variables which hold along the characteristic curves are readily found to be

$$\frac{\sqrt{M_f^2-1}}{\rho q^2}\frac{\partial p}{\partial \nu_\mp} \pm \frac{\partial \theta}{\partial \nu_\mp} + \frac{1}{M_f}\left\{\sum_\alpha \frac{\sigma_\alpha}{q}\frac{Dc_\alpha}{Dt} + \sum_\alpha \sum_\beta \varepsilon_\alpha C_{\alpha\beta}\frac{1}{q}\frac{DT_{\alpha\beta}}{Dt}\right\} = 0 \qquad 2.2(2)$$

which hold along lines given by equation (2.2(1)) $\nu_\mp$ are lengths measured along the characteristic curves. The characteristic relations holding along the streamline characteristics exist naturally and are given by equations (2.1(3), (21.(4) and (2.1(5).

2.2.1 Integration of the Characteristic equations

Now that the equations have been reduced to a system of ordinary differential equations they may be readily written in finite difference form and integrated step-by-step throughout the flow field provided suitable initial data are posed. If the initial data is given on some curve (Fig. 2.2(1) which is not coincident with any of the characteristic curves, the solution can be progressed away from this initial line.

If points (1) and (2) lie on the data curve then provided the points 1 and 2 are sufficiently close together the position of a point 3 may be located by letting the characteristic lines through 1 and 2 be represented by straight lines based on the slope of the frozen mach lines at 1 and 2 and determining the intersection point. This naturally introduces an error (of order of the mesh size) which may be reduced by iteration (to order of the mesh size squared) and overall errors in many cases can be reduced by reducing mesh size. (This is only true provided the truncation error is not an important factor). Having located point 3 the pressure and flow angle may be

deduced from equations (2.2(2) written in finite difference form. Before the other flow variables can be determined the intersection of the streamline through the point 3' with the initial data line must be located. To a first approximation this is accomplished by extrapolating the tangent at point 3' to intersect the data curve. Then by interpolation all the dependent variables may be found at the point of intersection and hence by equations (2.1(4) and (2.1(5) the values of c_* and T_{*_μ} at point 3' may be evaluated. Using the energy equation $h + q^2/2 =$ constant and the thermal and caloric equations of state all the dependent variables are determined at the point 3. By iteration through the whole cycle the results can be improved. This is the computation scheme which is used in section 2.3.

The restrictions associated with prescribing the initial data is well formulated for general quasi-linear systems and for the systems associated with non-equilibrium flow fields Der (1963) and Napolitano (1960) discuss the implications of these restrictions. In particular Der points out in detail the importance of these restrictions when designing supersonic non-equilibrium nozzles. One result of importance to fluid dynamicists is that it is impossible to design a nozzle for prescribed uniform exit conditions.

In passing it may be noted that two relatively simple solutions arise when the flow is considered to be in either a frozen or equilibrium state.

(i) Frozen Flow : In regions where the flow times are fast compared with the chemical rates or relaxation times then the right hand side of the rate equations tend to zero and the non-homogeneous terms in equations (2.2(2) vanish. In this situation the flow will occur isentropically with a constant ratio of specific heats and solutions in many cases may be constructed analytically.

(ii) Equilibrium Flow : For the other extreme when the flow times are slow compared with chemical rates or relaxation times the chemical reactions and internal adjustments of the molecules occur infinitely quickly. In this situation the disturbance fronts propagate with the equilibrium speed of sound and in the limit it is found

that the characteristic directions change discontinuously to

$$\frac{dy}{dx} = \tan(\theta \pm \mu_e) \qquad 2.2(3)$$

where $\mu_e = \sin^{-1}\frac{1}{M_e}$ and μ_e is the Mach number based on the equilibrium speed of sound. For finite relaxation or chemical times, no matter how small, the characteristic directions will be given by equation (2.2(1) and not equation (2.2(3).

Along the curves given by equation (2.2(3) there holds

$$\frac{\sqrt{M_e^2-1}}{\rho_e q_e^2}\, dp_e \pm d\theta = 0$$

$$\rho_e q_e\, dq_e + dp_e = 0$$

$$\rho_e\, dh_e - dp_e = 0$$

where the subscript e indicates that the dependent variables are evaluated for equilibrium conditions. The rate equations used to determine $c_\alpha, \tau_{v\rho}$ are now replaced by the equilibrium relations connecting $c_{\alpha_e}, \tau_{v\rho_e}$ with the translational temperature and pressure. In this case no analytical solutions exist since the composition and vibrational temperatures vary throughout the flow field and numerical techniques must be resorted to. However since the independent variables are now a function of only two state variables (p, T) say, the computation is simpler than the non-equilibrium situation. Provided information concerning the chemical kinetics and thermodynamics of the fluid is available the dependent variables may be computed in a step by step manner similar to that already described.

2.3 Numerical Solution for the two Dimensional Expansion of an Ideal Dissociating Gas.

As an example of the general method discussed in the previous section the method of characteristics is applied to the supersonic flow of a 'Lighthill' type Ideal Dissociating gas around a sharp corner.

We consider only one chemical reaction and the equation describing the reaction may be written formally as

$$A_2 + X \underset{k_r}{\overset{k_f}{\rightleftharpoons}} 2A + X \qquad 2.3(1)$$

where x is any third body, which in collision with a molecule or atom may act as a heat sink or source. For a diatomic gas this third body may be an atom or a molecule. k_f and k_r are the specific reaction rate coefficients for dissociation and recombination, both being dependent on local temperature.

If c is the concentration by mass of the atomic species and c_e, which may be evaluated from the law of mass action $\frac{c_e^2}{1-c_e} = \frac{\rho_0}{\rho} \exp -T_0/T$, is the concentration evaluated as if it were in equilibrium with the local values of the pressure and the temperature, then the rate equation pertinent to the above reaction (cf Clarke 1960) is

$$\frac{Dc}{Dt} = \frac{k_r}{m^2} \rho^2 \left\{ \frac{c_e^2 - c^2}{1 - c_e^2} \right\} \qquad 2.3(2)$$

It may be noted that $m^2/k_r\rho^2$ has the dimensions of time and may be treated as a characteristic chemical time. is the mass of the atomic species.

Notice that for this gas

$$\sigma = \frac{(1+c)(1+T_0/T) - (4+c)}{(1+c)(4+c)} \qquad 2.3(3)$$

where T_0 is the characteristic temperature (59,000°K for O_2) for dissociation, and since no internal modes exist equation 2.2(2)

reduces to

$$\frac{\sqrt{M_f^2-1}}{\rho q^2}\frac{\partial p}{\partial \nu_+^-} \pm \frac{\partial \theta}{\partial \nu_+^-} + \frac{1}{M_f}\left\{\frac{(1+c)(1+\tau\gamma_T)-(4+c)}{(1+c)(4+c)}\right\}\frac{p^2}{q}\left\{\frac{c_e^2-c^2}{1-c_e^2}\right\} = 0 \qquad 2.3(4)$$

which holds along the characteristic directions

$$\frac{dy}{dx} = \tan(\theta \pm \mu_f) \qquad 2.3(5)$$

In (2.3(4) the length has been made non-dimensional with the product of the free stream velocity and the chemical relaxation time $m^2/k_{r_\infty}\rho_\infty^2$. k_r is strictly a function of temperature but for the purpose of the present calculations it has been assumed constant. Along the streamlines

$$\rho\frac{Dh}{Dt} - \frac{Dp}{Dt} = 0 \qquad 2.3(6)$$

and $$\rho q\frac{Dq}{Dt} + \frac{Dp}{Dt} = 0 \qquad \text{holds.} \qquad 2.3(7)$$

The system of equations is completed by the thermal equation of state

$$p = \rho(1+c)RT \qquad 2.3(8)$$

and the caloric equation of state

$$h = (4+c)RT + RT_0 c \qquad 2.3(9)$$

At the corner the flow is completely frozen and the solution is identical to that of Prandtl-Meyer flow for an isentropic gas with $\gamma_f = \frac{4+c}{3}$.

At large distances from the corner the flow time is long compared with the chemical reaction time, and the flow will occur as it were in equilibrium and a solution is obtained in a step-by-

step manner as indicated in the last section. The full non-equilibrium equations have been solved by the method of characteristics discussed in the last section.

2.3:1 Discussion of the Characteristic Calculations

To check the results of Appleton (1960) a full solution was obtained for oxygen for the same initial conditions with $M_{f_\infty} = 2.0$ $T_\infty = 3540\,^\circ K$, $c = 0.52427$ and $p = 0.21$ atmospheres. More recent calculations by Glass and Takano (1963) treat a similar case and this is discussed below.

The characteristic mesh, see figure 2.2(1), was constructed in the physical plane and the basic computing procedure was identical to that described in section 2.2:1. The iterative procedure followed standard practice (cf Isenberg (1952)), with the coefficients in the difference scheme being replaced by mean values of the coefficients at points 2,3' and 1,3' , and the whole process was repeated until successive guesses at the new point 3' differed by less than one part in ten thousand.

The assessment of the optimum mesh size needed to ensure stability and convergence of the computing scheme was made by trial and error. Choice of the best angular increment at the corner (see figure 2.2(2)) was made by comparing the numerical solution with the exact Prandtl-Meyer solution which exists at the corner. It was found that 0.25° intervals gave satisfactory agreement to better than one part in ten-thousand for a 10° corner. The increment in the initial radial distance Δ h along the leading characteristic was then varied and the results compared. The density along the wall, figure 2.3(10), displayed the greatest change in character (not magnitude) to variations in mesh size, with the rest of the dependent variables being affected to some degree (see figures 2.3(1) to 2.3(4)). The programme was too long (timewise) to choose an even smaller mesh size.

By suitable combinations of initial mesh sizes the density could be made to increase or decrease, figure 2.3(10), and thus it would appear that one must proceed with some care in the neighbourhood

of the singular point at the corner. These rather incomplete calculations suggest that it is possible to produce at will, curves similar to those of Appleton 1960, who found initial increases in the density for the larger expansion angles of 20° and 30°. The numerical solutions which produced an initial increase in density also show that the flow angle just away from the corner over-expanded. This will produce compression waves as the flow becomes parallel to the wall and thus the characteristics will tend to converge. Although these preliminary computations did not proceed far enough to see whether the characteristics actually intersect, one may conjecture that incorrect numerical calculations could produce a shock of the type first suggested by Feldman (1958) and like the one which Glass and Takano (1963) claim to have discovered.

As pointed out by Wood and Parker (1958), who studied the unsteady expansion of a relaxing gas the gradients of the flow variables at the frozen wave head may be evaluated exactly, once the rate laws are known. For the particular case of an Ideal Dissociating Gas and for plane flow, Appleton (1960) has shown for steady flow that the decay of the gradients can be written

$$\frac{\left[\frac{\partial}{\partial\varphi}(u_i(r,\varphi))\right]_{\varphi=\varphi_F}}{\left[\frac{\partial}{\partial\varphi}(u_i(0,\varphi))\right]_{\varphi=\varphi_F}} \frac{kr\exp -kr}{1-\exp -kr} \qquad 2.3(10)$$

where $K = \frac{1}{2}\frac{\left(\frac{4+\epsilon_\infty}{3}\right)M_{f\infty}}{\sqrt{M_{f\infty}^2-1}}\, c_\infty^2(1+\epsilon_\infty)\sigma_\infty^2$

and φ is the angular position in the expansion fan and φ_F is its value along the leading characteristic. u_i is any dependent variable.

In the computations equation 2.3(10) was used to assess the accuracy of the mesh size rather than incorporate this extra data into the solution. A comparison between the exact solution 2.3(10) and the gradients of pressure obtained from numerical results is made in

figure 2.3(11). The values of the pressure, temperature and concentration within the expansion fan, referred to free stream conditions, were plotted against radial position in the fan and distance from the corner, figures 2.3(6), 2.3(7), 2.3(8). The results were found to agree closely with those of Appleton.

Since considerable departures from equilibrium occur within the expansion fan (i.e. at the corner after a 10° expansion $c = 0.52427$ and $c_e = 0.11400$) the region downstream of the corner is one where energy is being fed into the system through recombination of atoms and this results in a corresponding readjustment of the dependent variables to some new equilibrium state. The 'a priori' prediction of this asymptotic equilibrium state does not appear possible due to the finite entropy and vorticity production associated with real gas flows. Since the infinite rate equilibrium solution is an isentropic process it is difficult to see what relation it bears to the asymptotic solution other than the fact that the isentropic equilibrium solution gives a fair approximation, see figures (2.3(1) - 2.3(5)).

The results indicate that the pressure, temperature and density are tending to approach the infinite rate equilibrium values but to the extent of the present calculations a small but finite difference exists.

Arguments put forward by Appleton (1963) show by momentum considerations that the final value of pressure far downstream of the corner will tend towards the equilibrium value. A result which is borne out by the present calculations. Overshoots in the wall pressure occur and are probably associated with the vorticity production within the expansion. It is however interesting to note that a reduction of the mesh size (see figure 2.3(1)) reduces this overshoot considerably and one may conjecture that the overshoot is a result of the numerical solution. The formal second order analysis of section 2.5 shows no evidence of an overshoot and could perhaps be a further indication that the choise of a smaller mesh size would completely eliminate the overshoot.

The more recent calculations of Glass and Takano (1963)

cannot be truly compared with those presented here because they use a gas model which assumes that the vibrational energy is always completely excited whereas the present solutions use the Ideal Dissociating Gas which assumes that only half the vibrational energy is in equilibrium with the translational degree of freedom. More serious is the fact that their problem is incorrectly posed. For on the one hand they assume that the vibrational mode is always in equilibrium with the translational mode, and on the other, they assume that truly frozen flow (i.e. the vibrational energy and the dissociation fraction remain equal to their free stream values) exists at the corner and the disturbances can be felt along the initial truly frozen Mach line. Both these assumptions are incompatible if the vibrational energy mode is in equilibrium.

Fortunately the difference between the frozen and partially frozen states is small and thus their calculations behave fairly well away from the corner. The results agreeing on the whole with the present calculations. But in the region of the corner which is very sensitive, the calculations are meaningless and their discovery of a recombination shock is probably a result of the fictitious problem they have formulated.

2.3.2 Comparison of the numerical calculations with the available theories

In view of the essentially non-linear character of non-equilibrium flow problems numerical techniques have to be used. However approximate theories have been developed and it is of interest to see their range of validity. So far two approaches have been used; a fully linearised theory and a co-ordinate perturbation technique.

(i) Linearised Theory

Classical linearised theory was first applied to non-equilibrium problems independently by Clarke (1960) and Moore and Gibson (1960) for the expansion of a reacting gas. Moore and Gibson approximate the basic equation by the telegraph equation and Clarke solves it exactly by transform techniques. The solution at the

wall* is compared with the numerical solution in figures 2.3(1 to 5). As may be expected agreement between the two becomes worse as the expansion angle is increased but for a 5° corner agreement is good, especially when one bears in mind that the entropy and vorticity production is neglected to first order. In all cases the extent of the relaxation zone is well predicted for the 5° corner. Obviously, for the larger angles, the fact that the relaxation time is proportional to the inverse of the density squared, the linear theory will tend to underestimate the zone, as shown in figures 2.3 (1) and 2.3(6). The fact that the temperature and concentration agree so well appears to be quite fortuitous.

(ii) Co-ordinate Perturbation Solution.

An alternative approach to the problem was proposed by Napolitano (1960) and Stulov (1962), who suggested a series solution to the problem with the independent variables expanded as a power series in r, the radial distance from the corner. Thus they assumed

$$u_i(r,\theta) = \sum_{\alpha=0}^{n} r^{\alpha} u_{i\alpha}$$

where u_i is any dependent variable. Writing the governing equations in polar co-ordinates centred at the apex of the expansion and substituting the above series solution, and then collecting together terms of like order i.e. of $o(r^{\alpha})$ a system of equations for $u_{i\alpha}$ was obtained. In practice only first order terms u_i, can readily be obtained due to the complexity of the algebra. The zeroth solution

---

* For further details see Clarke (1960) and section (2.4) where linearised theory is discussed for more than one relaxing mode and for which the above problem would be a special case.

yields the frozen flow solution which exists at the corner. The first order solution is independent of the radial distance r and is only a function of the angular position within the fan and of the frozen solution, and the dependent variables up to the first order can be evaluated. For details of the algebra see the papers cited above. The solution to the first order has been evaluated for this particular problem and the pressure, temperature and atom concentration are compared with the computed solutions in figures 2.3(6) to 2.3(8).

As can be seen, the results show moderate agreement for the pressure and temperature for only quite small values of the radial distance. As r increases, the solution rapidly diverges and becomes quite meaningless after $r = 0.24$. In a recent paper by Shanatian and Inger (1962) this small radius of convergence for the first order solution was also found. These results also show that the radial mesh size in the characteristic solution must be chosen carefully and suggest that even quite small values of radial mesh size just away from the corner will probably overestimate the increases in p, ρ, T etc. These errors may be sufficient to cause the erratic variation of the density downstream of corner shown in figure 2.3(10).

From figure 2.3(9) it may be noted that the characteristic lines are distinctly non-linear. This non-linearity can be predicted quite well with this approach to the problem. The characteristic lines emanating from the corner are given by

$$\frac{dy}{dx} = \tan(\theta + \mu)$$

Letting $\theta + \mu = \theta_0 + \mu_0 + r(\theta_1 + \mu_1)$, where the subscripts 0 and 1 denote the zercth and first order solutions and substituting in the above equation we have

$$\frac{dy}{dx} = \tan(\theta_0 + \mu_0) + \sec^2(\theta_0 + \mu_0)(\theta_1 + \mu_1)r$$

Since the characteristics to a first approximation are the straight frozen ones, r can be written as $x/\cos(\theta_0 + \mu_0)$. Thus very approximately

$$y \simeq \tan(\theta_0+\mu_0)\,x + \sec^3(\theta_0+\mu_0)\,\frac{x^2}{2}(\theta_1+\mu_1) + \cdots \qquad 2.3(11)$$

represents the equation of the characteristic lines. θ_1 and μ_1 are unwieldy expressions and are not given here but with reference to the paper of Napolitano (1961) they may easily be derived. In figure 2.3(9) the last characteristic in the expansion fan is compared with the above approximation and the result is surprisingly good.

Since the density variation downstream of the last characteristic of the expansion is small, 2%, interferograms will tend to indicate the position of this line. Comparison of the observed characteristic with equation 2.3(11) could yield an estimate of the relaxation time.

2.4 Linearised Non-Equilibrium Flow with more than one relaxing internal mode

The previous sections have shown that any non-equilibrium plane flow problem, with an arbitrary number of relaxing or reacting modes, can in principle be solved, at least by numerical techniques, provided the flow is supersonic. However section 2.3 indicates that even for a simple flow with only one relaxing mode this is a lengthy method of solving the problem. Thus before embarking on solutions with more than one relaxing mode it is advisable to look first for approximate but analytical solutions. The underlying principles of such a solution have been proposed by Moore and Gibson (1960) and Clarke (1960) who applied acoustic theory to solve the non-equilibrium equations with just <u>one</u> relaxing mode. It is now proposed to extend this analysis to a gas with two relaxing modes (and eventually to n relaxing modes). The original work of Moore and Gibson and Clarke then becomes a special case of the resulting analysis. To give some

physical significance to the analysis an example is evaluated for Carbon Dioxide.

Apart from the rate equations the basic equations governing the flow of a relaxing gas with more than one mode remain the same and applying the usual small perturbation technique the basic equations reduce to

$$u_\infty \frac{\partial p_1}{\partial x'} + \rho_\infty \left(\frac{\partial u_1}{\partial x'} + \frac{\partial v_1}{\partial y'} \right) = 0 \qquad 2.4(1)$$

$$\frac{\rho_\infty u_\infty^2}{p_\infty} \frac{\partial u_1}{\partial x'} + \frac{\partial p_1}{\partial x'} = 0 \qquad 2.4(2)$$

$$\frac{\rho_\infty u_\infty^2}{p_\infty} \frac{\partial v_1}{\partial x'} + \frac{\partial p_1}{\partial y'} = 0 \qquad 2.4(3)$$

and

$$\rho_\infty u_\infty \frac{\partial E_1}{\partial x'} + p_\infty \left(\frac{\partial u_1}{\partial x'} + \frac{\partial v_1}{\partial y'} \right) = 0 \qquad 2.4(4)$$

where u_1 and v_1 are the components of velocity in the x' y' directions ρ density and p_1 is the pressure, the subscripts on the dependent variables indicating a perturbed quantity. The total specific internal energy is

$$E_1 = e_1 + e_{2_1} + e_{1_1} \qquad 2.4(5)$$

where e_1 is the energy contained in the translational plus active modes and e_{1_1} and e_{2_1} are the linearised amounts of energy associated with the first and second modes. The thermal equation of state for a relaxing gas becomes

$$p = \rho R T \qquad 2.4(6)$$

The above system of equations constitute six equations for eight unknowns. Therefore, to complete the system it is necessary to specify how the internal modes re-adjust themselves once a non-equilibrium state is established.

2.4:1 The Rate Equations

For only one internal mode the classical Landau-Teller theory shows that the rate of re-adjustment of the internal energy will occur in a linear manner proportional to the difference of the actual internal energy from the equilibrium value of the internal energy, evaluated so that it is in equilibrium with the local value of the translational temperature. Little published work exists which describes how individual rate processes occur when a molecule has more than one internal mode. In view of this lack of detail, for the purpose of the present analysis it is assumed that all re-adjustments of the internal modes will occur in a linear manner. To this extent the description of the rate processes follow the ones presented by K. F. Herzfeld (19). Allowing for some degree of coupling between the internal modes a possible description of the way by which the internal modes may re-adjust themselves is

$$\frac{De_1}{Dt} = \frac{e_1(T) - e_1}{\tau'} + \frac{e_2 - e_2(T_1)}{\tau'''} \qquad 2.4(7)$$

and

$$\frac{De_2}{Dt} = \frac{e_2(T) - e_2}{\tau''} + \frac{e_2(T_1) - e_2}{\tau'''} \qquad 2.4(8)$$

T is the translational temperature and T_1 is the vibrational temperature of the first mode. In this approximate description the first mode is allowed to gain energy from the translational mode by collision and at the same time be allowed to lose some to the second mode by internal leakage. Similarly the second mode may adjust its internal energy by the same processes. τ', τ'' and τ''' are the relaxation times associated with the different mechanisms by which

energy exchanges may occur. Equations 7 and 8 imply that for both modes the rate at which energy is gained from the translational mode is proportional to deviation of the actual internal energy from the equilibrium value evaluated with the local translational temperature. In addition it is also specified that the rate at which the two modes exchange energy internally is proportional to the deviation of the actual internal energy of the second mode from the equilibrium value of this mode valuated as if it were in equilibrium with the local vibrational temperature T_1 of the first mode. Obviously such representations are approximate but from the point of view of dealing with linearised gas flows it is hoped that it will be adequate to indicate aspects peculiar to gases with two relaxing modes.

K. F. Herzfeld (Princeton Series on High Speed Aerodynamics) in discussing absorption and dispersion of acoustic waves propagating into relaxing gas mixtures discusses two mode relaxing gases for the extreme situations of equations 7 and 8. In the case when no coupling exists between the modes $\tau_{\infty}^{III} = \infty$ and only translational collisions are important. Herzfeld refers to this situation as excitation of the modes in parallel. If on the other hand it is assumed that the second mode receives little energy directly from translational then $\tau^{II} = \infty$ and the situation is commonly referred to as excitation in series.

2.4:2 Non-Equilibrium equation for two modes

Provided we let τ' τ'' and τ''' take their undisturbed free-stream values the rate equations 2.4(7) and 2.4(8) are in a linearised form provided $e_1 \propto T_1$ and $e_2 \propto T_2$. It is now possible to eliminate all the dependent variables in equations $\frac{(2.4)}{7-8}$ in favour of the pressure perturbation p_1 and the following is the linearised non-equilibrium equation pertinent to gases with the relaxing modes

$$C_{P_{f\infty}}\left(\frac{\tau'_\infty \tau''_\infty u_\infty^2}{L^2}\right)\frac{\partial^2}{\partial x^2}\left[B^2_{f\infty}\frac{\partial^2 p_1}{\partial x^2}-\frac{\partial^2 p_1}{\partial y^2}\right]+\left(C_{p_{f\infty}}+C_{v_1}\right)\left(\frac{\tau''_\infty u_\infty}{L}\right)\frac{\partial}{\partial x}\left[B^2_{1\infty}\frac{\partial^2 p_1}{\partial x^2}-\frac{\partial^2 p_1}{\partial x^2}\right]$$

$$+\left(C_{p_{f\infty}}+C_{v_2}\right)\left(\frac{\tau'_\infty u_\infty}{L}\right)\frac{\partial}{\partial x}\left[B^2_{2\infty}\frac{\partial^2 p_1}{\partial y^2}-\frac{\partial^2 p_1}{\partial y^2}\right]+C_{p_f}\left(1+\frac{\omega_2}{\omega_1}\right)\left(\frac{\tau'_\infty \tau''_\infty}{\tau'''_\infty}\frac{u_\infty}{L}\right)\frac{\partial}{\partial x}\left[B^2_{f\infty}\frac{\partial^2 p_1}{\partial x^2}-\frac{\partial^2 p_1}{\partial y^2}\right]$$

$$+C_{p_{e\infty}}\left(1+\frac{\omega_2}{\omega_1}\frac{\tau'_\infty}{\tau'''_\infty}+\frac{\tau''_\infty}{\tau'''_\infty}\right)\left[B^2_{e\infty}\frac{\partial^2 p_1}{\partial x^2}-\frac{\partial^2 p_1}{\partial y^2}\right]=0 \qquad 2.4(9)$$

It will be noted that by introducing a second mode into the system the order of the partial differential equation has been raised by one above that for a single relaxing mode.* In fact it is not difficult to generalise the situation to a gas which has n relaxing modes, in which case the order of the equation is increased to $(n+2)$. To a linearised approximation the flow field is irrotational and hence equation 2.4(9) could have been written in terms of velocity potential.

In equation 9 the independent variables have been made non-dimensional with some characteristic length L such that $x = x'/L$ and $y = y'/L$. $C_{p_{f\infty}}$ is the specific heat at constant pressure, obtained by assuming there is no contribution from the internal modes $C_{v_{1\infty}}$ and $C_{v_{2\infty}}$ are the heat capacities of the first and second modes such that $e_1 = \omega_1 T_1$ and $e_2 = \omega_2 T_2$, T_1 and T_2 being the corresponding vibrational temperatures of the modes. $C_{p_e} = C_{p_f} + \omega_1 + \omega_2$ is the equilibrium heat capacity at constant pressure.

$B^2_{f\infty}$ is the Ackeret factor $\left(\frac{u_\infty^2}{a_{f\infty}^2}-1\right)$ based on the frozen speed of sound $a_{f\infty} = \left\{\frac{C_{pf}}{C_{vf}}RT\right\}^{1/2}$ and $B_e^2 = \left(\frac{u_\infty^2}{a_e^2}-1\right)$. $a_e^2 = \left(C_{pe}/C_{ve}\right)RT$ is the square of the equilibrium sound speed obtained by considering that all the modes take an active part. For

---

* For the case of only one relaxing mode Clarke (1960) Vincenti (1960) and Moore and Gibson (1960) show that the governing linearised equation is given by $\tau_\infty u_\infty \frac{\partial}{\partial x}\left[B^2_{f\infty}p_{1xx}-p_{1yy}\right]+\left[B^2 p_{1xx}-p_{1yy}\right]=0$.

a gas with two modes two other natural sound speeds exist.

$$a_1^2 = \frac{C_{pf} + C_{v1}}{C_{vf} + C_{v1}} \cdot RT \qquad 2.4(10)$$

and

$$a_2^2 = \frac{C_{pf} + C_{v2}}{C_{vf} + C_{v2}} \cdot RT \qquad 2.4(11)$$

The subscript indicating which mode has been considered as taking an active part. It may be noted that

$$a_f > a_2 \geq a_1 > a_e$$

provided the first mode contains more energy than the second. These two extra speeds introduce the corresponding Ackeret factors B_1 and B_2 in equation 9.

In the case where only one relaxing mode participates the choice of L becomes a natural one when no other length characteristic to the problem exists. For example, L is taken as equal to the product of the freestream velocity and the relaxation time. For gases with more than one relaxation time the choice of L is wide. Inspection of equation 9 now indicates that if L is set equal to either $u_\infty \tau'$ or $u_\infty \tau''$ then a situation can arise such that one mode may never take an active part within the flow field, whose coordinates have been non-dimensionalised with $u_\infty \times$(relaxation time of the other mode). In such cases the total solution has to be obtained by superposition. Naturally the situation becomes more complex as the number of modes is increased.

The characteristics of equation 9 are the streamlines and the lines $dy/dx = \pm \frac{1}{B_{f\infty}}$, provided both τ' and τ'' are greater than zero. However in the limit of either τ' or τ'' equalling zero the characteristics of the system change discontinuously to

$dy/dx = \pm 1/B_{1\infty}$ or $dy/dx = \pm 1/B_{2\infty}$ respectively. In the event of both $\mathcal{T}'$ and $\mathcal{T}''$ being zero then the characteristics change discontinuously to $dy/dx = \pm 1/B_{e\infty}$. This discontinuous change is characteristic to non-equilibrium equations and was first discussed at length by Boa-Teh-Chu (1957). One interesting feature not obtained in the simple case is when $\mathcal{T}''' \to 0$, i.e. when energy is exchanged internally between modes infinitely quickly, then the order of the equation is reduced but the characteristics remain equal to the frozen ones.

Before continuing the analysis several deductions may be made. When $\mathcal{T}' = \mathcal{T}'' = 0$ the classical Prandtl-Gluaert equation for equilibrium flow results. When $\mathcal{T}' = \mathcal{T}'' = \infty$ the corresponding equation for frozen flow is obtained. When $\mathcal{T}'$ and $\mathcal{T}''$ remain finite but $\mathcal{T}''' = 0$ the system reduces to the familiar third order equation characteristic to non-equilibrium problems. See for example Vincenti (1959) Moore and Gibson (1960) and Clarke (1960)

2.4:3 The solution for a sharp cornered expansion in supersonic flow

Truly supersonic flow is said to exist when $M_e > M_1 > M_2 > M_f > 1$. The interesting transonic region is not dealt with here.

To examine the flow past a sharp corner equation 2.4(9) is solved subject to the following boundary condition*

$$\frac{\partial p_1(x,0)}{\partial y} = \gamma_e M_e^2 \frac{\partial}{\partial x}\left(H(x)\right)$$

which holds along $y = 0$. $H(x)$ is the unit step function. The solution of equations 2.4(9) subject to the above boundary condition is most easily solved by transform techniques. Define the Laplace transform of $p_1(x,y)$ as

$$\bar{p}_1(z,y) = \int_0^\infty p_1(x,y)\, \exp -zx \, dx$$

---

* There is of course, no need to restrict the solution to a sharp corner. As with all linearised problems flow past arbitrary boundary shapes may be considered.

Choosing $L = U_\infty \tau'_\infty$ in equation 2.4(9), multiplying by $\exp -\lambda z$ and integrating from zero to infinity yields the following ordinary differential equation in the transform plane.

$$\frac{d^2\bar{p}_1}{dy^2} = (z B_{f_\infty})^2 \left\{ \frac{z^2 + \left[\frac{C_{p_c}+C_{v_2}}{C_{p_f}} \frac{B_c^2}{B_f^2} \frac{\tau'}{\tau''} + \frac{C_{p_c}+C_{v_1}}{C_{p_f}} \frac{B_c^2}{B_f^2} + \frac{C_{v_1}+C_{v_2}}{C_{v_1}} \frac{\tau'}{\tau'''} \right] z + \frac{C_{p_c}}{C_{p_f}} \frac{\tau'}{\tau''} \left[1 + \frac{C_{v_2}}{C_{v_1}} \frac{\tau'}{\tau'''} + \frac{\tau''}{\tau'''} \right] \frac{B_c^2}{B_f^2} }{ z^2 + \left[\frac{C_{p_f}+C_{v_2}}{C_{p_f}} \frac{\tau'}{\tau''} + \frac{C_{p_c}+C_{v_1}}{C_{p_f}} + \frac{C_{v_1}+C_{v_2}}{C_{v_1}} \frac{\tau'}{\tau'''} \right] z + \frac{C_{p_c}}{C_{p_f}} \frac{\tau'}{\tau''} \left[1 + \frac{C_{v_2}}{C_{v_1}} \frac{\tau'}{\tau'''} + \frac{\tau''}{\tau'''} \right] } \right\} \bar{p}_1 \qquad 2.4(12)$$

For convenience let the roots of the quadratics within the curly brackets $\alpha\ \beta\ \delta$ and σ then equation 2.4(12) becomes

$$\frac{d^2\bar{p}_1}{dy^2} - (z B_{f_\infty})^2 \left\{ \frac{(z+\delta)(z+\sigma)}{(z+\alpha)(z+\beta)} \right\} \bar{p}_1 = 0 \qquad 2.4(13)$$

For an outgoing wave system a possible solution of 2.4(13) is

$$\bar{p}_1 = A \exp -z B_{f_\infty} \sqrt{\frac{(z+\delta)(z+\sigma)}{(z+\alpha)(z+\beta)}}\, y \qquad 2.4(14)$$

The arbitrary constant may be evaluated by utilising the transformed boundary condition. Evaluating the constant A, the transformed pressure perturbation is given by

$$\bar{p}_1 = \frac{\gamma_{f_\infty} M_{f_\infty}^2}{B_{f_\infty}} \frac{1}{z} \sqrt{\frac{(z+\alpha)(z+\beta)}{(z+\delta)(z+\sigma)}} \exp -z B_{f_\infty} \sqrt{\frac{(z+\delta)(z+\sigma)}{(z+\alpha)(z+\beta)}}\, y \qquad 2.4(15)$$

A general solution of equation 2.4(15) is not easily obtained due to the essential singularities at $z = -\alpha$, $z = -\beta$ which occur in the exponential, but as in the case of one relaxing mode (Clarke 1960) the inversion of equation (15), when y = 0, i.e. (along the wall), is readily accomplished. From the standard inversions listed in Erdelyi, Oberhettinger and Tricomi (1954) used in conjunction with the convolution theorem, the pressure perturbation at the boundary y = 0

in the physical plane is

$$\frac{B_f}{\gamma_f M_f^2} p_1(x,0) = I_0\left[\frac{\alpha-\delta}{2} x\right] \exp\left[-\frac{\alpha+\delta}{2} x\right]$$

$$+\alpha\int_0^x I_0\left[\frac{\alpha-\delta}{2} u\right] \exp\left[-\frac{\alpha+\delta}{2} u\right] du$$

$$+\int_0^x \frac{\beta-\sigma}{2} \exp\left[-\frac{(\beta+\sigma)}{2}(x-t)\right]\left\{I_1\left[\frac{\beta-\sigma}{2}(x-t)\right]+I_0\left[\frac{\beta-\sigma}{2}(x-t)\right]\right\}\cdot$$

$$\left\{I_0\left[\frac{\alpha-\delta}{2} t\right]\exp\left[-\frac{(\alpha+\delta)}{2} t\right]+\alpha\int_0^t I_0\left[\frac{\alpha-\delta}{2} u\right]\exp\left[-\frac{\alpha+\delta}{2} u\right] du\right\} dt \qquad 2.4(16)$$

where I_0 and I_1 are modified Bessel functions of the zeroeth and first order.

Since the parameters α, β, δ and σ are functions of τ', τ'' and τ''' there exists an infinity of possible combinations for which equation 2.4(16) can be evaluated. It is therefore convenient to select certain extreme cases for discussion.

To give some physical interest to the solution of the equation an example has been evaluated for the polyatomic molecule of carbon dioxide. Carbon dioxide has a linear symmetric molecule and has four vibrational modes: a doubly degenerate bending mode with a characteristic temperature of 959°K and two stretching modes with characteristic temperatures of 1920°K and 3380°K. Some doubt exists about the mechanism by which the modes are excited and as such the simple description of the rate equation may be quite adequate. Although carbon dioxide has three vibrational modes, provided the temperature is sufficiently low, $< 1000\ ^{\circ}K$, the energy contained in the last stretching mode is negligibly small and in such circumstances the molecule may be treated as one which has two active modes of

vibration. This situation has been discussed by Witteman (1961) who assumes that the first stretching mode is excited only by internal leakage. His analysis suggests that the relaxation time associated with the transfer of energy from the bending mode to stretching mode is smaller than the relaxation time associated with the direct excitation of the bending mode. Schwartz (1954) on the other hand indicated that the reverse situation would prevail.

The specific freestream conditions chosen were ones that could be generated in the steady supersonic flow region that follows a normal shock in a shock tube. With T_∞ = 1000°K and an equilibrium Mach number of M_e = 2. this condition would correspond roughly to a shock Mach number of about 4 to 4.5 in a shock tube. The energy contained in the various modes is as follows:- 1200 R, 330 R and 188 R. Thus it can be seen that neglect of the last mode is possible.

2.4:4 Parallel Excitation of the internal modes, $\tau''' = \infty$.

As noted earlier $\tau''' = \infty$ indicates that the two internal degrees of freedom only gain energy from translation. The choice of $\tau''' = \infty$ allows α, β, δ and σ to be determined for a range of values of τ''/τ'. For the specific conditions cited above that may exist for Carbon Dioxide this case has been evaluated in figure 2.4(1) for a range of τ''/τ'. Particularly simple solutions arise for the limiting cases of $\tau''/\tau' = 0$; $\tau''/\tau' = 1$ and $\tau''/\tau' = \infty$.

(i) For $\tau''/\tau' = 0$ the highest order derivatives in equation 2.4(9) are removed and it degenerates to a third order equation. Relative to the first mode the second mode adjusts itself infinitely quickly and thus it may be noted that the pre-cursor signals will always be felt along lines given by $\frac{dy}{dx} = \pm 1/M_2$ rather than the frozen ones. The pressure distribution along the wall then simplifies to

$$-\frac{B_2(p-p_\infty)}{\gamma_f M_f^2\,\theta} = \exp\left[-\frac{C_{p_f}+C_{v_2}}{2C_{p_f}}\left(\frac{B_2^2}{B_f^2}+1\right)x\right] I_0\left[\frac{C_{p_f}+C_{v_2}}{2C_{p_f}}\left(\frac{B_2^2}{B_f^2}-1\right)x\right]$$

$$+\frac{C_{p_f}+C_{v_2}}{C_{p_f}}\int_0^x \exp\left[-\frac{C_{p_f}+C_{v_2}}{2C_{p_f}}\left(\frac{B_2^2}{B_f^2}+1\right)x\right] I_0\left[\frac{C_{p_f}+C_{v_2}}{2C_{p_f}}\left(\frac{B_2^2}{B_f^2}-1\right)x\right] dx \quad 2.4(17)$$

(ii) For $\tau''/\tau' = 1$ the unwieldy expression under the root sign in equation 2.4(12) factorises and allows the inversion to be written as

$$-\frac{B_{f_\infty}(p-p_\infty)}{\gamma_f M_f^2\,\theta} = \exp\left[-\frac{C_{p_e}}{2C_{p_f}}\left(\frac{B_e^2}{B_f^2}+1\right)x\right] I_0\left[\frac{C_{p_e}}{2C_{p_f}}\left(\frac{B_e^2}{B_f^2}-1\right)x\right]$$

$$+\frac{C_{p_e}}{C_{p_f}}\int_0^x \exp\left[-\frac{C_{p_e}}{2C_{p_f}}\left(\frac{B_e^2}{B_f^2}+1\right)x\right] I_0\left[\frac{C_{p_e}}{2C_{p_f}}\left(\frac{B_e^2}{B_f^2}-1\right)x\right] dx \quad 2.4(18)$$

(iii) For $\tau''/\tau' = \infty$ equation (2.4(9) indicates that the pressure will never return to its full equilibrium value. This arises of course because of the way in which the independent variables have been made non-dimensional. For this case a first integral of equation can be obtained and the resulting third order equation gives the following solution

$$-\frac{B_{f_\infty}(p-p_\infty)}{\gamma_{f_\infty} M_{f_\infty}^2\,\theta} = \exp\left[-\frac{C_{p_f}+C_{v_1}}{C_{p_f}}\frac{1}{2}\left(\frac{B_1^2}{B_f^2}+1\right)x\right] I_0\left[\frac{C_{p_f}+C_{v_1}}{C_{p_f}}\frac{1}{2}\left(\frac{B_1^2}{B_f^2}-1\right)x\right]$$

$$+\frac{C_{p_f}+C_{v_1}}{C_{p_f}}\int_0^x \exp\left[-\frac{C_{p_f}+C_{v_1}}{C_{p_f}\,2}\left(\frac{B_1^2}{B_f^2}+1\right)x\right] I_0\left[\frac{C_{p_f}+C_{v_1}}{2C_{p_f}}\left(\frac{B_1^2}{B_f^2}-1\right)x\right] dx \quad 2.4(19)$$

2.4:5 Series Excitation of the internal modes $\tau'' = \infty$

In this case it is assumed that energy can only be fed into the second mode by internal leakage. Once again equation 2.4(9) may be simplified for limiting values of τ'''/τ'

(i) When $\tau'''/\tau' = \infty$ the system behaves as if it has only one active internal mode. A first integral can be obtained and the solution for the pressure distribution along the wall is identical to equation 2.4(19). The pressure never recovers to its full equilibrium value.

(ii) When $\tau'''/\tau' = 0$ the highest order derivatives are removed but in this case the characteristics associated with possible discontinuities in the pressure, velocity etc. remain unchanged but one streamline characteristic is removed. The solution is

$$-\frac{B_{f\infty}(p-p_\infty)}{\gamma_\infty M_{f\infty} B} = \exp\left[-\frac{c_{v1}}{c_{v1}+c_{v2}}\cdot\frac{1}{2}\cdot\left(\frac{B_e^2}{B_f^2}+1\right)x\right] I_0\left[\frac{c_{v1}}{c_{v1}+c_{v2}}\cdot\frac{1}{2}\cdot\left(\frac{B_e^2}{B_f^2}+1\right)x\right]$$

$$+\frac{c_{v1}}{c_{v1}+c_{v2}}\int_0^x \exp\left[-\frac{c_{v1}}{c_{v1}+c_{v2}}\cdot\frac{1}{2}\cdot\left(\frac{B_e^2}{B_f^2}+1\right)x\right] I_0\left[\frac{c_{v1}}{c_{v1}+c_{v2}}\cdot\frac{1}{2}\cdot\left(\frac{B_e^2}{B_f^2}-1\right)x\right] dx \quad 2.4(20)$$

Both cases (i) and (ii) are given in figure.

Of particular interest in this section are the results of Witteman (1961) who suggests that for carbon dioxide the most probable means of energy distribution to the stretching modes is through internal leakage i.e. $\tau_\infty'' = \infty$. His work suggests that at $T = 1000\,^\circ K$, $\tau''/\tau' \sim 0.25$ and this case would lie between cases (i) and (ii) presented in figure 2.4(2). The difference between the profiles $\tau'''/\tau' = \infty$ and $\tau'''/\tau' = 0$ is so small that it is unlikely that experimental determination of the actual pressure distribution would ever be accurate enough to asses the ratio of τ'''/τ'.

2.4:6 A particular example of parallel and series excitation.

When it is assumed that the energy can be transferred internally at an infinitely fast rate $T''' = 0$ equation 2.4(9) reduces to

$$C_{p_f}\left(1+\frac{c_{v_2}}{c_{v_1}}\right)\frac{\tau'\tau''}{L}u_\infty\frac{\partial}{\partial\xi}\left[B_{f_\infty}^2 p_{,xx}-p_{,yy}\right]+C_{p_e}\left(\frac{c_{v_2}}{c_{v_1}}\tau'+\tau''\right)\left[B_e^2 p_{,xx}-p_{,yy}\right]=0$$

letting $L = u_\infty \tau'$ three simple cases arise 2.4(21)

(i) When $\tau''/\tau' = 0$ the solution is just the equilibrium limit

(ii) When $\tau'''/\tau' = 1$ the solution is given by equation 2.4(18)

(iii) When $\tau'''/\tau' = \infty$ the solution is given by equation 2.4(20)

These are shown in figure 2.4(3)

2.4:7 Decay of the Pressure Perturbation Along the leading characteristic

To determine the flow field in the vicinity of the first frozen Mach line it is convenient to work in a semi-characteristic co-ordinate system rather than the rectangular cartesian system used in equation (9). Let $\xi = x - B_{f_\infty} y$ and $\eta = B_{f_\infty} y$ then equation (9) transforms to

$$C_{p_f}\left(\frac{\tau'\tau''a_\infty^2}{L^2}\right)\frac{\partial^2}{\partial\xi^2}\left[-p_{,\eta\eta}+2p_{,\xi\eta}\right]+\left(C_{p_f}+c_{v_2}\right)\left(\frac{\tau' u_\infty}{L}\right)\frac{\partial}{\partial\xi}\left[\left(B_2^2-1\right)p_{\xi\xi}+2p_{\xi\eta}-p_{\eta\eta}\right]$$

$$+\left(C_{p_f}+c_{v_1}\right)\left(\frac{\tau'' u_\infty}{L}\right)\left[\left(B_1^2-1\right)p_{\xi\xi}+2p_{\xi\eta}-p_{\eta\eta}\right]+C_{p_f}\left(1+\frac{c_{v_2}}{c_{v_1}}\right)\left(\frac{\tau'\tau''}{\tau'''}\right)\frac{u_\infty}{L}\frac{\partial}{\partial\xi}\left[-p_{,\eta\eta}+2p_{\xi\eta}\right]$$

$$+C_{p_e}\left(1+\frac{c_{v_2}}{c_{v_1}}\frac{\tau'}{\tau''}+\frac{\tau''}{\tau'''}\right)\left[\left(B_e^2-1\right)p_{\xi\xi}+2p_{\xi\eta}-p_{,\eta\eta}\right]=0 \qquad 2.4(22)$$

Defining a Laplace transform as in equation (11) and applying the boundary condition equivalent to equation (10) gives the following

solution for the pressure perturbation in the transform plane

$$-\frac{B_{f\infty}}{\gamma_{f\infty} M_{f\infty}^2 \theta}\,\bar{p} = \frac{1}{z}\sqrt{\frac{(z+\alpha)(z+\beta)}{(z+\delta)(z+\sigma)}}\,\exp\left\{z - z\sqrt{\frac{(z+\delta)(z+\sigma)}{(z+\alpha)(z+\beta)}}\right\}\eta \qquad 2.4(23)$$

where α, β, δ and σ take on the same values indicated in equation 2.4(13).

To look at the behaviour for small ξ (i.e. near the first characteristic) Laplace transform theory shows that this corresponds to large z. Expanding equation 2.4(23) in inverse powers of z and neglecting powers of $(1/z)^2$ gives

$$-\frac{B_{f\infty}}{\gamma_{f\infty} M_{f\infty}^2 \theta}\,\bar{p} = \frac{1}{z}\exp -\frac{1}{2}\left(\delta+\sigma-\alpha-\beta\right) \qquad 2.4(24)$$

Inverting equation 2.4(24) and substituting for $\delta+\sigma-\alpha-\beta$ shows that at the wave head the pressure perturbation decays like

$$-\frac{B_{f\infty}}{\gamma_{f\infty} M_{f\infty}^2 \theta}\left(p-p_\infty\right) = \exp -\frac{1}{2}\left\{\frac{C_{p_f}+C_{w_2}}{C_{p_f}}\,\frac{\tau'}{\tau''}\left(\frac{B_2^2-1}{B_f^2}\right) + \frac{C_{p_f}+C_{w_2}}{C_{p_f}}\left(\frac{B_1^2}{B_f^2}-1\right)\right\}\eta \qquad 2.4(25)$$

Remembering that η is made non-dimensional with $u_\infty \tau'$. It will be noted that the decay is independent of any internal relaxations and is only a function of the relaxation processes associated with direct energy transfer by collisions from the translational mode and thus if energy transfer is by internal leakage only then observation of the decay of the head of the fan could yield a technique for measuring the true τ' for a wide temperature range, (See section (3.30) for further discussion on this point).

The limiting case $\tau''/\tau' \to 0$ suggests that the decay will

occur in an infinitely small distance from the corner. This of course corresponds to the discontinuous change of the characteristics due to the higher order terms vanishing.

2.4:8 Extension of linear theory to n active internal modes

Before concluding this chapter on the application of linearised theory to the problem of plane expansion it may be pointed out that the proceeding work for two modes may formally be extended to cope with any number of modes.

Since the analysis is only algebraically difficult, the general form of the solution for n modes will be derived for excitation of the modes in parallel only. The more general case of parallel and excitation only adds difficulties in manipulation.

Equations 2.4(1), 2.4(2), 2.4(3), and 2.4(4) remain the same but now

$$E = e + \sum_{i=1}^{n} e_i \qquad 2.4(26)$$

where e_i is the specific internal energy of the i^{th} mode. Further, instead of the two general rate equations 2.4(7), 2.4(8) there exist n equations

$$\frac{De_\alpha}{Dt} = \frac{e_\alpha(T) - e_\alpha}{\tau_\alpha} \qquad \alpha = 1, \ldots, n \qquad 2.4(27)$$

which have no coupling by internal energy transfer. Letting $e_\alpha = c_{v\alpha} T_\alpha$ to a linear approximation where T_α is the vibrational temperature of the α^{th} mode then substituting the equation of state into the energy equation there results to first order

$$\frac{\partial p_1}{\partial x} + \frac{\rho_\infty a_{f\infty}^2}{p_\infty}\left(\frac{\partial u_1}{\partial x} + \frac{\partial v_1}{\partial y}\right) + \frac{p_\infty R}{c_{vf}\rho_\infty}\sum_{i=1}^{n} c_{vi}\frac{\partial T_{i1}}{\partial x} = 0 \qquad 2.4(28)$$

By means of the momentum equation the velocity perturbations may be eliminated to give

$$B_{f\infty}^2\frac{\partial^2 p_1}{\partial x^2} - \frac{\partial^2 p_1}{\partial y^2} + \frac{\rho_\infty R\, u_\infty^2}{c_{vf}\rho_\infty a_{f\infty}^2}\sum_{i=1}^{n} c_{vi}\frac{\partial^2 T_{i1}}{\partial x^2} = 0 \qquad 2.4(29)$$

Eliminating the translational temperature between the energy equation and the rate equations gives

$$c_{v_f}\left(q_\infty \tau_\alpha \frac{\partial}{\partial x}+1\right)\frac{\partial T_\alpha}{\partial x^2} = \frac{B_E^2 p_{xx}-p_{yy}}{\frac{p_\infty u_\infty^2 R}{c_{v_f} p_\infty a_{f_\infty}^2}} + \frac{1}{\gamma_\infty M_\infty^2}\left(p_{xx}+p_{yy}\right) \qquad \alpha = 1,\ldots,n. \qquad 2.4(30)$$

Eliminating the vibrational temperatures between 2.4(29) and then equation 2.4(30) in favour of the pressure gives after a considerable amount of manipulation the following equation

$$\sum_{r=0}^{n} \frac{1}{(Lq_\infty)^{r-1}} \frac{\partial^{n-r}}{\partial x^{n-r}} \left\{ \sum_{\alpha_1 \ldots \alpha_r} \frac{c_{p_f}+c_{v_{\alpha_1}}+\ldots c_{v_{\alpha_r}}}{\tau_{\alpha_1}\tau_{\alpha_2}\ldots\tau_{\alpha_r}} \left\{ \left[M^2_{\alpha_1\ldots\alpha_r} - 1 \right] \frac{\partial^2 p}{\partial x^2} - \frac{\partial^2 p}{\partial y^2} \right\} \right\} = 0 \qquad 2.4(31)$$

α_s may take any value between 1 and n and the symbol $\sum_{\alpha_1 \ldots \alpha_r}$ represents the sum of all possible products taken r at a time from the 'n' possible values of α_s. Thus for a given r there will exist ${}^nC_r = n!/r!\,(n-r)!$ ways of choosing possible combinations of α_s taken r at a time. The Mach Number $M_{\alpha_1 \ldots \alpha_r}$ is based on the speed of sound

$$a^2_{f_{\alpha_1\ldots\alpha_r}} = \frac{c_{p_f}+c_{v_{\alpha_1}}+\ldots+c_{v_{\alpha_r}}}{c_{v_f}+c_{v_{\alpha_1}}+\ldots+c_{v_{\alpha_r}}} \frac{p_\infty}{\rho_\infty} \qquad 2.4(32)$$

For the specific case of n = 2 this equation reduces to equation 2.4(9) with $\tau_{\alpha\alpha} = \infty$.

In principle equation 2.4(30) may be solved by Laplace transform techniques. For the case of a sharp corner the transform of the pressure perturbation is of the form

$$\bar{p} = \frac{1}{z}\sqrt{\frac{\prod_1^n (z-\beta_i)}{\prod_1^n (z-\delta_i)}}\ \exp -zB_f\sqrt{\frac{\prod_1^n (z-\delta_i)}{\prod_1^n (z-\beta_i)}}$$

δ_i and β_i are roots of n^{th} order equations in z.

The n essential singularities at $z = \beta_i$ make it difficult to evaluate for a general y, but at the boundary y = 0

$$\bar{p} = \frac{1}{z}\sqrt{\frac{\hat{\Pi}(z-\beta_i)}{\hat{\Pi}(z-\delta_i)}}$$

and may be inverted by repeated application of the convolution theorem.

2.5 A Second Order Solution For Plane Supersonic Non-Equilibrium Flow.

For small departures from equilibrium, linearised theory describes the general features of many non-equilibrium flows remarkably well. However, some aspects of the problem are not made apparent because some of the non-linearities which are peculiar to such systems are removed in the process of linearisation. For example, for the flow past a sharp corner it is not immediately apparent, in the exact solution, what the final asymptotic values of the dependent variables are far downstream of the corner. As mentioned earlier, this query arises because of the finite production of vorticity and entropy associated with non-equilibrium flows. The linearised theory automatically implies that the asymptotic values will be the same as the infinite rate equilibrium values, since to this approximation the entropy and vorticity production is zero. Linear theory also fails to predict the phenomena of freezing first discovered by Bray (1959) and later predicted (on an analytical basis by Blythe (1963). In view of these essential differences it would thus appear desirable to seek a higher approximation which accounts in some measure for the non-linearities and hope that it will shed light on the numerical solutions and perhaps explain in a more satisfactory way the observed results. For isentropic flow with a constant ratio of specific heats higher approximations have generally yielded a better answer (for example see Van Dyke (1951)). In particular the formal second order solution for the plane flow around a corner

is known to yield the Busemann approximation and has proved to be a satisfactory improvement.

The aim of the present study is to seek an analogous solution for non-equilibrium flow in two dimensions.

2.5:1 The Iteration Procedure

Unlike the case dealt with by Van Dyke (1951), a general equation in one dependent variable (In isentropic flow this is the velocity potential) does not exist. Thus, it is assumed that any dependent variable u_i (say) may be represented by the series

$$u_i(x,y) = \sum_r u_{i_r}(x,y)\,\delta^r \qquad 2.5(1)$$

where δ is some small parameter. Substituting this series into the basic equations of motion 2.1(1), 2.1(7) and collecting together terms of order δ^r yield r sets of equations for u_{i_r}. Each of the set equations is linear in $u_{i_r}(x\ y)$ and has right hand sides depending on the solutions of the previously computed $(r-1)$ solutions. The complexity of using such a technique increases rapidly with each successive approximation. In practice it is rare that it is ever possible to proceed beyond the second approximation and thus a discussion of the convergence of such a series is virtually impossible. In fact, there is no 'a priori' guarantee that the second order solution will be better than the first. It is hoped however that, for sufficiently small δ the extra terms will show an improvement. The degree of success can only be assessed 'a posteriori' by comparing with other techniques of solution, in this instance with the numerical solution.

Since non-equilibrium effects are very dependent on the thermal and chemical kinetics of the problem it is necessary to choose from the outset a specific example. Thus in the following discussion the problem of the expansion of a relaxing gas is considered. The basic equations describing the flow then simplify

from those in section 2.1 to the following.

$$u\frac{\partial p}{\partial x} + v\frac{\partial p}{\partial y} + \rho a_f^2\left(\frac{\partial u}{\partial x} + \frac{\partial v}{\partial y}\right) + R\frac{c_{v_1}}{c_{v_f}} \cdot p \cdot \frac{DT_v}{Dt} = 0$$

$$\rho u\frac{\partial u}{\partial x} + \rho v\frac{\partial u}{\partial y} + \frac{\partial p}{\partial x} = 0$$

$$\rho u\frac{\partial v}{\partial x} + \rho v\frac{\partial v}{\partial y} + \frac{\partial p}{\partial y} = 0 \qquad 2.5(2)$$

$$\left(u\frac{\partial}{\partial x} + v\frac{\partial}{\partial y}\right)\left(c_{v_f}T + c_{v_1}T_v\right) + \frac{p}{\rho}\left(\frac{\partial u}{\partial x} + \frac{\partial v}{\partial y}\right) = 0$$

$$\left(u\frac{\partial}{\partial x} + v\frac{\partial}{\partial y}\right)T_v = \frac{T - T_v}{\tau}$$

For a simple harmonic vibrator

$$c_{v_1} = \left(\frac{\Delta v}{T}\right)^2 \exp\frac{\Delta v}{T} \Big/ \left(\exp\frac{\Delta v}{T} - 1\right)^2 \qquad 2.5(3)$$

but to help to simplify the algebra the specific heat associated with the internal mode is treated as a constant. This is generally not a very severe restriction and does not seriously affect the non-equilibrium character of the problem. In the above equations Tv is the vibrational temperature and the rest of the variables take on their usual significance. τ is the relaxation time and in general, experiment has shown that it is of the form

$$\frac{\tau}{\tau_\infty} = \frac{\exp b\left(T^{-1/3} - 1\right)T_\infty^{-1/3}}{\rho/\rho_\infty} \qquad 2.5(4)$$

where b* is a constant determined by experiment and the subscript ∞ represents some reference state. The variations of τ can be very significant in non-equilibrium problems (for example it is the

* For Carbon Dioxide $b = 60\ (^\circ K)^{\frac{1}{3}}$

primary reason why 'freezing' occurs in nozzle flows), but in the present example of corner flow for small angles of expansion it may not be too significant and for the moment τ is treated as a constant. However some comment is made later about the possibility of including this variation and its subsequent effect on the theory.

Substituting the series expansion 2.5(1) into the above system of equations and collecting terms of order θ gives the linearised form of the equations. As in section 2.4 all the dependent variables may be eliminated in favour of the pressure perturbation p_1 to give the following third order partial differential equation

$$\frac{C_{p_f}}{C_{p_e}} \tau_{\infty} u_{\infty} \frac{\partial}{\partial x}\left\{(M_e^2-1)\frac{\partial^2 p_1}{\partial x^2} - \frac{\partial^2 p_1}{\partial y^2}\right\} + \left\{(M_e^2-1)\frac{\partial^2 p_1}{\partial x^2} - \frac{\partial^2 p_1}{\partial y^2}\right\} = 0 \qquad 2.5(5)$$

This is a special case of the more general problem treated in section (2.4) Equation 2.5(5) can be solved by transform techniques, (cf Clarke 1961, Der 1963) or by Greens functions (cf Clarke-Cleaver 1963). Approximate solutions have also been obtained by treating $\left(\frac{M_e^2-1}{M_f^2-1} - 1\right)$ as an additional small parameter characteristic to the problem. Utilising this parameter Moore and Gibson reduce equation 2.5(5) to the telegraph equation and obtain a closed form solution valid over the whole flow field. Napolitano (1961) also makes use of this extra parameter to obtain a series solution of equation 2.5(5) Morrison (1956) solves the equation exactly. In all cases the solution is relatively complex for a general field point. Since the second order solution, as will be seen, depends on the first order solution difficulties may be anticipated even at this stage.

For this supersonic case $M_e > M_f > 1$, equation 2.5(5) is hyperbolic and thus no disturbances from the given boundary will be felt ahead of the first frozen characteristic. Therefore when dealing with flow fields which are unbounded on one side, it is convenient to transform to a semi-characteristic co-ordinate system by letting $\xi = x - B_{f_\infty} y$ and $\eta = B_f y$ with $B_{f_\infty} = \sqrt{M_f^2 - 1}$.
In transformed co-ordinates the linearised equation becomes

$$-\left(\frac{C_{pf}}{C_{pe}}\tau_w u_\infty \frac{\partial}{\partial \xi}+1\right)\left\{\frac{\partial^2 p_2}{\partial \eta^2}-2\frac{\partial^2 p_2}{\partial \xi \partial \eta}\right\}+\left(B^2-1\right)\frac{\partial^2 p_2}{\partial \xi^2}=0 \qquad 2.5(6)$$

Substituting the series expansion 2.5(1) in the governing equations and collecting terms of order θ^2 and transforming to a semi-characteristic co-ordinate system $\xi = x - B_f y$, $\eta = B_f y$, the following second order system of equations may be obtained.

$$\left[\gamma_f M_f^2 u_{2\xi} + p_{2\xi}\right] = -\gamma_f M_f^2\left\{(\rho_1+u_1)u_{1\xi} + B_f v_1(u_{1\eta}-u_{1\xi})\right\} = -\varphi(\xi,\eta) \quad 2.5(7)$$

$$\left[\gamma_f M_f^2 v_{2\xi} + B_f(p_{2\eta}-p_{2\xi})\right] = -\gamma_f M_f^2\left\{(\rho_1+u_1)v_{2\xi} + B_f v_1(v_{1\eta}-v_{1\xi})\right\} = -\psi(\xi,\eta) \quad 2.5(8)$$

$$\left[p_{2\xi} + \frac{\rho_\infty a_f^2}{p_\infty}\left(u_{2\xi} + B_{f\infty}(v_{2\eta}-v_{2\xi})\right) + \frac{c_{v1}}{c_{vf}}T_{v2\xi}\right] = -\left\{u_1 p_{1\xi} + B_{f\infty}v_1(p_{1\eta}-p_{1\xi})\right.$$

$$\left. + \gamma_f\left(p_1 u_{1\xi} + B_f p_1(v_{1\eta}-v_{1\xi})\right) + \frac{c_{v1}}{c_{vf}}\left((\rho_1+u_1)T_{v1\xi} + v_1 B_f(T_{v1\eta}-T_{v1\xi})\right)\right\} = -\Omega(\xi,\eta) \quad 2.5(10)$$

$$\left[T_{2\xi} + \frac{T_{v2}-T_2}{\tau_\infty u_\infty}\right] = -\left\{u_1 T_{v1\xi} + v_1 B_f(T_{v1\eta}-T_{v1\xi})\right\} = -\Lambda(\xi,\eta) \quad 2.5(11)$$

and

$$\left[p_{2\xi} - T_{2\xi} + u_{2\xi} + B_{f\infty}(v_{2\eta}-v_{2\xi})\right] = -\left\{(u_1-T_1)p_{1\xi} + B_f v_1(p_{1\eta}-p_{1\xi})\right.$$

$$\left. -\left((p_1-2T_1+u_1)T_{1\xi} + B_f v_1(T_{1\eta}-T_{1\xi})\right) + \left(p_1 u_{1\xi} + B_{f\infty}p_1(v_{1\eta}-v_{2\xi})\right)\right\} = -\vartheta(\xi,\eta) \quad 2.5(13)$$

The above set of equations for u_{i2} are linear with terms on the right hand side φ, ψ, Ω, Λ, ϑ which are functions of the first order solution only. The second order perturbation components may be

eliminated in favour of the pressure perturbation to give

$$-\left(\Gamma_\infty \frac{\partial}{\partial \xi}+1\right)\left\{\frac{\partial^2 p_2}{\partial \eta^2}-2\frac{\partial^2 p_2}{\partial \xi \partial \eta}\right\}+(B^2-1)\frac{\partial^2 p_2}{\partial \xi^2}=\frac{1}{B_{f_\infty}^2}\left\{\left(\Gamma_\infty \frac{\partial}{\partial \xi}+1\right)\left(\varphi_\xi - M_{f_\infty}^2 \Omega_\xi\right)\right. \qquad 2.5(14)$$

$$\left.+\left(\Gamma_\infty \frac{\partial}{\partial \xi}+1\right)\left(\psi_\eta-\psi_\xi\right)B_{f_\infty}+\frac{\omega_1}{c_{p_e}}M_{f_\infty}^2\Omega_\xi-\gamma_{f_\infty}M_{f_\infty}^2\frac{\omega_1}{c_{p_e}}\vartheta_\xi+\frac{\omega_1}{\omega_f}M_{f_\infty}^2\Lambda_{\xi\xi\xi}\right\}=\frac{F(\xi,\eta)}{B_{f_\infty}^2}$$

where $\Gamma_\infty = u_\infty \tau_\infty c_{p_f}/c_{p_e}$ and $F(\xi,\eta)$ represents the terms in the curly brackets.

Before continuing with the general solution of equation 2.5(14) it is of interest to examine the vorticity and entropy production terms.

2.5:2 Vorticity Production

The vorticity $\zeta(\xi,\eta)$ is defined as

$$\zeta(\xi,\eta)=\frac{\partial v}{\partial \xi}-B_{f_\infty}\left(\frac{\partial u}{\partial \eta}-\frac{\partial u}{\partial \xi}\right) \qquad 2.5(15)$$

and from the generalisation of Croccos theorem (cf Clarke-McChesney (1964)) to include flows with relaxing or reacting modes, it follows that ζ is only zero when the flow is completely frozen or when it is in equilibrium. Substituting the series 2.5(1) into 2.5(15) it is readily shown that the vorticity to first order is zero and hence a velocity potential may be defined. However to second order this is no longer true and on collecting together terms of order θ^2 and using equations 2.5(7) and 2.5(8) it is found that the second order vorticity is given by

$$\zeta_2(\xi,\eta)=\int_0^\xi \left\{B_{f_\infty}(\varphi_\eta-\varphi_\xi)-\psi_\xi\right\} d\xi \qquad 2.5(16)$$

Thus in the second order system a velocity potential cannot be defined. Equation 2.5(16) also shows that the vorticity is simply a function of first order products and can thus be evaluated directly. Inspection of the definitions of φ and ψ show that along the wall the vorticity is zero at the corner and will steadily decrease to some new constant value far downstream. In the far field away from the corner φ , ψ and their derivatives become very small. At infinity $\varphi \longrightarrow \varphi_e$ and $\psi \longrightarrow \psi_e$, their equilibrium values, which can be shown to be zero, and hence the vorticity becomes zero. The variation of vorticity along the wall has been evaluated (Appendix D) for a specific example of Carbon dioxide discussed in more detail in Section 2.5:9 and is presented in figure 2.5(3). It may be shown that $\xi_2 \sim O(B^2-1)^2$, where $B^2 = \frac{M_e^2-1}{M_f^2-1}$, and since for many flows $B^2 \sim 1$ this suggests, that if (B^2-1) is chosen to be of order θ then to second order a velocity potential could be defined.

2.5:3 Entropy Production

For only one relaxing mode the entropy production along a streamline, equation 2.1(10) reduces to

$$\frac{Ds}{Dt} = c_1 \frac{(T - Tv)}{T\,Tv} \cdot \frac{DTv}{Dt} \qquad 2.5(17)$$

To first order this is zero but collecting terms of order θ shows that the entropy production is given by

$$S_\infty \frac{\partial s}{\partial \xi} = \omega_1 \frac{C_{pf}}{C_{pe}} (T_1 - Tv_1)^2 \qquad 2.5(18)$$

where S_∞ is the entropy in the undisturbed state ahead of the corner.

Once again the right hand side is a function only of first order products and may quickly be evaluated. The evaluation is carried out in appendix (E) and is presented in figure 2.5(2). Since $(T_1 - Tv_1)$ is finite at the corner and tends to zero as $\xi \longrightarrow \infty$ the entropy perturbation, which is equal to the integral of $\frac{\omega_1}{C_{pe}} \omega_f (T_1 - Tv_1)^2$ varies from zero at the corner to some new constant value along

way downstream on the wall. Far away from the corner T_t and T_v approach their equilibrium values therefore $T_{t\,e} \simeq T_{v\,e}$ and thus the entropy is zero. Therefore like the vorticity, a long way downstream an entropy layer exists going from a constant value at the wall to zero at infinity.

2.5:4 General solution of the second order equation

The flow is rotational and therefore a velocity potential cannot be defined and some other dependent variable must be chosen. In this case the pressure perturbation was chosen for, in the particular case of the expansion, (as seen in section 2.3), of all the dependent variables the pressure is the one that will tend to the infinite rate equilibrium value, downstream of the corner. Thus if the expansion procedure is valid the solution of 2.5(14) should show that p_2 approaches p_{2e} as $\xi \to \infty$.

The basic task therefore is to solve

$$-\left(\frac{\partial}{\partial\xi} + 4\left\{\frac{\partial^2 p_2}{\partial\eta^2} - \frac{\partial^2 p_2}{\partial\xi\partial\eta}\right\} + (B^2-1)\frac{\partial^2 p_2}{\partial\xi^2} = \frac{F(\xi,\eta)}{B_e^2}\right. \qquad 2.5(19)$$

subject to some appropriate boundary conditions. ξ, η have now been made non-dimensional with Γ_∞. In this instance equation 2.5(19) is tackled by Laplace transform techniques.

Define the Laplace transform of any independent variable as u_{i2}

$$\bar{u}_{i_2}(z,\eta) = \int_0^\infty u_{i_2}(\xi,\eta)\exp -z\xi \, d\xi \qquad 2.5(20)$$

and its inverse as

$$u_{i_2}(\xi,\eta) = \frac{1}{2\pi i}\int_{c-i\infty}^{c+i\infty} \bar{u}_{i_2}(z,\eta)\exp z\xi \, dz \, .$$

Operating on both sides of equation (2.5(19)) and performing the infinite integrals shows that the transform of the pressure perturbation is governed by

$$\frac{d^2\bar{p}_2}{d\eta^2} - 2z\frac{d\bar{p}_2}{d\eta} - (B^2-1)\frac{z^2}{1+z}\bar{p}_2 = -\frac{\overline{F(z,\eta)}}{B_c^2(1+z)} \qquad 2.5(21)$$

where $\bar{F}(z,\eta)$ is the transform of $F(\xi,\eta)$.

By the method of Variation of Parameters a general solution of equation 2.5(21) is

$$\bar{p}_2 = -\frac{1}{C}\left\{\int_A^\eta \frac{\overline{F(z,\eta)}}{B_c^2(1+z)} f_1(u)\exp-\int^u 2z\,dt\,du\right\} f_2(\eta)$$

$$+\frac{1}{C}\left\{\int_B^\eta \frac{\overline{F(z,u)}}{B_c^2(1+z)} f_2(u)\exp-\int^u 2z\,dt\,du\right\} f_1(\eta) \qquad 2.5(22)$$

where C is given by

$$f_1\frac{\partial f_2}{\partial\eta} - f_2\frac{\partial f_1}{\partial\eta} = C\exp\int^\eta 2z\,dt \qquad 2.5(23)$$

and f_1 and f_2 are two particular solutions of the homogeneous equation given by

$$f_1 = \exp(z-a)\eta \text{ and } f_2 = \exp(z+a)\eta$$

where for convenience a is defined as

$$a = z\sqrt{\frac{B^2+z}{1+z}} \quad . \qquad 2.5(24)$$

The undetermined constants have to be determined from the boundary conditions. For an outgoing wave system it is necessary to put $B = \infty$.

To determine A the boundary condition along the wall must be imposed.

Along the wall given by

$y_{wall} = T(x)$ (say), there holds the following condition

$$\left(\frac{dy}{dx}\right)_{wall} = \frac{(x, y_{wall})}{(x, y_{wall})} .$$

Letting $V = V_1 (x\ y_{wall})\ \theta + V_2 (x\ y_{wall})\ \theta^2$
and $u = 1 + u_1(x, y_{wall})\ \theta + u_2(x, y_{wall})\ \theta^2$ and substituting for y_{wall} and expanding in powers of θ gives

$$v_1(x,0)\,\delta + T(x)\,\delta^2 \frac{\partial v_1}{\partial y}(x,0) + \delta^2 v_2(x,0) \simeq \delta T'(x) + \delta^2 T'(x)\, u_1(x,0)$$

Collecting terms of order θ gives

$$V_1 (x, 0) = T'(x)$$

which is the familiar linearised boundary condition. Collecting terms of order θ^2 gives

$$v_2(x,0) = T'(x)\, u_1(x,0) - T(x) \frac{\partial v_1}{\partial y}(x,0) \qquad 2.5(25)$$

Both these boundary conditions are imposed along $y = 0$. The following analysis is primarily concerned with the solution for $T(x) = x$ but it may be extended to fairly general values of $T(x)$.

The connection between V_2 and p_2 arises through the momentum equation 2.5(8) and therefore along $\eta = 0$ equation 2.5(22) must be solved subject to

$$B_{\infty} \left(\frac{\partial \bar{p}_2}{\partial \eta}(z,0) - z\, \bar{p}_2(z,0) \right) + \gamma_{\infty} M_{\infty}^2 z\, \bar{v}_2(z,0) = -\bar{\psi}(z,0) \qquad 2.5(26)$$

Substituting equation 2.5(22) for p_2 into the above b.c gives an equation for A. Substituting for A and B shows that

$$\bar{p}_2(z,\eta) = \frac{1}{2a}\int_0^{\infty} \frac{\bar{F}(z,\eta_0)}{B_{\epsilon_\infty}^2(1+z)} \exp\left\{-(z+a)\eta_0+(z-a)\eta\right\} d\eta_0$$

$$+ \frac{1}{2a}\int_{\eta}^{\infty} \frac{\bar{F}(z,\eta_0)}{B_{\epsilon_\infty}^2(1+z)} \exp\left\{-(z+a)(\eta_0-\eta)\right\} d\eta_0$$

$$+ \frac{1}{2a}\int_0^{\eta} \frac{F(z,\eta_0)}{B_{\epsilon_\infty}^2(1+z)} \exp\left\{-(z-a)(\eta_0-\eta)\right\} d\eta_0$$

$$+ \frac{\gamma_{\epsilon_\infty} M_{\epsilon_\infty}^2}{B_{\epsilon_\infty}}\left\{\frac{z}{a}\bar{V}_2(z,0)+\frac{1}{a}\bar{\Psi}(z,0)\right\}\exp(z-a)\eta \qquad 2.5(27)$$

It is now possible to invert formally the above equation provided the inversion is accomplished before the η_0 integration. This can be done if the integrands are well behaved.

By definition

$$F(\xi,\eta) = \frac{1}{2\pi i}\int_{c-i\infty}^{c+i\infty} \bar{F}(z,\eta_0)\exp\xi z\, dz \qquad 2.5(28$$

In addition define

$$H(\xi,\eta) = \frac{1}{2\pi i}\int_{c-i\infty}^{c+i\infty} \frac{\exp\left(-(z+a)\eta_0+(z-a)\eta\right)}{2a(1+z)}\exp\xi z\, dz \qquad 2.5(29)$$

$$G(\xi,\eta) = \frac{1}{2\pi i}\int_{c-i\infty}^{c+i\infty} \frac{\exp -(z+a)(\eta_0-\eta)}{2a(1+z)}\exp\xi z\, dz \qquad 2.5(30)$$

and

$$I(\xi,\eta) = \frac{1}{2\pi i}\int_{c-i\infty}^{c+i\infty} \frac{\exp -(z-a)(\eta_0-\eta)}{2a(1+z)}\exp\xi z\, dz \qquad 2.5(31)$$

where $\sigma > 0$.

Although the general inversion of H, G, I is not simple for general η it will be noted that for the integrals in equations 2.5(29 - 31) to exist the following conditions must be satisfied for

equation (2.5(29) $\quad \xi - 2\eta_0 > 0 \qquad \eta_0 > 0$ 2.5(32)

(2.5(30) $\quad \xi - 2(\eta_0 - \eta) > 0 \qquad \eta_0 > \eta$ 2.5(33)

(2.5(31) $\quad \xi > 0 \qquad \eta_0 < \eta$ 2.5(34)

With the above definitions it is possible to invert equation 2.5(27). Making use of the convolution theorem the second order pressure perturbation is

$$\frac{p}{p_2}(\xi,\eta) = \int_0^{\frac{\xi}{2}} \int_0^{\xi-2\eta_0} \frac{F(\xi_0,\eta_0)}{B_{f_\infty}^2} H(\xi-\xi_0;\eta_0;\eta)\, d\xi_0 d\eta_0$$

$$+ \int_\eta^{\frac{\xi}{2}+\eta} \int_0^{\xi-2(\eta_0-\eta)} \frac{F(\xi_0,\eta_0)}{B_{f_\infty}^2} G(\xi-\xi_0;\eta_0;\eta)\, d\xi_0 d\eta_0$$

$$+ \int_0^{\eta} \int_0^{\xi} \frac{F(\xi_0,\eta_0)}{B_{f_\infty}^2} I(\xi-\xi_0;\eta_0;\eta)\, d\xi_0 d\eta_0$$

$$+ \frac{\gamma_{f_\infty} M_{f_\infty}^2}{B_{f_\infty}} \int_0^{\xi} \psi(\xi_0,0)\, J(\xi-\xi_0,\eta)\, d\xi_0$$

$$+ \frac{\gamma_f M_f^2}{B_{f_\infty}} \int_0^{\xi} V_2(\xi_0,0)\, K(\xi-\xi_0,\eta)\, d\xi_0 \qquad 2.5(35)$$

where $$J(\xi,\eta) = \frac{1}{2\pi i} \int_{c-i\infty}^{c+i\infty} \frac{\pi}{a} \exp\{(z-a)\eta + \xi z\}\, dz \qquad 2.5(36)$$

$$K(\xi,\eta) = \frac{1}{2\pi i}\int_{c-i\infty}^{c+i\infty} \exp\{(z-a)\eta + \xi z\}\,dz \qquad 2.5(37)$$

In the above equation the limits of the ξ_0 and η_0 integration have arisen from the restrictions given in equations 2.5(32) to 2.5(34).

The domains of integration are shown in figure 2.5(1) and in conformity with a hyperbolic equation it is seen that the point ξ,η is only influenced by points bounded by the linearised characteristics DE and BF, the leading characteristic and the bounding wall. For any given position of ξ there is a constant contribution, given by the first integration over ABC, to the pressure no matter what the value of η. The second and third integrals give the contributions for $\eta_0 > \eta$ and $\eta_0 < \eta$, the last two integrals arising from the boundary conditions.

In principle the problem is now solved for any field point (ξ,η) provided the first order solution is available. However the first order solution is itself algebraically complex, ref. Morrison (1956) and since the evaluation of G, H, I, J, K are equally complex the integrations must be performed numerically. This would probably be more cumbersome than the solution by the method of characteristics. It is therefore difficult to argue that a numerical solution is justifiable.

Because of the above difficulties an approximate solution is desirable. Three possibilities present themselves, (i) Find an approximation to F, G, H in the physical plane and perform the integrations. For example one could attempt to use the approximate analysis of Moore and Gibson (1960) to obtain F, G, H over the whole field. (ii) Seek a formal series expansion in (B^2-1) in the physical plane in a similar manner to that attempted by Napolitano (1961) for the first order problem. (iii) To revert back to the transform plane and make the approximation in that plane.

It is proposed to tackle the problem by method (iii) but before attempting the full non-equilibrium second order solution the two limits of $\Gamma_\infty \to 0$ and $\Gamma_\infty \to \infty$ are interesting in themselves.

2.5:5 The Second Order Solution for Frozen Flow: $\Gamma_\infty = \infty$

When $\Gamma_\infty = \infty$ the governing second order equation 2.5(14) becomes for frozen flow

$$-\frac{\partial}{\partial \xi}\left[\frac{\partial^2 p_2}{\partial \eta'^2} - 2\,\frac{\partial^2 p_2}{\partial \xi \partial \eta'}\right] = \frac{1}{B_{f\infty}^2}\frac{\partial}{\partial \xi'}\left[\varphi'_{\xi'} + B_{f\infty}(\psi'_{\eta'} - \psi'_{\xi'}) - M_{f\infty}^2\,\Omega'_{\xi'}\right] \qquad 2.5(38)$$

where the primes on the independent variables signify that they have not been made non-dimensional. φ' and ψ' are defined as in equations 2.5(7) and 2.5(8) but now $\Omega' = u_1 p_{1\xi'} + B_f v_1 (p_{1\eta'} - p_{1\xi'}) + \gamma_{f\infty}\left[p_1 u_{1\xi'} + B_{f\infty}(u_{1\eta'} - u_{1\xi'})\rho_1\right]$
A first integral of 2.5(38) with respect to ξ may be obtained and the constant which is a function of η must be zero since the free stream is specified to be uniform.

Taking the Laplace transform equation 2.5(38) becomes

$$\frac{d^2\bar{p}_2}{d\eta'^2} - 2z\,\frac{d\bar{p}_2}{d\eta'} = -\frac{1}{B_{f\infty}}\left[z\bar{\varphi}' + B_{f\infty}(\bar{\psi}_{\eta'} - \bar{\psi}_{\xi'}) - M_{f\infty}^2 z\,\bar{\Omega}'\right] = -\frac{\bar{F}(z,\eta)}{B_{f\infty}^2} \qquad 2.5(39)$$

where the bar signifies that it is a transformed quantity.

To be specific equation 2.5(39) is solved subject to the second order boundary condition which for a sharp cornered expansion reduces to $B_{f\infty}\left(\frac{d\bar{p}_2}{d\eta'}(z,0) - z\,\bar{p}_2(z,0)\right) + \gamma_{f\infty} M_{f\infty}^2\,\bar{u}_1 = -\bar{\psi}(z,0)$
in the transform plane.

For the case of a sharp corner the first order quantities are $u_1 = -1/B_{f\infty}$, $p_1 = \gamma_{f\infty} M_{f\infty}^2 / B_{f\infty}$ and $\rho_1 = M_{f\infty}^2/B_{f\infty}$. $\bar{F}(z,\eta)$ may be evaluated by means of the complex convolution theorem.* It can then be shown that $\bar{\varphi}' = \bar{\psi}' = 0$ and that the only contribution to $\bar{F}$ arises through $\bar{\Omega}'$. For this example

$$M_{f\infty}\,\bar{\Omega}' = -\frac{(\gamma_{f\infty}+1)\,M_{f\infty}^2}{2B_{f\infty}^2} \qquad 2.5(40)$$

* If $P(z)$ is the transform of $p(\xi)$ and $Q(z)$ is the transform of $q(\xi)$ then the transform of $p(\xi)q(\xi) = \frac{1}{2\pi i}\int_{d-i\infty}^{d+i\infty} P(q)Q(z-q)\,dq$ with $R_e(z-q) > 0$ and $d > 0$. Also see Appendix (A) where the convolution theorem has been used to evaluate φ, ψ etc.

Recalling that the general solution is given by inverting equation 2.5(27) and noting the limits on the η integration

$$\frac{p_2(\xi',\eta')}{\gamma_{f_\infty} M_{f_\infty}^2} = \frac{(\gamma_f+1)M_{f_\infty}^4}{4B_{f_\infty}^4}\left\{\int_0^{\frac{\xi'}{2}}\frac{1}{2\pi i}\int_{c-i\infty}^{c+i\infty} \exp\{-2z\eta_0'+\xi' z\}\,dz\,d\eta_0'\right.$$

$$+\int_{\eta'}^{\eta'+\frac{\xi'}{2}}\frac{1}{2\pi i}\int_{c-i\infty}^{c+i\infty}\exp\{-2z(\eta_0'-\eta')+\xi' z\}\,dz\,d\eta_0'$$

$$\left.+\int_0^{\eta'}\frac{1}{2\pi i}\int_{c-i\infty}^{c+i\infty}\exp \xi' z\,dz\right\}$$

$$-\frac{1}{2\pi i}\int_{c-i\infty}^{c+i\infty}\frac{1}{z\,B_f^2}\exp \xi' z\,dz \qquad 2.5(41)$$

Performing the integrations shows that

$$\frac{p_2(\xi',\eta')}{\gamma_f M_f^2} = \frac{(\gamma_f+1)M_f^4}{4B_{f_\infty}^4} - \frac{1}{B_f^2} \qquad 2.5(42)$$

(In equation 2.5(41) the third integral vanishes because Laplace transform theory shows that $\int_{c-i\infty}^{c+i\infty}\exp \xi' z\,dz = \delta(0^-)$ which is outside the range of interest).

Equation 2.5(42) is the Busemann solution and agrees with the results obtained by Van Dyke (1951) who discovered particular integrals of the second order equation.

For the case of a parabolic wall the second order pressure perburbation is

$$\frac{p_2}{\gamma_f M_f^2} = \left[\frac{(\gamma_f+1)M_f^4}{4B_f^4} - \frac{1}{B_f^2}\right]\xi' + \frac{(\gamma_f+1)M_f^4}{2B_f^4}\xi'\eta' + \frac{\xi'^2}{2} \qquad 2.5(43)$$

which again agrees with Van Dyke.

The solution for the parabolic wall reveals the non-uniformities in η which exist in the isentropic case. Thus it may be anticipated that the non-equilibrium case could have a similar non-uniformity. Whether a further one exists with respect to ξ remains an open question at this stage.

2.5:6 The Second Order Solution for Equilibrium Flow, $\Gamma_\infty = 0$

In the case where the relaxation process is occurring infinitely quickly the second order equation reduces to

$$-\left(\frac{\partial^2 p_{2e}}{\partial \eta'^2} - 2\frac{\partial^2 p_{2e}}{\partial \eta' \partial \xi'}\right) = \varphi_{e\xi'} + B_e\left(\psi_{e\eta'} - \psi_{e\xi'}\right) - M_e^2 \Omega_{e\xi'} \qquad 2.5(44)$$

The subscripts e indicate that the terms are evaluated under equilibrium conditions. The primes on the independent variables now indicate that the co-ordinate system is based on the equilibrium characteristics, thus $\eta' = B_{e\infty} y$ and $\xi' = x - B_{e\infty} y$.

As pointed out by Boa - Teh - Chu and discussed in section 2.4, one of the singular features of non-equilibrium flow is the way in which the characteristics change discontinuously as the limit $\Gamma_\infty \to 0$ is taken.

When $\Gamma_\infty = 0$

$$\varphi_e = (\rho_{e_1} + u_{e_1})u_{e_1\xi'} + B_{e\infty} v_{e_1}(u_{e_1\eta'} - u_{e_1\xi'}) \qquad 2.5(45$$

$$\psi_e = (\rho_{e_1} + u_{e_1})v_{e_1\xi'} + B_{e\infty} v_{e_1}(v_{e_1\eta'} - v_{e_1\xi'}) \qquad 2.5(46)$$

$$\text{and } \Omega_e = \left[u_{e_1} p_{e_1\xi'} + B_{e\infty} v_{e_1}(p_{e_1\eta'} - p_{e_1\xi'}) + \gamma_e p_{e_1\xi'} u_{e_1\xi'} + \gamma_e p_{e_1} B_{e\infty}(v_{e_1\eta'} - v_{e_1\xi'})\right] \qquad 2.5(47)$$

and ϑ, Λ are zero.

In cases where the specific heat is considered as a function of temperature $c_{v_1} \neq$ constant then Ω_e will have extra terms in it which represent the variation of γ_e through the expansion. However for the rather simplified gas considered here it will be noticed that the form of the frozen and equilibrium equations are identical and thus the equilibrium pressure to second order is

$$\frac{P_{2e}(\xi',\eta')}{\gamma_e M_e^2} = \left[\frac{(1+\gamma_e)}{4 B_e^4} - \frac{1}{B_e^2}\right] \qquad 2.5(48)$$

Equations 2.5(42) and 2.5(48) show that the second order solutions for the two limits are consistent with results obtained by other techniques for isentropic flow.

2.5:7 The Non-Equilibrium Case, $0 < \Gamma_\infty < \infty$

For finite Γ_∞ the corner problem has no absolute length associated with it and it is thus convenient to work in ξ, η co-ordinates. As pointed out earlier inspection of the general solution immediately suggests that a simple closed form solution is unlikely to be discovered due to the intrinsic difficulties associated with the first order solution. Therefore an approximate solution is sought which if it is to be general for any field point, implies that some extra small parameter exists. The parameter which presents itself is $(B^2 - 1)$ and has been used previously by Moore and Gibson (1960) and Napolitano (1961) to obtain approximate solutions for the first order problem. In the following analysis it is assumed that the transform $\bar{F}(\xi,\eta)$ of the right hand side of equation 2.5(21) may be written as a series expansion in $(B^2 - 1)$ in the following form.

$$\bar{F}(z,\eta) = \sum_{r=0}^{n} \bar{F}_r(z,\eta)(B^2-1)^r \qquad 2.5(49)$$

where $\bar{F}_r(z,\eta)$ is assumed to be of order unity. No justification for this expansion appears possible and it can only be hoped that the series is convergent for some suitably small value of (B^2-1). For example one may always take (B^2-1) to be of order θ. A further query also arises whether it is correct to make the approximation to F but not to the left hand side of equation 2.5(19). Collecting

terms of order (B^2-1) from both sides of equation 2.5(19) is equivalent to the series expansion developed by Napolitano who showed that terms up to $(B^2-1)^4$ are needed. For the second order problem this leads to an excessive amount of algebra and thus the approximations are made only to the right hand side. A further point of interest is the technique suggested by Moore and Gibson (1960). Their approach was to make the transformation $\bar{\xi} = CB^2(\xi')$ and $\bar{\eta} = (B^2-1)\,B^2\eta'$ which transforms the first order equation 2.5(6) into

$$p_{\bar{\xi}\bar{\eta}} + p_{\bar{\xi}} + p_{\bar{\eta}} = 0 \qquad 2.5(50)$$

which is the telegraph equation and which has been obtained by judicious choice of the constant C. This equation is correct to order (B^2-1) and gives a very good approximation over the whole field. However to second order the technique is complicated by the right hand side and now the governing equation is

$$\left(\frac{\partial}{\partial\bar{\xi}} - \frac{\varepsilon}{2C}\frac{\partial}{\partial\eta}\right)\left(p_{2\bar{\xi}\bar{\eta}} + p_{2\bar{\xi}} + p_{2\bar{\eta}}\right) + O(B^2-1)^2 = \frac{F(\bar{\xi},\bar{\eta})}{2C^2B^6}\,B^2(B^2-1) \qquad 2.5(51)$$

where C has been chosen as $1 - \frac{3}{2}$ (B). With F = 0 and letting $p_2 = p_2^0 + p_2^1(B^2-1))$ etc. exactly the same equation as Moore and Gibson is recovered, but with F finite this technique renders the right hand side of $O(\frac{1}{B^2-1})$ which is large for sufficiently small (B^2-1). Thus the technique suggested for solving the first order problem breaks down in the second order case. This probably arises because the third order equation has been described by a second order one.

Inspection of $\overline{F_1}$ in equation 2.5(49) reveals that in the expansion procedure suggested here that the solution is unlikely to be uniformly valid in z and η. Generally $\bar{F}(z,\eta)$ consists of products first order quantities $p_i(\xi,\eta)\, q_i(\xi,\eta)^*$ (say). The transforms

---

* p and q are terms like u_1 p_1, $u_{1\bar{\xi}}$, $p_{1\xi}$, $u_{1\bar{\eta}}$, $p_{1\eta}$ etc. occurring in equation 2.5(14) and 2.5(17) to 2.5( ). Also see Appendix (A).

of p_i and q_i are of the form $P_i(z)\exp\left(z - z\sqrt{\frac{B^2+z}{1+z}}\right)\eta$ and $Q_i(z)\exp\left(z - z\sqrt{\frac{B^2+z}{1+z}}\right)\eta$ therefore by using the convolution theorem $\bar{F}(z,\eta)$ may be written

$$\bar{F}(z,\eta) = \frac{1}{2\pi i}\int_{d-i\infty}^{d+i\infty}\sum_i g_i(z)P_i(q)Q_i(z-q)\exp\left\{q - q\sqrt{\frac{B^2+q}{1+q}} + z - q\right\}^{\left\{(z-q)\sqrt{\frac{B^2+z-q}{1+z-q}}\right\}}dq \qquad 2.5(52)$$

where $g_i(z)$ have been obtained by taking the transform of $F(\xi,\eta)$. The sum of over i formally indicates all the possible product terms that can occur in F.

It is now necessary to expand Pi, Qi and the exponential term in (B^2-1). Thus $\bar{F}r(z,\eta)$ are specific to the problem under consideration. Because of the essential singularity at z = -1, it is also necessary to expand the exponential terms of (B^2-1) as well, Then the components $\bar{F}r(z,\eta)$ of F contain only powers of order η^r and thus the approximation to F will be valid only close to the wall. Due to the integration over η, the extent of the region covered by this expansion procedure will depend on the number of terms considered in the expansion and will thus only be valid near to the corner.

To simplify the problem further the analysis is restricted to looking at the behaviour of the perturbation terms near the wall $\eta = 0$.

2.5:9 Non-Equilibrium solution for $\eta = 0$, $0 < \xi_\infty < \infty$.

For $\eta = 0$

$$p(\xi,0) = 2\int_0^{\frac{\xi}{2}}\frac{1}{2\pi i}\int_{c-i\infty}^{c+i\infty}\frac{1}{2B_\infty^2 z(1+z)}\sqrt{\frac{1+z}{B^2+z}}\left\{\sum_{r=0}^{n}\bar{F}_r(z,\eta)(B^2-1)^r\exp\left\{-\left(z+z\sqrt{\frac{B^2+z}{1+z}}\right)\eta_0+\xi z\right\}\right.$$
$$\left. dz\,d\eta_0\right.$$
$$+\frac{\gamma_\infty M_\infty^2}{B_\infty}\frac{1}{2\pi i}\int_{c-i\infty}^{c+i\infty}\left\{\frac{\bar{\psi}(z,0)}{a}+\bar{V}_2(z,0)\frac{z}{a}\right\}\exp\xi z\,dz \qquad 2.5(53$$

which to order (B^2-1) can be written as

$$p_2(\xi,0) \simeq 2\int_0^{\xi/2}\frac{1}{2\pi i}\int_{c-i\infty}^{c+i\infty}\left[\bar{F}_0(z,\eta_0)+\left\{\bar{F}_1(z,\eta_0)-\frac{\bar{F}_0(z,\eta_0)}{2(1+z)}-\frac{\bar{F}_0(z,\eta_0)}{2(1+z)}z\eta_0\right\}(B^2-1)+\cdots\right]$$

$$\times\frac{\exp -2z\eta_0+\xi z}{2B_f^2\, z(1+z)}\,dz\,d\eta_0$$

$$+\frac{\gamma_{f_\infty}M_{f_\infty}^2}{B_{f_\infty}^2}\frac{1}{2\pi i}\int_{c-i\infty}^{c+i\infty}\left[\bar{\psi}_0(z,0)+\left\{\bar{\psi}_1(z,0)-\frac{\bar{\psi}_0(z,0)}{2(z+1)}\right\}(B^2-1)+\cdots\right]\frac{\exp\xi z}{z}\,dz$$

$$+\frac{\gamma_{f_\infty}M_{f_\infty}^2}{B_{f_\infty}}\frac{1}{2\pi i}\int_{c-i\infty}^{c+i\infty}\left[\bar{V}_2(z,0)+\left\{\bar{V}_{2_1}(z,0)-\frac{\bar{V}_{2_0}(z,0)}{2(1+z)}\right\}(B^2-1)+\cdots\right]\frac{\exp\xi z}{z}\,dz \qquad 2.5(54)$$

Substituting for $\bar{F}o$, $\bar{F}$ etc and performing the integration (see Appendix (A) for more details) the pressure perturbation to order (B^2-1) becomes after some considerable manipulation

$$\frac{p_2(\xi,0)}{\gamma_{f_\infty}M_{f_\infty}^2}=\frac{(1+\gamma_{f_\infty})M_{f_\infty}^4}{4B_{f_\infty}^4}-\frac{1}{B_{f_\infty}^2}+\frac{c_{v_1}(\gamma_f-1)M_f^4}{c_{p_e}4B_{f_\infty}^4}(1-\exp-\xi)$$

$$+\left[\left\{\frac{32M_{f_\infty}^2-17M_{f_\infty}^4-\gamma_{f_\infty}M_{f_\infty}^4-5\gamma_fM_f^2-24}{16B_{f_\infty}^4}\right\}(1-\exp-\xi)\right.$$

$$+\left\{\frac{M_f^2}{2B_f^2}-\frac{3(\gamma_f-1)M_f^4c_{v_1}}{16B_f^4\,c_{p_e}}\right\}(1-(1+\xi)\exp-\xi)$$

$$\left.+\frac{\xi}{2}\exp-\xi\right](B^2-1)+O(B^2-1)^2 \qquad 2.5(55)$$

The inelegant form of 2.5(55) immediately suggests that higher order terms in (B^2-1) will be increasingly tedious to obtain.

Inspection of equation 2.5(55) shows that at $\xi = 0$ the flow is frozen and equals the Busemann approximation corresponding to equation 2.5(42), i.e.

$$\frac{p_2(0,0)}{\gamma_{f\infty} M_{f\infty}^2} = \frac{(1+\gamma_{f\infty}) M_{f\infty}^4}{4 B_{f\infty}^4} - \frac{1}{B_{f\infty}^2} \qquad 2.5(56)$$

It may also be noted that if the neglect of (B^2-1) can be tolerated then the second order non-equilibrium solution still retains some simplicity, i.e.

$$\frac{p_2(\xi,0)}{\gamma_{f\infty} M_{f\infty}^2} = \frac{(1+\gamma_f) M_{f\infty}^4}{4 B_{f\infty}^4} - \frac{1}{B_{f\infty}^2} + \frac{c_{v_1}(\gamma_f - 1) M_f^4}{c_{p_e} 4 B_f^4} \left(1 - \exp -\xi\right) \qquad 2.5(57)$$

To discuss the solution further a specific example must be considered since it is difficult to assess the relative values of the terms as they stand. The vibrating gas is chosen as Carbon Dioxide and the conditions taken are those that could be obtained behind the primary shock in a shock tube. For a shock Mach Number of 3, $T_\infty \sim 600^\circ K$, $\gamma_{e\infty} \sim 1.24$, $M_e \sim 1.6$, $M_f = 1.51$, $c_{v_1} = 1.62R$. c_{v_1} has been chosen as the specific heat of the bending mode of CO_2 and it has been assumed that the other modes have a negligible effect. For this example $(B^2-1) = 0.23$ which will provide a fairly severe test of the validity of the expansion in (B^2-1).

Recalling that*

$$\frac{p}{p_\infty} = 1 + p_1 \theta + p_2 \theta^2 + \cdots$$

the total pressure variation along the wall for a 10° expansion for the above conditions is plotted in figure 2.5(4). As can be

---

* Where $\frac{p_1(\xi,0)}{\gamma_{f\infty} M_{f\infty}^2} = \exp -\left(\frac{B^2+1}{2}\right)\xi \, I_0\left[\frac{B^2-1}{2}\right]\xi + \int_0^\xi \exp -\left(\frac{B^2+1}{2}\right)\xi \, I_1\left[\frac{B^2-1}{2}\right]\xi \, d\xi.$

seen the asymptotic value tends very closely to the equilibrium value, and in the light of the results obtained in section 2.5(9), which show that the exact asymptotic value equals the infinite rate equilibrium value, it suggests that even to order (B^2-1) the expansion procedure for p_2 is satisfactory. The inclusion of higher order terms of (B^2-1) would not change this value appreciably since the neglected terms will probably be less than $(B^2-1)\ \theta^2$ which for the present example is 0.002.

It will be noted however that the approximation given by equation 2.5(57) is not satisfactory, see figure 2.5(4), away from the corner and the inclusion of the (B^2-1) term is necessary. However if (B^2-1) was smaller, equation 2.5(57) may still yield a satisfactory improvement.

A further check on the validity and accuracy of the expansion procedure can be made by comparing the 'exact' gradient of the flow variables with respect to ξ at the corner, with the approximate gradient. It can be show, see Appendix (B) for more details, that the exact pressure gradient at the corner is given by

$$\frac{1}{\gamma_f M_f^2}\frac{\partial p_2}{\partial \xi}(\xi=0,\eta=0) = \frac{(B^2-1)}{4}\left(\frac{1}{B_f^2}-1\right) - \frac{(B^2-1)M_f^2}{8B_f^4}\left\{2+4\gamma_f+M_f^2-\gamma_f M_f^2\right\}$$

$$+\frac{(\gamma_f-1)M_f^4}{4B_f^4}\frac{c_{v_1}}{c_{p_e}} - \frac{c_{v_1}(B^2-1)}{c_{p_e}2B_f^2}\left\{2M_f^2-\gamma_f M_f^2-1\right\}$$

$$-\frac{(B^2-1)M_f^2}{2B_f^2} + \frac{(B^2-1)}{B_f^2}$$

This can be compared with the approximate gradient by taking the derivative of p_2 in equation 2.5(55). In figure 2.5(4) the slopes of the pressure at the corner for the exact second order solution and the approximate second order solutions given by equations 2.5(55) and 2.5(57) are plotted. Now whereas the asymptotic

pressure agreed with the infinite rate value to within $(B^2-1)^2\ \theta^2$ it can be seen that the gradients at the origin show considerable variation and implies that further terms in (B^2-1) are needed before the slope converges to the exact value. Choosing a smaller value of (B^2-1) will obviously improve the situation. It is also interest- to note that the rate at which the pressure recovers is less than the linearised solution and is thus in qualitative agreement with the numerical solutions. To the order of the approximation the second order theory does not show up an overshoot in the pressure.

Evaluation of the second order velocity perturbation along the wall is readily obtained. Since $q = \left\{(1+U_1\theta+U_2\theta^2+\ldots)^2+(V_1\theta+V_2\theta^2+\ldots)\right\}^{1/2}$ then $q_2 = U_2 + V_1^2/2$, thus by using the ξ wise momentum equation q_2 is

$$q_2 = -\frac{1}{\gamma_{f_\infty} M_{f_\infty}^2} p_2(\xi,0) - \int_0^\xi \varphi(\xi,0)\,d\xi + 1 \qquad 2.5(58)$$

which to order (B^2-1) is given by

$$q_2 \simeq -\frac{1}{\gamma_f M_f^2} p_2(\xi,0) - \left(\frac{B^2-1}{2}\right)\left(1-\exp-\xi\right) + O(B^2-1)^2 \qquad 2.5(59)$$

This is plotted in figure 2.5(5) and as can be seen a noticeable difference exists between the asymptotic value of 2.5(59) and the equilibrium value. Since equation 2.5(55) shows that $p_2 \to p_{2e}$ very closely, and in fact it can be shown (see section 2.5:9) that $p_2 = p_{2_e}$ exactly as $\xi \to \infty$, then q_2 will always be different by $\int_0^\xi \varphi(\xi,0)\,d\xi$. This is in qualitative agreement with the numerical solutions discussed in section (2.3), as can be seen from figure 2.3(2). To evaluate the density, use is made of the continuity equation which in the transform plane to second order is given by

$$\bar{p}_2 + \bar{u}_2 + B_{f_\infty}\left(\bar{v}_2\eta - \bar{v}_2\xi\right) = \bar{x} \qquad 2.5(60)$$

where $\bar{\chi}$ is the transform of $+\rho_1 u_{1\xi} + u_1 \rho_{1\xi} + B_f\{\rho_1(v_{1\eta} - v_{1\xi}) + v_1(\rho_{1\eta} - \rho_{1\xi})$
Eliminating $\bar{u}_2$ and $\bar{v}_2$ by the momentum equation gives

$$\bar{\rho}_2 = \frac{1}{\gamma_f M_f^2}\left\{ M_{f_\infty}^2 \bar{\rho}_2 + \frac{B_f^2}{z^2}\left(\rho_{2\eta\eta} - 2z\rho_{2\eta}\right) + \frac{\bar{\Phi}}{z} + \frac{B_f}{z^2}\left(\bar{\psi}_\eta - \bar{\psi}z\right) - \frac{\bar{\chi}}{z} \right. \qquad 2.5(61)$$

but $$\bar{\rho}_{2\eta\eta} - 2z\bar{\rho}_{2\eta} = \frac{(B^2-1)z^2}{1+z}\bar{\rho}_2 - \frac{\bar{F}(z,\eta)}{B_f^2(1+z)}$$

$$\therefore \bar{\rho}_2 = \frac{1}{\gamma_f M_f^2}\left\{\left(M_f^2 + \frac{B_f^2(B^2-1)}{(1+z)}\right)\bar{\rho}_2 - \frac{\bar{F}(z,\eta)}{B_f^2(1+z)} + \frac{\bar{\Phi}}{z} + \frac{B_f}{z^2}\left(\bar{\psi}_\eta - z\bar{\psi}\right)\right\} - \frac{\bar{\chi}}{z} \qquad 2.5(62)$$

Substituting for $\bar{F}(z,\eta)$ gives

$$\bar{\rho}_2 = \frac{1}{\gamma_f M_f^2}\left\{\left(M_f^2 + \frac{B_f^2(B^2-1)}{(1+z)}\right)\bar{\rho}_2 - \left(-M_f^2\frac{\bar{\Omega}}{z} + \frac{\omega_1 M_f^2 \bar{\Omega}}{c_{p_e} z(1+z)} - \gamma_f M_f^2 \frac{\omega_1 \bar{\vartheta}}{c_{p_e} z(1+z)} + M_f^2 \frac{\omega_1}{c_{p_e}}\frac{\bar{\Lambda}}{1+z}\right)\right\} - \frac{\bar{\chi}}{z}$$

Substituting for $\bar{\Omega}$, $\bar{\vartheta}$ and $\bar{\Lambda}$ and $\bar{\chi}$, then up to (B^2-1) it is found that along the wall the density perturbation is given by

$$\rho_2 = \frac{M_f^2 \rho_2(\xi,0)}{\gamma_f M_f^2} + \frac{B_f^2(B^2-1)}{\gamma_f M_f^2}\int_0^\xi e^{\xi'-\xi}\rho_2(\xi,0)\,d\xi - \frac{(\gamma_f-1)M_f^4}{2B_f^2}$$

$$- \frac{(\gamma_f-1)M_f^4\omega_1}{2B_f^2 c_{p_e}}(1-e^{-\xi}) + \left\{\frac{2\gamma_f M_f^2 - \gamma_f M_f^4 + 3M_f^4 - 4M_f^2}{2B_f^2}\right\}(1-e^{-\xi})(B^2-1)$$

$$+ \frac{(\gamma_f-1)M_f^4\omega_1}{2B_f^2 c_{p_e}}(B^2-1)\left\{1-(1+\xi)\exp-\xi\right\} + M_f^2(B^2-1)\,\xi\exp-\xi. \qquad 2.5(63)$$

Once again a relatively simple solution is obtained if terms containing (B^2-1) are neglected. Then the density perturbation is given by

$$\rho_2 = M_{f\infty}^2 \left\{ \frac{(1+\gamma_f) M_f^4}{4 B_f^4} - \frac{1}{B_f^2} - \frac{(\gamma_f - 1) M_f^2}{2 B_f^2} \right.$$

$$\left. + \frac{(2 - M_f^2)\, \omega_1 (\gamma_f - 1) M_f^4}{4 B_f^4 C_{p_e}} \left(1 - \exp - \frac{\xi}{\xi}\right) \right\} \qquad 2.5(64)$$

Adding to ρ_2 to the linear solution allows the overall density to be obtained. This has been evaluated and is plotted in figure 2.5(6). Like the density variation in the numerical solutions this, as can be seen in figure 2.5(6), appears to be extremely sensitive to the approximation used. For whereas the contribution to the overall density perturbation from terms independent of (B^2-1) show a monotomic decrease from the frozen value at the corner to a value below the infinite rate equilibrium value, the inclusion of terms of order (B^2-1) indicate that first the density increases and then decreases in a similar way to the inexact numerical solutions discussed earlier (see figure 2.3(10)). The <u>exact</u> value to second order of the density gradient at the origin, see Appendix (C), is given by

$$\frac{\partial \rho_2}{\partial \xi}(\xi_1 = 0, \eta = 0) = M_f^2 \frac{\partial \rho_2}{\partial \xi} + (B^2-1) M_f^2 \left\{ \frac{(\gamma_f + 1) M_f^4}{4 B_f^2} - \frac{1}{B_f^2} \right\}$$

$$+ (\gamma_f - 1) M_f^2 \left\{ - \frac{(B^2-1)}{4 B_f^2} \left(1 + \frac{1}{B_f^2}\right) - \frac{\omega_1}{C_{p_e}} \frac{M_f^2}{2 B_f^2} - \frac{B^2-1}{2} \right\}$$

$$- \frac{(\gamma_f - 1) M_f^2}{B_f^2} \left\{ 1 - \frac{M_f^2}{2} \left(1 + \frac{1}{B_f^3}\right) \right\} (B^2-1)$$

$$+ (B^2-1) M_f^2 \qquad 2.5(65$$

For the example discussed this shows that the overall density gradient is negative and suggests that in the exact solution the density will monotomically decrease to its new asymptotic value, evaluated in section (2.5(9)). By comparison with the pressure variation downstream of the corner the density variation is small, i.e. about 30% of pressure variation. This may indicate that a delicate balance of terms of equal magnitude exists and that the small errors (due to the approximation) which exist in each of the terms can, when added up over all terms, give an overall error which is relatively large.

The error in the initial slope is sufficient to upset the whole of the result and now quite by chance the approximate solution tends very closely to the infinite rate equilibrium value rather than the true asymptotic value evaluated in section 2.5:9. This is in agreement with the numerical solutions and gives further justification for the disbelief in the overshoots of the density curves. Although a difference between the approximate asymptotic value and the exact asymptotic value exists it is only about 0.002, which is of $O(\theta^2(B^2-1)^2)$ and is thus accurate to the approximation made.

2.5:9 An Asymptotic Solution for $\eta = 0$, $\xi \to \infty$.

The preceding approximate analysis of the non-equilibrium region downstream of the corner resulted in an inelegant solution to the problem. Nevertheless several results obtained in the numerical solution have been repeated. In particular the approximate solution suggests that the pressure tends to the equilibrium value far downstream of the corner. On arguments based on the momentum equation in natural co-ordinates (i.e. $\rho q^2 \frac{\partial \theta}{\partial s} + \frac{\partial p}{\partial n} = 0$ where s and n are co-ordinates along and normal to the streamlines, θ the flow angle and ρ, q and p take their usual meanings), Appleton (1963) deduced that if the flow far away from the wall becomes parallel to the wall*

---

* Since the vorticity is non-diffusive in a relaxing gas flow, the flow must at large distance from the corner see the true wall and not the edge of some vorticity layer as is obtained with a boundary layer.

then the pressure must be constant far away from the corner and therefore the correct limit for the pressure on the wall is the infinite rate equilibrium value. So far numerical calculations and the approximate second order analysis substantiates this argument but do not conclusively prove it. Thus it is of interest to see whether an exact solution of equation 2.5(35), can be found when $\xi \to \infty$

Rather than beginning the problem with equation 2.5(35) it is more convenient to return to equation 2.5(27). After formally performing the inversion, equation 2.5(27) takes on the following form when $\eta = 0$

$$p_2(\xi, 0) = \frac{1}{2\pi i}\int_{c-i\infty}^{c+i\infty} \frac{1}{B_f^2(1+z)z}\sqrt{\frac{1+z}{B^2+z}}\, e^{\xi z}\int_0^\infty F(z,\eta_0)\exp -\left\{z+z\sqrt{\frac{B^2+z}{1+z}}\right\}\eta_0\, d\eta_0\, dz$$

$$+\frac{\gamma_f M_f^2}{B_f}\frac{1}{2\pi i}\int_{c-i\infty}^{c+i\infty}\left\{\frac{z}{a}\bar{v}_2(z,0)+\frac{1}{a}\bar{\psi}(z,0)\right\}\exp \xi z\, dz \qquad 2.5(66)$$

The second integral which arises from the boundary conditions presents no difficulties and thus will not be discussed for the moment.

It was noted in equation 2.5(52) that $\bar{F}$, the transform of first order products, may be evaluated by the convolution theorem. Substituting equation 2.5(52) into equation 2.5(66) gives, for the first integral

$$I(\xi, 0) = \frac{1}{2\pi i}\int_{c-i\infty}^{c+i\infty} \frac{e^{+\xi z}}{B_f^2 z(1+z)}\sqrt{\frac{1+z}{B^2+z}}\int_0^\infty \frac{1}{2\pi i}\int_{d-i\infty}^{d+i\infty}\sum'\left\{ g_i(z)\, Q_i(q)\, P_i\left(\frac{z-q}{\quad}\right)\right\}$$

$$\times \exp -\eta_0\left\{z\sqrt{\frac{B^2+z}{1+z}}+q\sqrt{\frac{B^2+q}{1+q}}+(z-q)\sqrt{\frac{B^2+z-q}{1+z-q}}\right\} dq\, d\eta_0\, dz$$

2.5(67)

Both c and d are greater than zero and from the convolution theorem $c - d > 0$. The integrand is well behaved along $\mathrm{Re}(q) = d$ and thus the order of the η_0 and q integrations may be changed. Integrating with respect to η_0 gives

$$I(\xi,0) = \frac{1}{2\pi i}\int_{c-i\infty}^{c+i\infty} \frac{1}{B_f^2 z}\sqrt{\frac{1+z}{B^2+z}}\,\frac{e^{\xi z}}{1+z}\,\frac{1}{2\pi i}\int_{d-i\infty}^{d+i\infty} \frac{\sum g_i(z) P_i(q) Q_i(z-q)}{\frac{z}{\sqrt{\frac{B^2+z}{1+z}}} + q\sqrt{\frac{B^2+z}{1+q}} + (z-q)\sqrt{\frac{B^2+z-q}{1+z-q}}}\,dq\,dz. \qquad 2.5(68)$$

The essential singularity at q = -1 has now been (apparently) removed and replaced by a denominator which has six roots not easily evaluated.

However the method of steepest descents suggests that the inversion w. r. t z will, for very large values of ξ, have a maximum contribution from the region $z \sim 0$.

Therefore,, let us formally expand the whole of the integrand w. r. t z for small z, i.e.

$$I(\xi,0) \simeq \frac{1}{2\pi i}\int_{c-i\infty}^{c+i\infty} \frac{\exp \xi z}{z\,B\,B_f^2}\,\frac{1}{2\pi i}\int_{d-i\infty}^{d+i\infty} \frac{\left[\sum g_i(0) P_i(q) Q_i(0-q) + \frac{\partial}{\partial z}\left[\sum g_i(0) P_i(q) Q_i(0-q)\right] z\right] dq\,dz}{\frac{q}{\sqrt{\frac{B^2+q}{1+q}}} - q\sqrt{\frac{B^2-q}{1-q}} + \left\{B + \sqrt{\frac{B^2-q}{1-q}} - \frac{q}{2}\sqrt{\frac{B^2-q}{1-q}}\left(\frac{1}{B^2-q} - \frac{1}{1-q}\right)\right\} z + o(z^2)} \qquad 2.5(69)$$

The denominator cannot be expanded further since the expansion would become invalid in the region of q = 0. Inspection of the definition of $\bar{F}(z, \eta_0)$ (see Appendix A) shows that all the $g_i(z)$ behave like z^n (n some integer >0) $\therefore$ $g_i(0) = 0$, but $\frac{\partial g_i}{\partial z} \neq 0$

$\therefore$

$$I(\xi,0) \simeq \frac{1}{2\pi i}\int_{c-i\infty}^{c+i\infty} \frac{\exp \xi z}{B\,B_f^2}\,\frac{1}{2\pi i}\int_{d-i\infty}^{d+i\infty} \frac{\sum P_i(q) Q_i(0-q)\left[\frac{\partial g_i}{\partial z}\right]_{z=0}}{\frac{q}{\sqrt{\frac{B^2+q}{1+q}}} - q\sqrt{\frac{B^2-q}{1-q}} + \left\{B + \sqrt{\frac{B^2-q}{1-q}} - \frac{q}{2}\right\}\frac{B^2-q}{1-q}\left(\frac{1}{B^2-q} - \frac{1}{1-q}\right)\Big\} z} dq\,dz$$

2.5(70)

Thus if equation (2.5(70) is to have a contribution as $\xi \to \infty (z \to 0)$ the integrand must behave at least as z^{-n} (n some positive integer). Judicious inspection of equation 2.5(70) shows that it is only in the region of $q = 0$ that this appears to occur. To evaluate the line integral let us close the contour to the left by a large semi-circle. Since $P_i Q_i$ behave at least like $\frac{1}{q}$ and the denominator behaves like q on the large semi-circle given by $R e^{i\theta}$, then as $R \to \infty$ the contribution vanishes. The simple pole at the origin arising from the terms $P_i Q_i$ gives a contribution $\frac{\sum \left[P_i(q) Q_i(z=0, q)\, q\right]_{q=0} \times \left(\frac{\partial q_i}{\partial z}\right)_{z=0}}{2 B_e^2}$

The roots of the denominator are not easily evaluated but it will be noted that in the region of $q = 0$ the denominator behaves like $-\frac{(B^2-1)q^2}{B} + 2Bz$ and thus approximately (exactly when $z = 0$) two poles exist at $q = \pm \sqrt{\frac{2B^2}{B^2-1} z}$ provided q and z are small. The use of the convolution theorem demands that $\mathrm{Re}(z - q) > 0$ always. Therefore since the integral is evaluated by closing the contour to the left the pole at $q = +\sqrt{\frac{2B^2}{B^2-1} z}$ must be excluded. Therefore in addition to the pole at $q = 0$ it is necessary to include the pole at $q = -\sqrt{\frac{2B^2}{B^2-1} z}$. Since $P_i Q_i$ behave as $\frac{1}{q}$ the pole will give a contribution $-\frac{\sum \left[P_i(q) Q_i(z=0, q)\right]_{q=-\sqrt{\frac{2B^2 z}{B^2-1}}} \left(\frac{\partial q_i}{\partial z}\right)_{z=0}}{4 B_e^2}$

thus as $z \to 0$,

$$I(\xi, 0) \underset{\xi \to \infty}{\simeq} \frac{\sum \left\{ P_i(q=0) Q_i(z=0, q=0) \left(\frac{\partial q_i}{\partial z}\right)_{z=0} \right\}}{4 B_e^2} \qquad 2.5(71)$$

Unfortunately the algebraic manipulations are too lengthy to include but associating P_i and Q_i with terms occuring in equations 2.5:7 to 2.5(13) and hence finding the Σ corresponding to $\bar{F}(z, \Omega_0)$, it can eventually be shown that equation 2.5(71) becomes

$$I(\xi,0) \underset{\xi\to\infty}{\simeq} \frac{1}{4B_e^2}\left\{\left(1-\frac{\omega_1}{c_{pe}}\right)\left[\frac{1+\gamma_f}{B_e^2}+(1+\gamma_f)\right]M_f^2+\frac{\omega_1}{c_{pe}}\left[\left\{1+(\gamma_f-1)M_f^2-B_f^2(B^2-1)\right\}\frac{\gamma_f M_f^2}{B_e^2}\right]\right.$$

$$+\frac{\omega_1}{c_{pe}}\left[\gamma_f M_f^2+\left\{(\gamma_f-1)M_f^2-B_f^2(B^2-1)\right\}\left\{\gamma_f M_f^2-2(\gamma_f-1)M_f^2+2B_f^2(B^2-1)-1\right\}\frac{1}{B_e^2}\right]$$

$$\left.+\frac{\omega_1}{c_{pe}}\left[-\left\{(\gamma_f-1)M_f^2-B_f^2(B^2-1)\right\}+\left\{M_f^2+B_f^2(B^2-1)\right\}\frac{M_f^2}{B_e^2}\right]\right. \qquad 2.5(72)$$

which on noting that $\gamma_e M_e^2 = \gamma_f M_f^2$, $B_f^2 B^2 = B_e^2$ and $\gamma_e = c_{pf}+\omega_1/c_{vf}+\omega_1$, reduces to

$$I = \frac{(\gamma_e+1)M_e^4}{4B_e^4} \qquad 2.5(73)$$

The $\bar{\psi}(z,0)$ occuring in the second integral of equation 2.5(66) combines with the ψ term in $F(z,\eta)$ and

$$\frac{1}{2\pi i}\int_{c-i\infty}^{c+i\infty}\frac{z}{a}\,\bar{v}_2(z,0)\exp\xi z\,dz \longrightarrow -\frac{1}{B^2B_f^2} \text{ as } z\to 0$$

$$\therefore \quad \frac{p_2(\xi,0)}{\gamma_e M_e^2} \to \frac{(\gamma_e+1)M_e^4}{4B_e^4}-\frac{1}{B_e^2} \text{ as } \xi\to\infty \qquad 2.5(74)$$

This is exactly the infinite rate equilibrium value obtained in sections 2.5:6. Thus to second order the asymptotic value of the pressure is the equilibrium value and gives further evidence that the numerical solution should eventually asymptote to the equilibrium value and the degree of divergence of the solution from this value may confidently be taken as an assessment of the error of the computing scheme.

The result also helps to justify the original expansion process 2.5(1) and suggests that non-uniformity w.r.t. ξ exists.

Having obtained equation 2.5(74) it is now possible to

evaluate the rest of the dependent variables and to assess (to within the accuracy of the second order theory) the deviation from the corresponding infinite rate equilibrium values.

(i) Evaluation of the second order temperature perturbation

T_2 can most easily be obtained by use of the energy equation

$$h + \frac{q_\infty^2}{h_\infty}\cdot\frac{a^2}{2} = \text{const.},$$

where the specific enthalpy h and the velocity have been made non-dimensional with their undisturbed values. Letting $h = 1 + \theta h_1 + \theta^2 h_2 + \cdots$ and $q^2 = (1 + \theta u_1 + \theta^2 u_2 + \cdots)^2 + (v_1\theta + v_2\theta^2 + \cdots)^2$ and collecting terms of order θ gives

$$h_2 + (\gamma_e - 1) M_e^2 \left(u_2 + \frac{v_1^2 + u_1^2}{2}\right) = 0$$

Since $h_2 = \left(c_{pf} T_2 + \omega_1 T_{v_2}\right) / c_{pf} + \omega_1$

then

$$\frac{c_{pf} T_2 + \omega_1 T_{v_2}}{c_{pf} + \omega_1} + (\gamma_e - 1) M_e^2 \left(u_2 + \frac{v_1^2 + u_1^2}{2}\right) = 0$$

As $\xi \to \infty$, $(\eta = 0)$ it is not difficult to show from equation 2.5(11) that $T_{v_2} \to T$

$$\therefore \text{ as } \begin{matrix}\xi \to \infty \\ \eta = 0\end{matrix}, \quad T_2 \to -(\gamma_e - 1) M_e^2 \left(u_2 + \frac{v_1^2 + u_1^2}{2}\right)$$

now $$\frac{u_1^2 + v_1^2}{2} \to \frac{M_e^2}{2 B_e^2} \quad \text{as } \xi \to \infty, \eta = 0$$

and from equations 2.5(58) and 2.5(74)

$$u_2 \to -\frac{p_{2e}}{\gamma_e M_e^2} - \int_0^{\xi=\infty} \varphi(\xi, 0)\, d\xi$$

$$\therefore \quad T_2 \to (\gamma_e - 1) M_e^2 \left\{ \frac{(\gamma_e+1) M_e^4}{4 B_e^4} - \frac{1}{B_e^2} \right\} - \frac{(\gamma_e - 1) M_e^4}{2 B_e^2}$$

$$+ (\gamma_e - 1) M_e^2 \int_0^\infty \varphi(\xi, 0)\, d\xi$$

$$= T_{2e} + (\gamma_e - 1) M_e^2 \int_0^\infty \varphi(\xi, 0)\, d\xi. \qquad 2.5(75)$$

Therefore to second order it can be seen that the temperature will be greater than the equilibrium temperature by an amount

$$A^2 (\gamma_e - 1) M_e^2 \int_0^\infty \varphi(\xi, 0)\, d\xi.$$

Since the infinite integral has a value = 0.104 the difference of the temperature from its infinite rate equilibrium value is $10.4(\gamma_e - 1) M_e^2 \theta^2$ per cent. For a 5° corner this is $0.08(\gamma_e - 1) M_e^2$ %.

(ii) Evaluation of the asymptotic second order density perturbation.

Since $\rho_2 = p_2 - T_2 - \rho_1 T_1$ it is not difficult to show that as $\xi \to \infty$ that

$$\rho_2 \to \rho_{2e} - (\gamma_e - 1) M_e^2 \int_0^\infty \varphi(\xi, 0)\, d\xi$$

thus to second order the density will fall below the infinite rate equilibrium value ρ_{2e} by an amount $(\gamma_e - 1) M_e^2 \int_0^\infty \varphi(\xi, 0)\, d\xi$. For the particular example under discussion this is shown in figure 2.5(6). This overshoot has not been found in the numerical solutions for the ideal dissociating gas. This could of course be simply because of the different non-equilibrium gas flow models used but in view of the fact that the approximate solutions tend to the equilibrium values it does suggest that there is probably still an error in the numerical solutions and that a more exact solution may show up this difference.

Although the differences that exist for the density and temperature are the same it must be remembered that as a percentage

of the total variation between the frozen and equilibrium, the density is large

$$\text{i.e. } \frac{(\gamma_e-1)M_e^2\int_0^\infty \varphi(\xi,0)\,d\xi}{\rho_F-\rho_e} > \frac{(\gamma_e-1)M_e^2\int_0^\infty \varphi(\xi,0)\,d\xi}{T_F-T_e}$$

i.e. 30% as compared with 5% for the temperature.

Before concluding this sub-section it is perhaps worth noting that if a variation of the relaxation time is allowed, then the solution appears to break down completely. For example if the variation of τ is considered to be that proposed by equation 2.5(4) then the right hand side of the second order rate equation 2.5(11) contains an extra term equal to $-(\rho_1 + bT_1/3T_\infty^{1/3})(T_1 - T_{v_1})$. Including this in the analysis for determining the exact gradients at the corner changes the overall pressure gradient from + 0.034 to −0.004. Corresponding, but exaggerated changes occur in the approximate solution. In fact if the second order rate equation is assumed to have no non-linearities associated with it and is taken simply as $\frac{\partial T_2}{\partial \xi} = \frac{T_2 - T_{V2}}{u_\infty \tau_\infty}$ overall improvement in the solution occurs, although the approximate solution still maintains similar initial increases in density, it is not so pronounced. Apart from the fact that (B^2-1) is not particularly small, at this stage it is not easy to see why the second order terms in the rate equation should make the solution so sensitive near the corner and yet have no overall effect on the frozen or asymptotic values. This obviously warrants further investigation.

A suitably small value of θ or (B^2-1) can correct most of the peculiarities of the theory when looking at the overall pressure, density etc.

2.5:10 The Role of the Characteristics of the Second Order System

Since the characteristics of hyperbolic equations play such an important part in the exact solution, it may be anticipated that any iteration process should be intimately connected with the characteristics. In fact the perturbation scheme* proposed keeps the undisturbed state characteristics for the characteristics at all stages of the iteration process and all the modifications that actually occur to the characteristics are transferred to the right hand side of the equations. Thus the role of the characteristics becomes buried in the algebra.

The form of the characteristics can however be looked at. Exactly, the equation of outgoing characteristics are given by

$$\frac{dy}{dx} = \tan(\theta+\mu)$$

Applying the perturbation procedure to θ and μ and collecting terms of order θ gives,

$$\frac{dy}{dx} = \tan\mu_\infty + \frac{\sec^2\mu_\infty}{\tan\mu_\infty}(\theta_1+\mu_1)\theta$$

For the frozen case $\mu_1 = \tan\mu_\infty\left(\frac{p_1-\rho_1}{\rho^2} - U_1\right)T'(x)$ where $T'(x)$ is the slope of the boundary. $\theta_1 = \theta(x - B_f y)$

$$\therefore (\theta_1+\mu_1) = \frac{(\gamma_f+1)M_f^2}{2B_f^2}T'(x-B_f y)$$

$$\therefore \frac{dy}{dx} = \frac{1}{B_{f\infty}} + \frac{(\gamma_f+1)M_f^4}{2B_f^3}\theta\, T(x-B_f y)$$

---

* Since charactersitic co-ordinates α,β (say) are natural ones it would be expected that some advantage may be gained by working in these co-ordinates. The main disadvantage is the determination of x and y in terms of α,β and the difficulty in applying the boundary conditions. Certainly if one could work, in these co-ordinates it would ensure that the correct characteristics are used at each stage of the iteration process.

For the non-equilibrium case the problem is complicated owing to the difficulty of evaluating p_1, ρ_1 and u_1 etc. for a general field point. Once again

$$\frac{dy}{dx} = \frac{1}{B_{f\infty}} + \theta \frac{M_{f\infty}^2}{B_{f\infty}} \left\{ \theta_1 + \frac{1}{B_{f\infty}} \left(\frac{p_1 - \rho_1}{2} - u_1 \right) \right\}$$

However it is possible to look at the solution for small $x - B_f y$, in which case the above may be written approximately

$$\frac{du}{dx} \simeq \frac{1}{B_{f\infty}} + \theta \frac{M_{f\infty}^4 (\gamma_{f\infty}+1)}{2 B_{f\infty}^3} H(x - B_f y) \exp -\frac{B^2-1}{3} B_f y$$

showing that near the wall and at the corner, the characteristics start off with the slope

$$\frac{du}{dx} \simeq \frac{1}{B_{f\infty}} + \frac{\theta M_f^4 (\gamma_f+1)}{2 B_f^3}$$

and tending to $\frac{dy}{dx} \to \frac{1}{B_{f\infty}}$ as $y \to \infty$,

thus the characteristics are convex downstream, see figure (2·5(7)) For the linearised corner problem of course this variation occurs in an infinitely thin strip adjacent to the linearised leading frozen characteristic. The equation may also be evaluated along the wall. For they will start off at the corner with the second order frozen characteristics and slowly increase until

$$\frac{dy}{dx}\Big(x, y=0\Big)_{x \to \infty} \to \frac{1}{B_{f\infty}} + \left\{ 1 + \frac{1}{B_{f\infty}} \left(\frac{(\gamma_{e\infty}-1)M_e^2+2}{2 B_{e\infty}} \right) \right\} \frac{M_{f\infty}^2 \theta}{B_{f\infty}}$$

which is in qualitative agreement with numerical solutions.

3.0 Experiments

The intention of this section is an attempt to provide some experimental support for the theoretical discussions of the previous section. To obtain a test gas which is at a sufficiently high temperature for the real gas effects (which have been studied in the earlier sections) to be present, the steady flow of gas following the primary shock in a shock tube has been used. Initially it was hoped to study the chemical kinetics of oxygen dissociation and recombination (hence the section on the flow of an ideal dissociating gas) but limitations of the experimental equipment available has restricted the work to looking at non-equilibrium effects associated with the vibrational relaxation of Carbon Dioxide.

3.1 The Shock Tube and associated equipment

The layout of the College of Aeronautics Shock Tube has been described by J.R. Busing (1962). In brief it is mounted vertically and is made of stainless steel with a 5.08 cm. internal diameter. The driving section is 1.22 metres long and the working section in the unexpanded part of the tube is situated 4.66 metres from the diaphragm. The diaphragms are allowed to break naturally and by scribing them repeatable shock Mach numbers could be obtained.

An Edwards Oil Diffusion pump, backed by a rotary pump is used to pump down the system to pressures of less than 10^{-4} TORR. The whole system was found to have a leak rate of about 0.25×10^{-3} TORR/min. in any twenty minutes after pumping for two to five hours. Longer pumping periods tended to reduce this leak rate.

Gas pressures are measured with an Alphatron vacuum gauge. This instrument has a range of 10^{-3} TORR $\sim$ 10^{3} TORR with an accuracy of 2% of the full scale deflection and has been calibrated with a Mcleod gauge in conjunction with a liquid nitrogen trap at the low pressures and with a master manometer at the higher pressures.

The shock velocity is recorded by timing the shock over 20 cms at a station just prior to the working section. The shock is detected by two thin film platinum resistance thermometers painted on a pyrex substrate and mounted flush to the tube walls. The output of these gauges are used to start and stop a microsecond counter.

The spark source designed by J.R. Busing consists of the barium titinate condensers charged to 12 kv. This has a relatively large light output with a spark duration of 3/10 m.secs. The spark was triggered via a digital delay unit from a thin film platinum gauge mounted in the working section.

A diagrammatic description of the instrumentation is given in figure 3.1(1).

3.1.1. The Mach Zehnder Interferometer.

The Mach-Zehnder interferometer has been constructed on similar lines to the one at The National Physical Laboratory and described by Tanner (1959). It consists of two fully reflecting mirrors and the half silvered mirrors (splitters) of dimensions (4" x 6.5" x 1") and placed on a horizontal heavy steel table figure 3.1(1). The whole table rests on sponge rubber pads which were found sufficient to absorb much of the surrounding vibrations. When the mirrors are mounted at 45° to the working section this allows a four inch square field of view. Mirror (2) and splitter (1) have only course adjustment, but mirror (1) has three degrees of freedom and splitter (2) has two degrees of freedom. After coarse adjustment, fine adjustment of rotation and translation of these componsnts is achieved through gear boxes which allows movements of the order of a wavelength of light to be made. Apart from a poorly mounted splitter, which caused extreme unsteadiness in the fringes and which was cured by extra damping, the fringes could be rapidly obtained (with practice) by utilising the new hand for cross hair method described by Tanner (1959). Once adjusted the fringes remained steady and stable for indefinite periods of time and only day to day adjustments for focus and contrast was needed.

The associated optical components consisted of a mercury vapour lamp, a spark source and two f2.5 - 12 inch focal length lenses, one for collimating the light and the other for collecting the light prior to focusing on the camera. The mercury vapour lamp was used for setting up the system and was first focussed on to the electrodes of spark and used for adjusting the interferometer.

A compensating chamber with dimensions equal to the working section was used so that the initial path differences in each circuit of the interferometer are equal.

A photograph and general layout of the equipment is shown in figure 3.1(1)

3.1.2. The Schlieren System

The Schlieren system is quite conventional and a diagram of the layout is shown is figure (3.1(2))

3.2.0 A study of the Normal Shock to determine the relaxation time for Carbon Dioxide

The intention of this section is not to discuss in detail the structure of shock waves, but to introduce briefly some experiments that were made to compare the relaxation times estimated by studying the structure of a plane expansion wave with relaxation times estimated by interferometric observation of the relaxation zone following the primary shock in a shock tube.

This is a well tried experimental technique and has been used extensively to determine relaxation and dissociation time data for gases at high temperatures. In particular it has been utilised by Smiley and Winkler (1954) and Griffith, Brickl and Blackman (1956) to determine relaxation times for carbon dioxide. A more recent paper by Johannesen, Zienkiewicz, Blythe and Gerrard (1962) reports a very careful series of experiments in which the Mach-Zehnder interferometer was used, in conjunction with an exact analysis developed by Johannesen (1961), to study the structure of the shock wave and hence determine the relaxation time for varying temperature . These measurements suggest that previous determinations of the relaxation times are too low, especially at the higher temperatures, and this they attribute to the extra care that was taken to ensure that the Carbon Dioxide used in the tests was extra dry. The available shock tube data is presented in figure (3.2.2).

Since it is difficult to assess the exact amount of impurity in the shock tube just prior to a run, the above experiments were repeated to assess, by comparison, the residual impurities that exist in the College of Aeronautics 5.08 cm shock tube system.

Provided the relaxation time τ and the vibrational specific heat Cp are assumed constant the equations governing the structure of the shock may be integrated. However τ and Cp can vary quite strongly and one must proceed with some care when developing an approximate solution. Blythe (1961) by comparing the many approximations that exist, with the exact solution, showed that the constant

enthalpy, pressure, Cp and τ approximation used by Blackman (1956) gives a good approximation to the structure of the wave, and that provided Cp and τ was represented by their mean values Cp_m, τ_m between the conditions just behind the shock front[a] and the final equilibrium value[2], then the relaxation time will be overestimated by a few per cent.

Bearing these limitations in mind the results have been evaluated on the assumption that the following density profile, given by Blackman, exists in the relaxation zone

$$\frac{\rho_2 - \rho}{\rho_2 - \rho_a} = \frac{\rho_2/\rho_a \quad \exp\left(-\frac{Cp_m}{CpF}\frac{x}{u_m \tau_m}\right)}{\left\{1 + \left(\frac{\rho_2}{\rho_a} - 1\right)\exp\left(-\frac{Cp_m}{CpF}\frac{x}{u_m \tau_m}\right)\right\}}$$

The density is evaluated from the interferogram and is obtained by means of the Mach-Zehnder interferometer. The relationship between the fringe shift and the density change is given by

$$\Delta\rho = \frac{\lambda}{KL}\Delta N$$

when $\Delta\rho$ is the density change across the shock, ΔN the fringe shift, λ the wavelength of the monochromatic light used, K the Gladstonedale count and L the width of the working section. K was determined by experiment and was found to equal 0.233.

A set of results for $M_S = 2.85$, $p_1 = 23.6$ mm. is shown in figure 3.2(3) and the plot of $\log\left(\frac{\rho_a}{\rho_2}\left(\frac{\rho_2 - \rho}{\rho_2 - \rho_a}\right)\right)$ indicates by the linearity how well this approximation describes the density profile.

Using the theoretical estimates for C_{p_m} and u_m the relaxation time may then be determined from the slope, for the mean temperature T_m. These are given in figure 3.2(2)

In view of the critical manner which water vapour affects the relaxation time, care was taken to ensure that the gas was dry. This consisted of using analytical grade carbon dioxide (water content specified as less than 1 part per 50 million) and was passed over a phosphorous pentoxide trap prior to being injected into the tube. In an attempt to reduce the outgassing to a minimum the tube was pumped for 2-5 hours after which time the final pressure was about 0.2μ Hg and the leak rate about 0.25μ Hg/min. over a period of about

20 minutes. This leak rate was comparable to that quoted by Johannesen et al but the ultimate pressure was higher. The time between stopping the pump and firing the tube was usually less than 5 minutes.

In spite of these precautions the final estimates of the relaxation times for the present series of experiments still lie lower than those of Johannesen et al and in the main, they tend to agree with those of Smiley and Winkler (1954) and Griffith et al (1956) (See figure 3.2(2)).

Because of the difficulties associated with the measurement of water vapour content at the pressures used it would appear that one must conclude that the gas is still relatively wet. Perhaps one may venture the suggestion that since the volume to surface area ratio of the tube used by Johannesen et al is approximately six times greater than the College of Aeronautics tube and the other workers, then for a fixed leak rate and initial pressure, the gas in the present experiments has the possibility of being about six times more wet.

In agreement with Johannesen it was found that the overall density ratio across the shock wave agrees with the assumption that all the degrees of freedom are in equilibrium downstream of the shock. (See figure 3.2(1).

3.3.0 Vibrational Relaxation Times for Carbon Dioxide obtained from expansion waves

Clarke (1960) as a consequence of discussing some theoretical aspects of linearised non-equilibrium flow fields suggested that the relaxation zone occuring downstream of a centred two dimensional expansion could provide an alternative means of determining the rate at which a relaxation process occurs. In a later paper Appleton (1960) indicated that a study of the decay of the gradients of the flow variables that occurs along the leading characteristic of the expansion might be a more profitable proposition from the experimental point of view. Although both papers were specifically concerned with dissociated gas flows the arguments are equally applicable to any situation in which a relaxation process may exist.

With these thoughts in mind, a feasibility study was made to determine whether relaxation times for Carbon Dioxide could be sensibly estimated by using a steady plane expansion. Carbon Dioxide was chosen because the vibrational modes of the molecule are readily excited and also because many independent experimental measurements of the relaxation time have been made. Considerable variation in the relaxation times exist (see figure 3.2(2)), but recent papers by Blythe (1962) and Johanneson et al (1962) have put much of the discrepancy into perspective. With this data available a ready comparison with the results obtained here can be made.

The steady supersonic flow following the primary shock in a shock tube was used to obtain samples of equilibrium Carbon Dioxide at high temperature. The plane expansion was generated by inserting a wedge into the unexpanded section of the two inch diameter shock tube described earlier. Since it is the gradient of the flow variables that decay along the leading characteristic, the Schlieren method is naturally suited to the experiment because of its sensitivity to density gradients. The gradients were obtained by measuring the image densities on the photographic plate.

3.3.1 The Density Gradient at the leading edge of the expansion

Appleton (1960), by adapting the work of Wood and Parker (1958) (who analysed the structure of a centred unsteady expansion wave), showed that the gradients of the flow variables decayed at the wave head of a centred steady expansion wave for the Lighthill type Ideal Dissociating Gas, see section (2.3). The analysis for a relaxing gas is the same as presented by Appleton (1960), but as background to the experiment these results are re-derived for the case of a simple vibrator. (For Carbon Dioxide it is considered, for the moment, that only the bending mode is important and that the energy contained in the other modes can be considered small enough to be neglected completely, an approximation which will certainly be wrong at the higher temperatures.)

The results are most easily derived by considering the governing equations in their characteristic form. For this particular case equations (2.2(2)) of section 2.2 reduce to

$$\frac{\partial\theta}{\partial\alpha} + \frac{\cot\mu}{\rho q^2}\frac{\partial p}{\partial\alpha} + \frac{\nu_\alpha}{RC_{p_f}TM_f q}\frac{DE_i}{Dt} = 0 \qquad 3.3(1)$$

which holds along $y_\alpha = \tan(\theta+\mu)x_\alpha$ and

$$\frac{\partial\theta}{\partial\beta} - \frac{\cot\mu}{\rho q^2}\frac{\partial p}{\partial\beta} - \frac{\nu_\beta}{RC_{p_f}TM_f q}\frac{DE_i}{Dt} = 0 \qquad 3.3(2)$$

which holds along $y_\beta = \tan(\theta-\mu)x_\beta$

α and β are characteristic parameters (as yet unassigned), θ the flow angle, p is the pressure, C_{p_f} the specific heat at constant pressure obtained by ignoring the energy contained in vibration, M_f the frozen Mach number and $\mu = \sin^{-1}(1/M_f)$. E_i is the internal energy associated with the bending mode and for equilibrium conditions this is given by.

$$E_i = 2R\theta_v/(\exp\theta_v/T - 1) \qquad 3.3(3)$$

θ_v being a characteristic temperature for vibration of the bending mode and equals 959°K.

It is now necessary to specify the time rate of change of the internal energy. In accordance with previous work it is assumed that the usual linear relaxation equation

$$\frac{DE_i}{Dt} = \frac{E(T) - E_i}{\tau(\rho, T)} \qquad 3.3(4)$$

holds, where E(T) is the internal energy evaluated as if it is in equilibrium with the local value of the translational temperature, E_i is the actual internal energy and $\tau(\rho, T)$ is a relaxation time associated with the vibrating mode and is a function of temperature and inversely proportional to the density. The experimental determination of the relaxation time discussed later will be obtained on the assumption that the above simple rate law holds. In addition to the characteristic relations 1 or 2 the streamlines represent a third characteristic direction and along these holds

$$\rho \frac{Dh}{Dt} - \frac{Dp}{Dt} = 0 \qquad 3.3(5)$$

where h is the specific enthalpy. These together with the thermal equation and caloric equation of state complete the basic system of equations. Let the parameter β label those characteristics originating at the apex of the expansion fan, then it may be noted that the derivatives of the dependent variables with respect to α will be zero at the leading edge of the expansion. Further, it is readily deduced that $y_\alpha(\alpha, \beta_0) + \tan \mu_\infty x(\alpha, \beta_0) = 0$, $E_{i\alpha}(\alpha, \beta_0) = 0$, $\rho_\infty h_\alpha(\alpha, \beta_0) - p_\alpha(\alpha, \beta_0) = 0$ and $\theta_\alpha(\alpha, \beta_0) - p_\alpha(\alpha, \beta_0)/\rho_\infty q_\infty^2 = 0$ where β_0 is the first characteristic in the fan and the subscript ∞ representing conditions upstream of the corner. By differentiating equation 3.3(1) with respect to β and utilising the conditions at the wave head the decay of the density gradients along the leading characteristic is

$$\left[\frac{\partial(\rho/\rho_\infty)}{\partial\beta}\right]_{\alpha,\beta_0} = C\exp-\left\{2\left(\frac{\theta_v}{T}\right)^2\frac{\exp\theta_v/T}{\left[\exp\frac{\theta_v}{T}-1\right]^2}\cdot\frac{1}{2}\cdot\frac{\gamma_c M_{\infty}}{B_F C_{PF}^2}\frac{1}{\tau_\omega q_\infty}\right\}^{\alpha} \qquad 3.3(6)$$

*

The constant C may be obtained from the frozen flow solution at the corner but for the present purpose however, there is no direct need to evaluate it. It is now necessary to assign to the characteristic parameters values pertinent to the problem. Following Appleton (1960) it is convenient to associate α with r the radial distance from the corner and β with an angle ϕ representing the inclination at the characteristics at the corner. Then it may be shown that

$$\left[\frac{\partial(\rho/\rho_\infty)}{\partial\varphi}\right]_{r,\varphi_0} = C\,\frac{kr\exp-kr}{1-\exp-kr} \qquad 3.3(7)$$

where k is given by the term in curly brackets in equation 3.3(6). Since the schlieren system is sensitive to gradients with respect to some physical length s (say) a more convenient form of (3.3(7)) is

$$\left[\frac{\partial(\rho/\rho_\infty)}{\partial s}\right]_{r,\varphi_0} = A\,\frac{\exp-kr}{1-\exp-kr} \qquad 3.3(8)$$

and A is some arbitrary constant. Thus for an ideally centred expansion the gradient tends to zero as r tends to infinity and to infinity as r tends to zero. Provided the gradient can be measured the constant k can be determined and with knowledge of all the dependent variables ahead of the corner, an estimate of the

---

* It is of interest to note that provided the energy exchange to the stretching modes is through internal leakage only then the decay of gradients will be the same as above, but if the excitation of the stretching arises through inelastic collisions involving energy transfer from translation to the stretching mode as well,, then the curly brackets in equation 3.3(6) contains extra terms associated with the other modes. This is in agreement with the linearised analysis for two modes discussed in section (2.4).

relaxation time can be made.

In practice the viscous interaction of the expansion wave with the boundary layer at the corner causes the toe of the expansion to spread and thus the result given by equation 3.3(8) for a centred expansion is not directly applicable to the real problem. In fact the upstream influence can be appreciable. Lighthill (1953) indicates that for a liminar boundary layer the upstream influence can be as much as ten boundary layer thicknesses and for a turbulent boundary the order of one boundary layer thickness. At the base of the leading characteristic of the fan the density gradient will be finite rather than infinite as indicated by equation 3.3(8). For evaluation assume that the first few characteristics of the fan, figure 3.3(2), which arise from the upstream influence of the corner, are effectively centred at some virtual point 0 distant r_o from the corner. Then relative to the measured value of the density gradient at r_o (i.e. at the outer edge of the boundary layer on the model) the decay of the density gradient at the wave head is given by

$$\frac{\left(\frac{\partial \rho}{\partial s}\right)}{\left(\frac{\partial \rho}{\partial s}\right)_{r_0}} = \left\{ \frac{1 - \exp -k r_0}{1 - \exp -k(r + r_0)} \right\} \exp -kr. \qquad 3.3(9)$$

Provided it is possible to measure r_o or at least ensure that kr_o is sufficiently large or r sufficiently small to render the term in brackets approximately one, then equation 3.3(9) may be used in conjunction with experiments to estimate the relaxation time.

3.3:2 Experimental Method

The experiments were performed in the 5.08 cm shock tube described in section (3.1) and the plane expansion was generated by inserting a wedge, figure 3.3(1) which spanned the working section. The leading portion of the wedge was mounted parallel to the gas flow to minimise the leading edge shock and the plane expansion is situated 2.54 cm from this leading edge.

In view of the recent experiments by N.H. Johannesen et al (1962) precautions were taken to ensure that impurities were kept to a minimum. The tube was pumped for at least two hours at $<10^{-4}$ TORR before performing the experiment and after this period of time the leak rate had reached $\cdot 25\ 10^{-3}$ TORR/hour. As in the normal shock experiments described in section (3.2) Analytical Grade Carbon Dioxide was used and has a water content of not more than one part per 50 million. It was further passed over a phosphorous pentoxide trap before being injected into the tube.

A conventional schlieren system was used to obtain density gradients throughout the flow field. Care was taken to ensure that the collimated light was aligned perpendicular to the wedge and that the image plane of the camera was focussed on the centre line of the tube. A barrier layer photo-cell was used to ensure that the knife edge was always adjusted to cut off just half the light. This, of Holder and North (1963), allows maximum and uniform sensitivity for a given range.

The spark source described in section 3.1 was used. The exposures were taken on Ilford L.N. fast blue sensitive plates and developed in a Leica bath (5 grams metol, 100 grams Sodium Sulphite and 1000 cc's water) for fifteen minutes at 65°F. A characteristic curve for this plate processed under the above conditions was obtained by exposing the plate with the spark source through a standard Kodak step filter. This is plotted in figure 3.3(3). The exposures of the actual schlieren pictures were then adjusted so that the required image density range to be measured always lay on the linear portion of the characteristic curve. This ensured that an approximately linear relationship existed between the image densities and the actual illumination of the schlieren image. The image densities on the photographic plate were measured with a Hilger and Watts micro-densitometer.

One of the major difficulties and source of error in analysing the photographic plates was the precise location of the leading characteristic of the expansion. To overcome this, scribes

spanning the working section, were made on the wedge upstream of the corner. These produced approximations to Mach lines and since for a relaxing gas flow disturbances are first felt along frozen Mach lines, the leading edge of this disturbance should approximate to these frozen Mach lines and should be parallel to the leading characteristic of the expansion. Far from the scribe, one may expect to see the disturbance diffused about the equilibrium Mach line but in the photographs taken where this phenomena could happen the Mach lines just became indistinct a long way from the disturbance. Comparison of the angle of the leading edge of the disturbance for a large number of runs are shown in figure 32(4) and as can be seen they scatter very closely around the theoretical frozen values.

The micro-densitometer was then aligned along these 'Mach lines' and moved until the expansion fan was just penetrated, the traverses being parallel to the Mach lines. Several traverses parallel to and near the estimated position of the wave head were then taken and the mean of the results used. (The error bands on Figure (3.3(8)) signify the scatter due to this

The Schlieren System appeared to be very sensitive to the boundary layer on the windows and this led to fairly rigid restrictions on the time at which the picture was taken. The delay was usually adjusted so that the picture was taken while the secondary wave system which developed just downstream of the corner was still in view see figure (3.3(6)). For these conditions it was estimated that the boundary layer on the windows would be laminar for most of the runs.

3.3:3 Results of wave head experiment

The series of experiments covered a shock Mach range of about 2.5 to 6.5. The low limit arising because the flow Mach number relative to the wedge becomes too low for shock attachment below this value.

Choice of the initial conditions in the low pressure part of the tube have been dictated mainly by the requirement that the

decay of the density gradients should be complete within the field of view. In fact since the effective centre of the leading portion of the expansion cannot be accurately located, it is necessary to choose initial conditions so that k is as large as possible. This means that relatively high initial pressures are best. This helps to compensate for the uncertainty in r_o.

A precise evaluation of r_o does not appear possible although estimates can be made from the schlieren and interferometer pictures. By traversing with the micro-densitometer along a line parallel to the boundary downstream of the corner and just outside the boundary layer results in figure (3.3(7) say. Since the resulting trace is proportional to the density gradient the peak represents the position where the expansion is occuring most rapidly and which will be somewhere in the fan. Unpublished results of tests performed by Zuckermann and Cleaver and Clark and Gibson (1962) in a 6" x 4" supersonic tunnel where the interaction of a Prandtl-Meyer expansion fan with a turbulent boundary was investigated, suggest that this peak gradient occured in the vicinity of the corner and thus the distance from the beginning of this trace to the peak, represents an order of magnitude estimation of the upstream influence. This distance was roughly 0.75 mm. see figure (3.3(7). If the boundary is laminar, theory suggests that the boundary thicknesss just ahead of the corner is about 0.05 mm. Lighthill (1953) suggests that the upstream influence will be about ten boundary layer thicknesses thus very approximately the two estimates agree. The interferograms and the pressure distribution obtained by Clark and Gibson (1960) suggest that at the most the flow has expandedby $2^{\circ} \sim 3^{\circ}$ just ahead of the corner thus a very crude estimate for r_o is given by $\frac{(0.5 * 0.75) \times 57.3}{(2 \sim 3)}$ which gives $10.\text{mm.} < r_o < 20\text{mm.}$ In most of the cases tested the value of k varied from 0.2 to 0.1 thus the factor $\left(\frac{1 - \exp - kr_o}{1 - \exp - k(r_o + r)}\right)$ varies from 1 at the reference point r = 0 to 0.6 at the worst estimate to 0.98 in the best circumstances. In evaluating the relaxation times this factor has

been taken as unity. Thus when taking a mean slope from the log $\left(\frac{\partial \rho}{\partial s} \Big/ \left(\frac{\partial \rho}{\partial s}\right)_{r=0}\right) \sim r$ it will tend to be exaggerated if a sample of points very far from the corner is taken, and hence the relaxation time obtained will be underestimated. However if conditions are chosen such that the decay of gradients is complete within a few millimetres of the corner, then this error will be small compared with the error associated with locating the wave head correctly.

An overall assessment of the experimental error does not appear possible at this stage apart from defining some limits associated with locating the wave head see figure (3·38). Of particular concern is the boundary layer growth on the shock tube wall which can affect the quality of the schlieren picture to a large extent and undoubtedly accounts for some of the large scatter of the measured relaxation times. Although care was taken to take the schlieren at approximately the same position in the hot flow behind the primary shock, variations in the quality of the pictures still occured;(the rate of charging of the driver section for example could influence the flow). In view of these fairly large errors no attempt was made to assess the effect of shock attenuation or the precise conditions existing ahead of the expansion which in the experiments have been taken as the equilibrium conditions behind the shock.

Despite all possible errors it was encouraging to find that final estimates of the relaxation time agreed fairly well with existing data. In particular they lie broadly in the same region as the measurements obtained by Johannesen et al (1962) and if anything, the relaxation times tend to be a little longer.

Of some concern is the discrepancy that exists between the relaxation times obtained from the expansion waves and those obtained from interferometric studies of the normal shock in the College of Aeronautics tube. Compare figures (3·38) and (3·2(2). As mentioned in section (3·2) it was not possible to measure the water content of the test gas just prior to a run and thus no absolute measurement of H_2O impurity was available. However it was

noted that for a given shock Mach number, hence temperature, the initial pressure in the shock tube was generally five times or more greater in the expansion wave experiments than the corresponding pressure needed to study the shock front. Thus for given impurities in the tube it is likely that the Carbon Dioxide could be five times drier in the expansion experiments, an amount which may be sufficient to explain the difference. While on the topic of dryness of the test gas it is particularly interesting to note the results of Daen-De Broer (1963). Their relaxation times, obtained by studying the normal shock with an integrated schlieren system, were longer than those of Johannesen and this they claim is because they baked their tube prior to a run at 300°C. to ensure that the tube was perfectly dry.

3.4 Interferometric observations of the expansion wave.

Preliminary calculations to determine the frozen and equilibrium conditions that exist downstream of a corner for the supersonic expansion of Carbon Dioxide showed that of all the state variables the density variation is the least sensetive to relaxation effects (see figure 3.4(1)). It was found that the temperature is the ideal measurement to make with the pressure lying in between the two. Owing to the size of the model, useful surface pressure measurements were not possible and at the present time the measurement of temperature is still a formidable problem. Thus the only immediate practical alternative was to use the Mach-Zhender interferometer to try to detect the rather insensitive density change which arises from the non-equilibrium effects.

The magnitude of the density change due to relaxation effects downstream of the corner for Carbon Dioxide is less than one per cent of the freestream density for a 20° expansion. To make this change correspond to a half of one fringe shift the initial channel pressures that are needed vary from 500 mm. Hg at a Shock Mach number of $M_s = 2.5$ to about 140 mm for $M_s = 5$. The corresponding

fringe shift through the expansion itself then range from 60.5 at M = 2.5 to 26 at Hg = 5. Thus, one is trying to detect a $\frac{1}{2}$ a fringe in 26 - 60 fringes. If the flow were inviscid and the density drop at the corner was discontinuous this may have been practical but unfortunately the viscous interaction of the boundary layer on the wedge with the expansion spreads out this theoretical drop to a considerable extent. With the initial perssures required to obtain a half a fringe shift the extent of the relaxation zone along the wall has shrunk to a few millimetres and has thus become blended with the viscous effects. Little data is available about the extent of the downstream effect the boundary layer has on the expansion but some experiments in an intermittent supersonic wind tunnel performed at the College of Aeronautics (Clarke and Gibson, and Cleaver and Zuckerman) show that this can be of the order of two or three boundary-layer thicknesses for a turbulent boundary layer. The flow situation is further complicated by the boundary layers on the window walls and for the initial pressures which are needed the fringe shift due to the side wall boundary layers can be greater than the fringe shift associated with the relaxation effects. Bearing these points in mind, the overall density change through the expansion was measured for several shock Mach numbers, see figure 3.4(2), and as can be seen the scatter from run to run is greater than the difference that one wishes to detect.

Thus the main conclusion of these interferometric investigations is that the viscous interactions downstream of the corner play such an important part in the expansion process that the measurement of the density in particular is severely handicapped. In fact this study suggests that a more detailed investigation of the viscous interaction of the boundary layer with an isentropic Prandtl-Meyer expansion would be a profitable one from both the theoretical and experimental point of view.

One further interesting point which was not pursued in detail is the possibility of utilising the upstream facing shock wave (see figure (3.4(2)), which is generated by the unsteady wave

processes, to determine relaxation times. In the present experimental arrangements the wedge cannot be made long enough to separate the shock wave from the expansion fan but if this could be done the wave (see figure (3.4/2)) is sufficiently plane for interferometric observations to be practically useful. If the expansion is made sufficiently small, this upstream shock is weak enough for it to be fully dispersed and may prove a useful way of observing fully dispersed wave in a dissociating gas.

4.0 Concluding Remarks

The problem of the non-equilibrium supersonic flow of a relaxing or reacting gas through a plane expansion has been discussed from the numerical, analytical and experimental points of view.

The numerical solutions of the supersonic flow of an Ideal Dissociating Gas agreed closely with those obtained by Appleton (1960). It was also shown that care must be exercised in choosing the mesh size near the corner, and that according to the choice of mesh size the density could be made to increase or decrease downstream of the corner. 'Correct' choice of the computing intervals indicated that the density decreases from its frozen value at the corner to the infinite rate equilibrium value. The pressure variation along the wall exhibited the overshoots in pressure obtained by Appleton and to the extent of the calculations it tended to the infinite rate equilibrium value, as did the temperature. This example also revealed the importance of the entropy and vorticity production associated with the non-equilibrium state of the gas and it was reflected in the inability to predict beforehand the final state of the gas far downstream of the corner. No recombination shock was discovered.

The formal second order theory which described in an approximate manner, how far the state of the gas, a long way downstream of the corner, deviated from the infinite rate equilibrium values, showed that for a rather simplified relaxing gas model, that on the wall

(i) the asymptotic pressure equalled the infinite rate equilibrium value,

(ii) the asymptotic temperature was greater than the infinite rate equilibrium value,

(iii) the asymptotic density was less than the infinite rate equilibrium value.

In addition, the theory showed that at the corner, where the flow is frozen, the second order Busemann solution is obtained and that the density will decrease and the pressure and temperature will increase to their asymptotic values.

An exact solution to the second order problem was not possible throughout the relaxation zone and an approximate solution was obtained by treating $\left(\frac{M_e^2-1}{M_\infty^2-1} - 1\right)$ as a small parameter. This gave a monotonic variation of the pressure between the corner and the asymptotic value. With this approximation the density was found to be extremely sensitive near the corner and it incorrectly predicted the gradient at the corner and overshoots were obtained which were similar in character to the numerical calculations which used the wrong mesh size.

The analysis, like so many second order solutions, is algebraically complex but in view of the time involved in the digital computor calculations of such problems it may well be worth while extending the present analysis to more complex but realistic situations.

It was found that linearised theory could readily be extended to gases with more than one relaxing or reacting mode, and could at the same time include coupling effects between the inert modes. An example was discussed for a two relaxing mode system with the object of assessing the importance of possible coupling effects between the bending and stretching modes of the Carbon Dioxide molecule in a plane expansion and it was concluded that although the differences were finite it would be difficult to detect them experimentally.

Overall interferometric observations of the supersonic flow of high temperature Carbon Dioxide through a plane expansion

have been inconclusive due to the excessive viscous interaction of the boundary layer on the model and on the windows. Analysis of the head of the expansion wave however, have borne fruitful results. By measuring the decay of the density gradient that occur along the wave-head in a relaxing gas with quantitative Schlieren methods estimates of the relaxation times have been obtained. This assumed that the conditions ahead of the expansion wave are the equilibrium conditions which exist behind the primary shock wave in the shock tube. The method has the advantage that relaxation times can be obtained for specific values of the temperature and density (say) for conditions which are near to equilibrium. The accuracy was not high but on the whole the results compare favourably with those of Johannesen et al (1961) who studied the non-equilibrium region behind a normal shock. Relaxation times were also estimated by interferometric observation of the normal shock and the two sets of results did not agree. This discrepancy could arise through the residual water vapour in the shock tube and it was concluded that since the initial pressures in the expansion wave experiments were always five or six times higher than the corresponding conditions in the shock wave experiments that the gas could be five or six times drier. This could be sufficient to cause the increase in the measured relaxation times.

These preliminary results do suggest that the technique may prove suitable for determining relaxation times or recombination rate coefficients for other gases.

5.0 References

Appleton, J.P. (1960). 'Structure of a Prandtl-Meyer expansion in an ideal dissociating gas.' U.S.A.A. rep. 146.

Appleton, J.P. (1963). 'Structure of a Prandtl-Meyer expansion in an ideal dissociating gas.' Phys. Fluids 6, 8.

Blythe, P.A. (1961). 'Comparison of exact and approximate methods for anlysing vibrational relaxation regions.' Journ.Fluid Mech. 10.

Blythe, P.A. (1963). 'Non-equilibrium flow through a nozzle.' Journ.Fluid Mech. 17, 1.

Bray, K.N.C. (1959) 'Atomic recombination in a hypersonic wind tunnel nozzle.' Journ.Fluid Mech. 6, 1.

Busing, J.R. (1962). 'The effect of surface catalytic efficiency on stagnation point heat transfer.' Archiwum Mechaniki Stosowanej 3/4, 14.

Chu, B.T. (1957). 'Wave propagation and the method of characteristics in reacting, gas mixtures with application to hypersonic flow.' Tech. Note W.A.D.C. 57-213.

Clarke, J.F. (1960). 'The linearised flow of a dissociating gas.' Journ.Fluid Mech. 7, 577.

Clarke, J.F. and Cleaver, J.W. (1963). 'Green's functions and the non-equilibrium equation with applications to non-equilibrium free streams.' College of Aeronautics Rep.No. 163.

Clarke, J.F. and McChesney M. (1963). 'The dynamics of real gases.' Butterworths, London.

Cleaver, J.W. (1959). 'The two dimensional flow of an ideal dissociating gas.'
College of Aeronautics Rep.No. 123

Courant and Friedrich. (1948). 'Supersonic flow and shock waves.'
Interscience publications.

Daen, J., and De Boer, D.C.T. (1962). 'Some studies on Argon, Helium and Carbon Dioxide with an integrated Schlieren Instrumentated shock tube.'
J. Chem. Phys. 36, 5.

Der, K.K. (1961). 'Linearised supersonic non-equilibrium flow past an arbitrary boundary.'
N.A.S.A. Tech. Rep. R-119.

Der, J.J. (1963). 'Theoretical studies of supersonic two dimensional and axisymmetrical non-equilibrium flow, including calculations through a nozzle.'
N.A.S.A. Tech. Rep. R-164.

Erdelyi, A, Magnus, W., Oberhettinger, F, and Tricomi, F.G. (1954). 'Tables of integral transforms.'
Vol.1. McGraw-Hill Book Co, inc.

Feldman, S. (1958). 'On the existence of recombination shocks.'
The physics of fluids. 1, 6.

Feldman, S. (1957). 'The chemical kinetics of air at high temperatures.'
AVCO Res. Rept. No. 4.

Glass, I.I. and Takano, A. (1963). 'Non-equilibrium expansion flow of dissociated oxygen around a corner.'
U.T.I.A. Rep. No. 91.

Griffith, W, Brickl, D. and Blackman, V.H. (1956). 'Structure of shock waves in polyatomic gases.'
Phys. Rev. 102.

Holder-North (1963). 'Schlieren Methods.'
Her Majesty's Stationary Office.

Isenberg, J.S. 'The method of characteristics in compressible flow.' Tech. Rept. No. F-TR-1173A-ND

Blythe, P.A., and Gerrard, J.H. (1962) 'Experimental and theoretical analysis of vibrational relaxation regions in Carbon Dioxide.' Journ. Fluid Mech. 13, 2.

Kirkwood, J.G. and Wood, W.W. (1957) 'Hydrodynamics of a reacting and relaxing fluid.' J. Appl. Phys. 28, pp. 395.

Lighthill, M.J. (1953) 'On boundary layers and upstream influence II.' Proc. Roy. Soc. Series A 217.

Moore, F.K. and Gibson, W.E. (1960) 'Propagation of weak disturbances in a gas subject to relaxation effects.' J. Aero. Space Sci's. 27, 117.

Morrison, J.A. (1956) 'Wave propagation in voigt materials' Quart. Appl. Maths 14.

Napolitano, L.G. (1960) 'Non-equilibrium centred rarefaction wave for a reacting mixture.' A.E.D.C. TN-60-129.

Napolitano, L.G. (1961) 'On two new methods for the solution of non-equilibrium flows.' University of Naples, I.A.Rep.No. 42.

Schwartz, R.N. (1954) 'The equations governing vibrational relaxation phenomena in Carbon Dioxide gas.' N.A.V.O.R.D. Rep.No. 3701.

Shanahan, R.J. and Inger, G.R. (1962). 'Non-equilibrium centred expansion of a dissociated supersonic gas flow.' Douglas Rep. SM-42 492.

Smiley, E.F. and Winkler, E.H. (1954) 'Shock tube measurements of vibrational relaxation.' J. Chem. Phys. 22

Stulov, V.P. (1962) 'The flow of an ideal dissociating gas about a convex angle corner with non-equilibrium taken into account.'
R.A.E. translation 1012.

Tanner, L.H. (1956) 'The optics of the Mach-Zehnder interferometers.'
R. & M. 3069.

Dyke, M.D. Van (1951) 'A study of second order supersonic flow theory.'
N.A.C.A. T.N. 2200.

Vincenti, W.G. (1959) 'Non-equilibrium flow over a wavy wall.'
J. Fluid Mech. 6.

Vincenti, W.G. (1961) 'Calculations of the one dimensional non-equilibrium flow of air through a hypersonic nozzle.
A.E.D.C.-TN-61-65.

Witteman, W.J. (1961) 'Vibrational relaxation in Carbon Dioxide.'
J. Chem. Phys. 35.

Wood, W.W. and Parker, F.R. (1958)
'Structure of a centred rarefaction wave in a relaxing gas.'
Phys. Fluids 1, 3.

List of reports consulted but not specifically mentioned in the text

Byron, S.R. 'Interferometric measurement of the rate of oxygen heated by strong shock waves.' Cornell University Aeronautical Engineering Rept. Contract N401 (25).

Clarke, J.F. (1958) 'The flow of chemically reacting mixtures.' College of Aeronautics Rep. No. 117.

Clarke, J.F., Cleaver, J.W. and Lilley, G.M. (1964) 'A review of analytical studies of reacting or relaxing gas flows' Inst. Mech. Eng.

Fowler and Guggenhiem (1949) 'Statistical Thermodynamics.' Cambridge University Press.

Lee, R.S. (1963) 'A unified analysis of supersonic non-equilibrium flow over a wedge.' I.A.S. paper 63 - 40.

Napolitano, L.G. (1963) 'Chemical relaxation for channel flow of of doubly reacting mixtures.' University of Naples, I.A. Rep.No.50.

Ferri, A. (1961) 'Fundamental Data obtained from shock tube experiments.' AGARDograph No. 41 High Speed Aerodynamics.

Spence, D.A. (1961) 'Unsteady shock propagation in a relaxing gas.' Proc. Roy. Soc. A 264.

Wegener, P.P. and Cole, J.D. (1960) 'Experiments on the propagation of weak disturbances in stationery supersonic nozzle flow of chemically reacting gas mixtures.' J.P.L. Rept. No. 20 - 134.

Appendix A

In this appendix a brief statement is made of some of the points underlying the manipulations that are needed to obtain the second order pressure perturbation.

1. The determination of $\bar{F}$.

Upon taking the transform of F, defined equation 2.5(14) it is found that

$$\bar{F}(z,\eta) = z(z+1)\bar{\varphi} + (z+1)\left(\frac{\partial\bar{\psi}}{\partial\eta} - z\bar{\psi}\right) - M_f^2 z(z+1)\bar{\Omega} + \frac{C_{v1}}{C_{pe}} M_f^2 z\bar{\Omega} - \gamma_f M_f^2 \frac{C_{v1}}{C_{pe}} z\bar{\vartheta} + M_f^2 \frac{C_{v1}}{C_{pe}} z^2\bar{\Lambda} \qquad A(1)$$

Before proceeding further it is necessary to discuss the individual terms.

(a) Evaluation of $\bar{Q}$

This like the rest of the terms appearing in A 1 may be obtained by use of the convolution theorem.*

---

* In applying the convolution theorem the transforms of the first order solutions are needed. These are

$$\bar{p}_1 = \frac{\gamma_f M_f^2}{B_f} \frac{1}{a} \exp(z-a)\eta$$

$$u_1 = \frac{1}{B_f} \frac{1}{a} \exp(z-a)\eta$$

$$\bar{\rho}_1 = \frac{1}{B_f}\left\{ M_f^2 + B_f^2(B^2-1)/1+z \right\} \frac{1}{a} \exp(z-a)\eta$$

$$\bar{T}_{v_1} = \frac{C_{pf}}{C_{v1}} \frac{B_f(B^2-1)}{(z+1)\,a} \exp(z-a)\eta$$

$$\bar{T}_1 = \left\{ (\gamma_f-1)M_f^2 - \frac{B_f^2(B^2-1)}{(1+z)} \right\} \frac{1}{B_f} \frac{1}{a} \exp(z-a)\eta$$

$$(\bar{T}_1 - \bar{T}_{v1}) = \frac{B_f(B^2-1)}{C_{v1}} \frac{C_{pe}}{1+z} \frac{z}{a} \exp(z-a)\eta$$

$$a = z\sqrt{\frac{B^2+z}{1+z}} \qquad a(z-q) = (z-q)\sqrt{\frac{B^2+z-q}{1+z-q}}$$

thus noting that $\varphi = \gamma M_f^2 \left\{ (\rho_1 + u_1) u_{1\xi} + B_{f\infty} v_1 (u_{1\eta} - u_{1\xi}) \right\}$ then

$$\bar{\varphi} = -\frac{\gamma_f M_f^2}{2\pi i} \int_{d-i\infty}^{d+i\infty} \left\{ \frac{1}{q} - \frac{1}{q\sqrt{(1+q)(B^2+z-q)}} \right\} e^{q - q\sqrt{\frac{B^2+q}{1+q}} + z - q - (z-q)\sqrt{\frac{B^2+z-q}{1+z-q}}} dq \qquad A(2)$$

It is not possible to evaluate this easily by complex variable theory because of the essential singularity at $q = -1$, but expanding in powers of (B^2-1) it is not difficult to show that

$$\bar{\varphi} = \gamma_f M_f^2 \frac{B^2-1}{2} \cdot \frac{1}{z+1} + O(B^2-1)^2 \qquad A(3)$$

In section (2.5.9) a solution is obtained along $\eta_0 = 0$ as $z \to 0$. Under these conditions A 2 reduces to

$$\bar{\varphi} = +\frac{2}{\pi}\sqrt{\frac{2}{B^2+1}} \int_0^\infty \left\{ \frac{B^2}{B^2+t^2} - \frac{1}{t^2+1} \right\} \sqrt{\frac{t^2 + \frac{B^2+1}{2}}{t^2 + 2B^2/B^2+1}}\, dt \qquad A(4)$$

This has not be solved analytically. The numerical value of this integral has been found as $\bar{\varphi} = 0.104$.

(b) Evaluation of $\bar{\Psi}$

$\Psi = +\gamma_f M_f^2 \left\{ (\rho_1 + u_1) v_{1\xi} + B_f v_1 (v_{1\eta} - v_{1\xi}) \right\}$ thus

$$\bar{\Psi} = \frac{\gamma_f M_f^2}{2\pi i} \int_{d-i\infty}^{d+i\infty} B_{f_\infty} \left\{ \frac{1}{q}\sqrt{\frac{B^2+q}{1+q}} - \frac{1}{q}\sqrt{\frac{B^2+z-q}{1+z-q}} \right\} \exp q - q(q) + z - q(q)(z-q) \qquad A(5)\, dq$$

which is given approximately by

$$\bar{\Psi} = -\gamma_f M_f^2 B_f \frac{(B^2-1)}{2} \frac{1}{1+z} + O(B^2-1)^2 \qquad A(\ )$$

(c) Evaluation of $\bar{\Omega}$

From equation 2.5(10)

$$\bar{\Omega} = u_1 p_{1\xi} + B_f v_1 (p_{1\eta} - p_{1\xi}) + \gamma_f \{ p_1 u_{1\xi} + B_f p_1 (v_{1\eta} - v_{1\xi}) \}$$

$$+ \frac{c_{u1}}{c_{uf}} \{ (p_1 + u_1) \bar{T}_{v_{1\xi}} + v_1 B_f (\bar{T}_1 - \bar{T}_f)$$

$$\therefore \bar{\Omega} = -\frac{\gamma_f M_f^2}{2\pi i} \int_{d-i\infty}^{d+i\infty} \left\{ \frac{1}{B_f^2} \frac{1}{q} \sqrt{\frac{1+q}{B^2+q} \frac{1+z-q}{B^2+z-q}} + \frac{1}{q} + \frac{\gamma_f}{B_f^2} \frac{1}{q} \sqrt{\frac{1+q}{B^2+q} \frac{1+z-q}{B^2+z-q}} + \frac{\gamma_f}{q} \sqrt{\frac{1+q}{B^2+q} \frac{B^2+z-q}{1+z-q}} \right\}$$

$$\times \exp \left[q - a(q) + z - q - a(z-a) \right] dq$$

$$+ \frac{\gamma_f B_f^2 (B^2-1) c_{uf}}{c_{u1}} \frac{}{2\pi i} \int_{d-i\infty}^{d+i\infty} \left\{ \frac{1}{q} \frac{1}{1+z-q} \sqrt{\frac{1+z-q}{B^2+z-q}} - \frac{1}{q} \frac{1}{1+z-q} \right\} \exp \left[q - a(q) + z - q - a(z-q) \right] dq$$

$$\bar{\Omega} = -\frac{\gamma_f M_f^2 (1+\gamma_f) M_f^2}{2 B_f^2} + \gamma_f M_f^2 \left[\frac{1+\gamma_f - B_f^2 \gamma_f}{B_f^2} \right] \frac{B^2-1}{2(1+z)} + \frac{\gamma_f M_f^2 M_f^2 (1+\gamma_f)(B^2-1) z}{B_f^2} \frac{}{2(1+z)} \eta_0 + O(B^2-1)$$

A(7)

(d) Evaluation of $\bar{\vartheta}$

From equation 2.5(13)

$$\bar{\vartheta} = \left\{ (u_1 - T_1) p_{1\xi} + B_f v_1 (p_\eta - p_{1\xi}) \right\} - \left\{ (p_1 - 2T_1 + u_1) T_{1\xi} + B_f v_1 (T_{1\eta} - T_{1\xi}) \right\} + \left\{ p_1 u_{1\xi} + B_f p_1 (v_{1\eta} - v_{1\xi}) \right\}$$

$$= -\frac{1}{2\pi i} \int_{d-i\infty}^{d+i\infty} \left\{ \frac{\gamma_f M_f^2}{B_f^2} \left(1 + (\gamma_f - 1) M_f^2 - \frac{B_f^2 (B^2-1)}{1+q} \right) \frac{1}{q} \sqrt{\frac{1+q}{B^2+q} \frac{1+z-q}{B^2+z-q}} + \frac{\gamma_f M_f^2}{q} \right\} \exp \left[q - a(q) + z - q - a(z-q) \right] \eta_0 \, dq$$

$$- \frac{1}{2\pi i} \int_{d-i\infty}^{d+i\infty} \left[\left\{ (2M_f^2 - \gamma_f M_f^2 - 1) + \frac{2B_f^2 (B^2-1)}{1+q} \right\} \left\{ (\gamma_f - 1) M_f^2 - \frac{B_f^2 (B^2-1)}{1+z-q} \right\} \frac{1}{B_f^2} \frac{1}{q} \sqrt{\frac{1+q}{B^2+q} \frac{1+z-q}{B^2+z-q}} \right.$$

$$\left. - \frac{1}{q} \left\{ (\gamma_f - 1) M_f^2 - \frac{B_f^2 (B^2-1)}{1+z-q} \right\} \right] \exp \left[q - a(q) + z - q - a(z-q) \right] \eta_0 \, dq$$

$$- \frac{1}{2\pi i} \int_{d-i\infty}^{d+i\infty} \left[\left\{ M_f^2 + \frac{B_f^2 (B^2-1)}{1+q} \right\} \left\{ \frac{1}{B_f^2} \frac{1}{q} \sqrt{\frac{1+q}{B^2+q} \frac{1+z-q}{B^2+z-q}} + \frac{1}{q} \sqrt{\frac{1+q}{B^2+q} \frac{B^2+z-q}{1+z-q}} \right\} \right]$$

$$\times \exp \left[q - a(q) + z - q - a(z-a) \right] \eta_0 \, dq$$

$$\simeq -\frac{(\gamma_f M_f^2)^2}{2B_f^2} - \frac{(\gamma_f-1)^2 M_f^4}{2B_f^2} - \frac{M_f^4}{2B_f^2}$$

$$+ \frac{(\gamma_f M_f^2)\left[1+(\gamma_f-1)M_f^2\right]}{B_f^2}\frac{B^2-1}{2(1+z)} + \frac{(\gamma_f M_f^2)^2}{B_f^2}\frac{z}{1+z}\eta_0\frac{B^2-1}{2}$$

$$+\left\{-\frac{(2M_f^2-\gamma_f M_f^2-1)}{(1+z)} - \frac{(\gamma_f-1)M_f^2(2M_f^2-\gamma_f M_f^2-1)}{2B_f^2}\left(\frac{1}{1+z}+\frac{z}{1+z}\eta_0\right)\right.$$

$$\left. + \frac{B_f^2}{1+z} + \frac{(\gamma_f-1)M_f^2}{2}\left(\frac{z}{1+z}\right)\eta_0\right\}(B^2-1)$$

$$+\frac{1}{2}\left(\frac{M_f^2}{B_f^2}-M_f^2\right)\frac{B^2-1}{1+z} + \frac{M_f^4}{2B_f^2}\frac{z}{1+z}\eta_0(B^2-1) + O(B^2-1)^2 \qquad A(8)$$

(e) Evaluation of $\bar{\Lambda}$

From equation 2.5(11)

$$\dot{\Lambda} = U_1 T_{v_{1\xi}} + B_{f_\infty} V_1 \left(T_{v_{1\eta}} - T_{v_{1\xi}}\right)$$

$$\bar{\Lambda} = -\frac{1}{2\pi i}\int_{d-i\infty}^{d+i\infty} \frac{\gamma_f(B^2-1)C_{uz}}{C_{u_1}}\left[\frac{1}{q}\frac{1}{1+z-q}\sqrt{\frac{1+q}{B^2+q}\frac{1+z-q}{B^2+z-q}} + \frac{B_f^2}{q(1+z-q)}\right]$$

$$\times \exp\left[q-a(q)+z-q-a\left|z-q\right.\right]\eta_0\, dq$$

$$\simeq -\frac{\gamma_f(B^2-1)C_{uz}}{C_{u_1}}\frac{M_f^2}{1+z} + O(B^2-1)^2 \qquad A(9)$$

2. Having obtained the transforms of $\bar{\Phi}$, $\bar{\Psi}$ etc then the collection of terms independent of (B^2-1) and then $(B^2-1)^2$ etc. from equations A(3), A(5), A(7), A(8) and A(9) gives after substitution into equation A(1) the coefficients $\bar{F}o(z,\eta)$, $\bar{F}_1(z,\eta)$ etc. These may now be substituted into equation 2.5(54). After performing the two integrations equation 2.5(55) results.

Appendix B : An asymptotic solution for $\frac{\partial p_2}{\partial \xi}$ for small ξ.

The gradient of the second order pressure perturbation can be written in the form

$$\frac{\partial p_2}{\partial \xi}(\xi,0) = \frac{1}{2\pi i}\int_{c-i\infty}^{c+i\infty} \frac{1}{B_\xi^2}\sqrt{\frac{1+z}{B^2+z}}\,\exp \xi z\,\frac{1}{1+z}\,\frac{1}{2\pi i}\int_{d-i\infty}^{d+i\infty} \frac{\sum_i g_i(z) P_i(q) Q_i(z-q)}{z\sqrt{\frac{B^2+z}{1+z}}+q\sqrt{\frac{B^2+q}{1+q}}+z-q\sqrt{\frac{B^2+z-q}{1+z-q}}}\,dq\,dz$$

$$+\frac{\gamma_c M_\xi^2}{B_\xi^2}\,\frac{1}{2\pi i}\int_{c-i\infty}^{c+i\infty}\sqrt{\frac{1+z}{B^2+z}}\,\bar{V}_2(z,0)\exp \xi z\,dz, \qquad \text{B(1)}$$

where the P_i, Q_i, g_i are as defined in equation 2.5(52). As $\exp \xi z$ is the only exponential term in the integrand transform theory shows that a solution for small ξ corresponds to the solution of B(1) for large Z. Therefore the first task is to evaluate the q integral for the case when z is large. When z is large the denominator behaves like 2z therefore one is left to deal with $\int_{d-i\infty}^{d+i\infty}\sum_i g_i(z)P_i(q)Q_i(z-q)\,dq = \bar{F}(z,0)$ In a similar manner to the last appendix it is necessary to evaluate $\bar{\Phi}, \bar{\Psi}$ etc. when z is large.

First note the following, which arise when z is large.

$$\text{(i)}\quad \frac{1}{2\pi i}\int_{d-i\infty}^{d+i\infty}\frac{1}{q}\sqrt{\frac{1+q}{B^2+q}\,\frac{1+z-q}{B^2+z-q}}\,dq \simeq \frac{1}{2}-\frac{B^2-1}{2z}$$

$$\text{(ii)}\quad \frac{1}{2\pi i}\int_{d-i\infty}^{d+i\infty}\frac{1}{q}\sqrt{\frac{1+q}{B^2+q}\,\frac{B^2+z-q}{1+z-q}}\,dq \simeq \frac{1}{2}+\frac{B^2-1}{2z}$$

$$\text{(iii)}\quad \frac{1}{2\pi i}\int_{d-i\infty}^{d+i\infty}\frac{1}{q}\sqrt{\frac{B^2+q}{1+q}\,\frac{1+z-q}{B^2+z-q}}\,dq \simeq \frac{1}{2}-\frac{B^2-1}{2z} \qquad \text{B(2)}$$

$$\text{(iv)}\quad \frac{1}{2\pi i}\int_{d-i\infty}^{d+i\infty}\frac{1}{q}\,\frac{1}{1+z-q}\sqrt{\frac{B^2+q}{1+q}\,\frac{1+z-q}{B^2+z-q}}\,dq \simeq \frac{1}{z}$$

$$\text{(v)}\quad \frac{1}{2\pi i}\int_{d-i\infty}^{d+i\infty}\frac{1}{q(1+z-q)}\,dq \simeq \frac{1}{z}$$

(vi) $$\frac{1}{2\pi i}\int_{d-i\infty}^{d+i\infty}\frac{1}{q}\frac{1}{1+q}\sqrt{\frac{1+q}{B^2+q}\frac{1+z-q}{B^2+z-q}}\,dq \simeq 0$$

(vii) $$\frac{1}{2\pi i}\int_{d-i\infty}^{d+i\infty}\frac{1}{q}\cdot\frac{1}{1+q}\cdot\frac{1}{1+z-q}\sqrt{\frac{1+q}{B^2+q}\frac{1+z-q}{B^2+z-q}}\,dq \simeq 0$$

B(2)

(viii) $$\frac{1}{2\pi i}\int_{d-i\infty}^{d+i\infty}\frac{1}{q}\cdot\frac{1}{1+z-q}\sqrt{\frac{1+q}{B^2+q}\frac{1+z-q}{B^2+z-q}}\,dq \simeq \frac{1}{z}$$

(ix) $$\frac{1}{2\pi i}\int_{d-i\infty}^{d+i\infty}\frac{1}{q^2}\sqrt{\frac{B^2+z-q}{1+z-q}}\,dq \simeq 0$$

If we now substitute the values of these integrals into equations A(2), A(5), A(7), A(8), A(9) to determine the values of $\bar{\varphi}(z,o)$, $\bar{\psi}(z,o)$ etc. and then substitute the values of $\bar{\varphi}$, $\bar{\psi}$ etc. into A(1) an equation for $\bar{F}(z,o)$ as $z\to\infty$ can be found. This is

$$\frac{\bar{F}(z,0)}{\gamma_f M_f^2} \simeq z(z+1)\left\{\frac{1}{2}+\frac{B^2-1}{2z}\right\} - B_f^2 z\sqrt{\frac{B^2+z}{1+z}}(z+1)\frac{B^2-1}{2z}$$

$$+\frac{z(z+1)M_f^2(B^2-1)}{2}\left\{\frac{(1+\gamma_f)}{B_f^2}\left(\frac{1}{2}-\frac{B^2-1}{2z}\right)+\frac{1}{2}+\gamma_f\left(\frac{1}{2}+\frac{B^2-1}{2z}\right)\right\}$$

$$-\frac{\omega_1}{C_{pe}}M_f^2 z\left\{\frac{1+\gamma_f}{B_f^2}\left(\frac{1}{2}-\frac{B^2-1}{2z}\right)+\frac{1}{2}+\gamma_f\left(\frac{1}{2}+\frac{B^2-1}{2z}\right)\right\}$$

$$+\frac{\omega_1}{C_{pe}}z\gamma_f M_f^2\left\{\frac{1+(\gamma_f-1)M_f^2}{B_f^3}\frac{1}{2}+\frac{1}{2}\right\}$$

$$+\frac{\omega_1}{C_{pe}}z\left\{\frac{M_f^2}{B_f^2}\left(\frac{1}{2}-\frac{B^2-1}{2z}\right)+M_f^2\left(\frac{1}{2}+\frac{B^2-1}{2z}\right)\right\}$$

$$+\frac{\omega_1}{C_{pe}}z\left\{\frac{(2M_f^2-\gamma_f M_f^2-1)(\gamma_f-1)M_f^2}{B_f^2}\left(\frac{1}{2}-\frac{B^2-1}{2z}\right)-\frac{(\gamma_f-1)M_f^2-B_f^2}{2}\right.$$
$$\left.-(2M_f^2-\gamma_f M_f^2-1)(B^2-1)\frac{1}{z}+\frac{B_f^2(B^2-1)}{z}\right\}-z^2\left(\frac{1}{z}+\frac{B_f^2}{z}\right)$$

The pressure gradient may then be written as the following when z is large.

$$\frac{1}{\gamma_f M_f^2}\frac{\partial P_2}{\partial \xi}(\xi=0,0) \sim \frac{1}{2\pi i}\int_{c-i\infty}^{c+i\infty}\left(1-\frac{B^2-1}{2z}\right)\frac{e^{\xi z}\,\bar{F}(z,0)}{2B_f^2 z(1+z)}\,dz + \frac{1}{2\pi i}\frac{1}{B_f}\int_{c-i\infty}^{c+i\infty}\sqrt{\frac{1+z}{B^2+z}}\,\bar{V}_2(z=0)e^{\xi z}\,dz$$

substituting for $\bar{F}(z, 0)$ and collecting terms which behave like $\frac{1}{z}$ gives the finite contribution to the gradient which exists at the corner. This is given by

$$\frac{1}{\gamma_f M_f^2}\frac{\partial P_2}{\partial \xi}(\xi=0,\eta=0) = \frac{(B^2-1)}{4}\left(\frac{1}{B_f^2}-1\right) - \frac{(B^2-1)M_f^2}{8B_f^4}\left(2+4\gamma_f+M_f^2-\gamma_c M_f^2\right)$$

$$+\frac{(\gamma_f-1)M_f^4}{4B_f^4}\frac{c_{vn}}{c_{pe}} - \frac{c_{vn}}{c_{pe}}\frac{(B^2-1)}{2B_f^2}\left(2M_f^2-\gamma_c M_f^2-1\right)$$

$$-\frac{(B^2-1)M_f^2}{2B_f^2} + \frac{(B^2-1)}{B_f^2}$$

Appendix C : An Asymptotic solution for $\frac{\partial \rho_2}{\partial \xi}$ for small ξ.

Starting with the energy equation $h + \frac{q_\infty^2}{2} q^2 = \text{constant}$ it is not difficult to show that

$$\frac{C_{pf_\infty} T_2 + C_{v_{1\infty}} T_{v_2}}{C_{pf_\infty} + C_{v_{1\infty}}} + (\gamma_e - 1) M_e^2 \left(u_2 + \frac{v_1^2 + u_1^2}{2} \right) = 0 \qquad C(1)$$

Noting that $\rho_2 = p_2 - T_2 - \rho_1 T_1$ and substituting for T_{v_2} from equation 2.5(11) C(1) can be written as

$$\frac{\partial \rho_2}{\partial \xi} = \frac{1}{2\pi i} \int_{c-i\infty}^{c+i\infty} \left[z \left\{ M_f^2 + \frac{B_f^2 (B^2-1)}{1+z} \right\} \bar{p}_2 + (\gamma_f - 1) M_f^2 \left\{ z - \frac{C_{v_1}}{C_{pe}} \frac{z}{1+z} \right\} \left\{ \frac{\overline{u_1^2 + v_1^2}}{2} - \frac{\bar{\Phi}}{z} \right\} \right.$$

$$\left. - z \overline{\rho_1 T_1} - \frac{C_{v_1}}{C_{pf}} \frac{z}{1+z} \bar{\Lambda} \right] \exp\{z\} \, dz \qquad C(2)$$

Noting that

$$\overline{\frac{u_1^2 + v_1^2}{2}} = \frac{1}{2} \cdot \frac{1}{2\pi i} \int_{d-i\infty}^{d+i\infty} \left\{ \frac{1}{q(z-q)} \sqrt{\frac{1+q}{B^2+q} \cdot \frac{1+z-q}{B^2+z-q}} + \frac{1}{q(z-q)} \right\} dq$$

and

$$\overline{\rho_1 T_1} = \frac{1}{2\pi i} \int_{d-i\infty}^{d+i\infty} \left\{ \frac{1}{B_f^2} \left((\gamma_f - 1) M_f^2 - \frac{B_f^2 (B^2-1)}{1+q} \right) \left(M_f^2 + \frac{B_f^2 (B^2-1)}{1+z-q} \right) \frac{1}{q(z-q)} \sqrt{\frac{1+q}{B+q} \frac{1+z-q}{B^2+z-q}} \right\} dq$$

and substituting for $\bar{p}_2$, $\bar{\Phi}$ and $\bar{\Lambda}$, then making use of the relations B(2) derived in Appendix (B) the density derivative can be evaluated. This is given in equation 2.5(65).

Appendix D : The vorticity production

The vorticity is given by

$$\frac{\zeta(\xi,\eta)}{\theta^2} = \frac{\partial v_2}{\partial \xi} - B_{f_\infty}\left(\frac{\partial u_2}{\partial \eta} - \frac{\partial u_2}{\partial \bar{\xi}}\right)$$

and is correct to second order. Substituting for u_2 and v_2 from the second order momentum equations then allows us to write

$$\frac{\zeta(\xi,\eta)}{\theta^2} = B_{f_\infty}\int_0^{\xi}\frac{\partial \varphi}{\partial \eta}\,d\xi - B_{f_\infty}\varphi - \psi$$

The first order solution is known exactly along the wall and therefore φ and ψ are known. This is a lengthy operation and a good approximation to the answer can be obtained by treating (B^2-1) as a small parameter. The transform of ζ along the wall is given by

$$\frac{\bar{\zeta}(z,\eta)}{\theta^2} = \frac{B_{f_\infty}}{z}\cdot\frac{\partial \bar{\varphi}}{\partial \eta} - B_f\bar{\varphi} - \bar{\psi}$$

Applying the convolution theorem to determine $\bar{\varphi}$ and $\bar{\psi}$ shows that

$$\frac{\bar{\zeta}(z,\eta)}{\theta^2} = -\frac{1}{2\pi i}\int_{d-i\infty}^{d+i\infty}\left[\frac{B_f}{z}\cdot\frac{1}{q}\left\{1-\sqrt{\frac{B^2+q}{1+q}\,\frac{1+z-q}{B^2+z-q}}\right\}\left\{q\sqrt{\frac{B^2+q}{1+q}}+(z-q)\sqrt{\frac{B^2+z-q}{1+z-q}}\right\}\right.$$
$$\left.+\frac{B_f}{q}\left\{\sqrt{\frac{B^2+q}{1+q}}-\sqrt{\frac{B^2+z-q}{1+z-q}}\right\}\right]dq$$

expanding in terms of (B^2-1) shows that

$$\frac{\bar{\zeta}(z,0)}{\theta^2} \simeq -\frac{(B^2-1)^2}{4}\left(\frac{1}{z}-\frac{1}{z+2}\right)+\cdots$$

Inverting this gives

$$\frac{\zeta(\xi,0)}{\theta^2} \simeq -\left(\frac{B^2-1}{2}\right)^2\left(1-e^{-2\xi}\right)+\cdots$$

Appendix E : Entropy production

To second order the entropy production along the streamlines is given by

$$\frac{S-S_\infty}{S_\infty \theta^2} = c_{v_1}\frac{C_{p_e}}{C_{p_e}}\int_0^{\xi}(T_1-T_{v_1})^2\,d\xi$$

T_1 and T_{v_1} are known exactly along the wall and therefore the integral can be evaluated. However, like the vorticity production a fairly simple, but approximate, answer can be obtained by treating (B^2-1) as a small parameter. Making use of the convolution theorem the transform of the entropy production is

$$\frac{C_{p_e}}{C_{v_1}C_{p_f}}\frac{\overline{S-S_\infty}}{S_\infty\theta^2} = \frac{1}{2\pi i}\int_{d-i\infty}^{d+i\infty}\frac{(\gamma_f-1)^2M_f^4}{B_f^2}\frac{1}{(1+q)(1+z-q)}\sqrt{\frac{1+q}{B^2+q}\frac{1+z-q}{B^2+z-q}}\,dq$$

Expanding in (B^2-1) gives

$$\frac{C_{p_e}}{C_{v_1}C_{p_f}}\frac{\overline{S-S_\infty}}{S_\infty\theta^2} = \left[\frac{(\gamma_f-1)M_f^2}{B_f}\right]^2\left\{\frac{1}{z(z+2)} - \frac{B^2-1}{2z}\left(\frac{z}{(z+2)^2}\right) + \frac{O(B^2-1)^2}{}\right\}$$

Inversint shows that

$$\frac{C_{p_e}}{C_{v_1}C_{p_f}}\frac{\overline{S-S_\infty}}{S_\infty\theta^2} = \left[\frac{(\gamma_f-1)M_f^2}{B_f}\right]^2\left\{1-e^{-2\xi} - (B^2-1)\left(\frac{1-e^{-\xi}}{4} - \frac{\xi}{2}e^{-2\xi}\right)\right\}+\cdots$$

Appendix E : Entropy production

To second order the entropy production along the streamlines is given by

$$\frac{S-S_\infty}{S_\infty \theta^2} = c_{v_1}\frac{C_{p_e}}{C_{p_e}}\int_0^{\xi}(T_1-T_{v_1})^2\,d\xi$$

T_1 and T_{v_1} are known exactly along the wall and therefore the integral can be evaluated. However, like the vorticity production a fairly simple, but approximate, answer can be obtained by treating (B^2-1) as a small parameter. Making use of the convolution theorem the transform of the entropy production is

$$\frac{C_{p_e}}{c_{v_1}C_{p_f}}\frac{\overline{S-S_\infty}}{S_\infty\theta^2} = \frac{1}{2\pi i}\int_{d-i\infty}^{d+i\infty}\frac{(\gamma_f-1)^2M_f^4}{B_f^2}\frac{1}{(1+q)(1+z-q)}\sqrt{\frac{1+q}{B^2+q}\frac{1+z-q}{B^2+z-q}}\,dq$$

Expanding in (B^2-1) gives

$$\frac{C_{p_e}}{c_{v_1}C_{p_f}}\frac{\overline{S-S_\infty}}{S_\infty\theta^2} = \left[\frac{(\gamma_f-1)M_f^2}{B_f}\right]^2\left\{\frac{1}{z(z+2)} - \frac{B^2-1}{2z}\left(\frac{z}{(z+2)^2}\right) + O(B^2-1)^2\right\}$$

Inversint shows that

$$\frac{C_{p_e}}{c_{v_1}C_{p_f}}\frac{\overline{S-S_\infty}}{S_\infty\theta^2} = \left[\frac{(\gamma_f-1)M_f^2}{B_f}\right]^2\left\{1-e^{-2\xi}-(B^2-1)\left(\frac{1-e^{-\xi}}{4}-\frac{\xi}{2}e^{-2\xi}\right)\right\}+\cdots$$

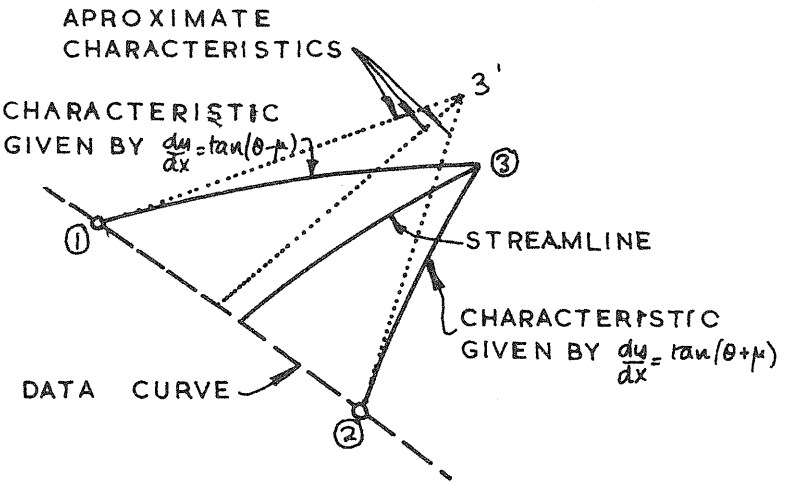

CHARACTERISTIC GRID
FIG. 2·2(1)

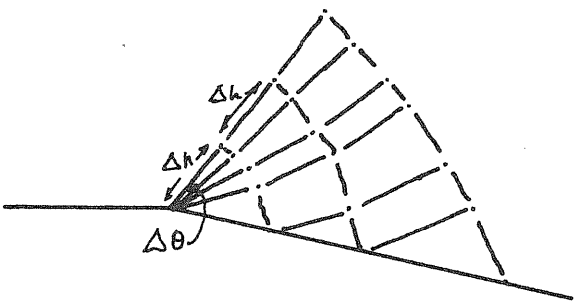

CHARACTERISTIC GRID NEAR THE CORNER
FIG. 2·2(2)

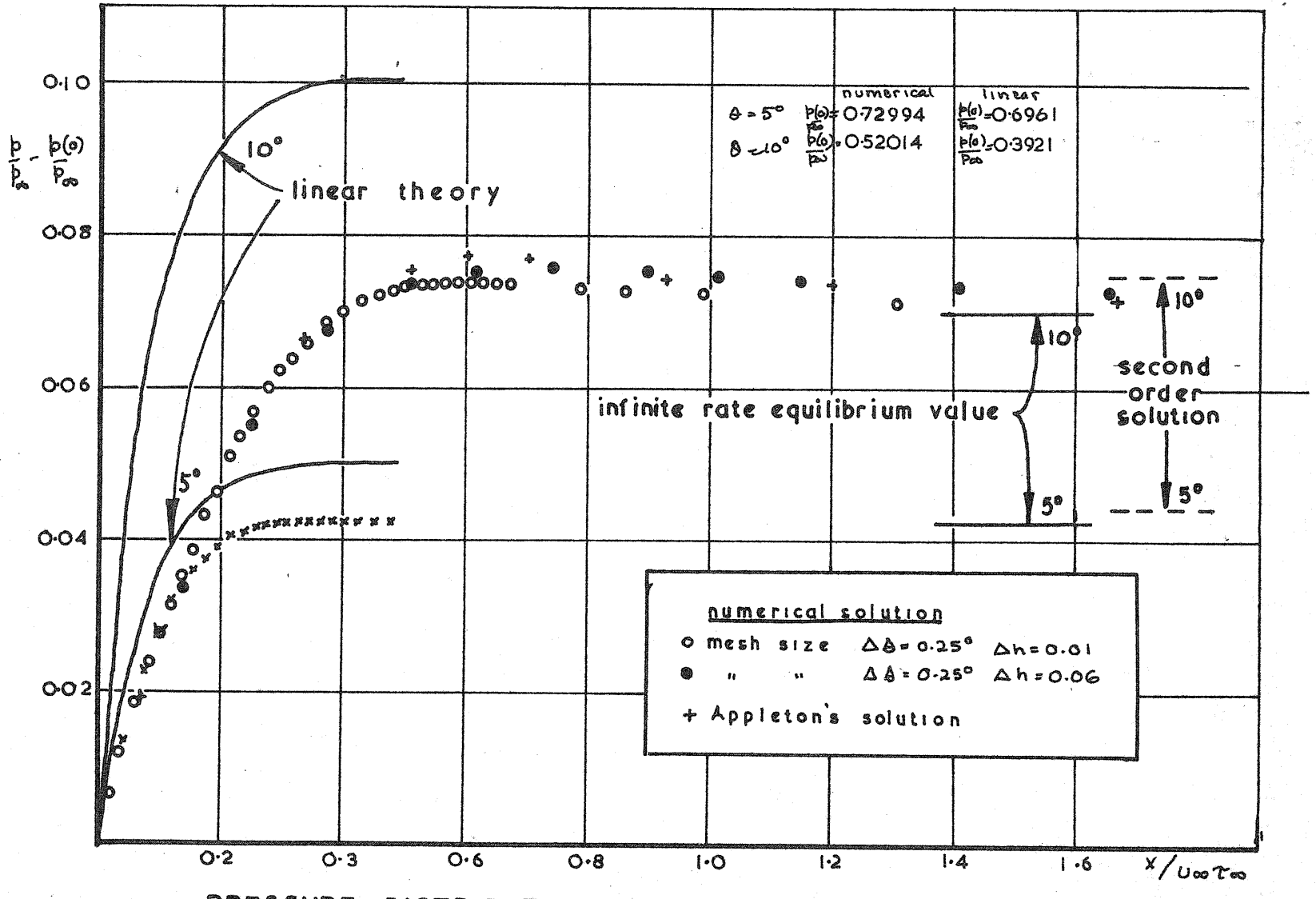

PRESSURE DISTRIBUTION ALONG THE WALL. FIG. 2·3(1)

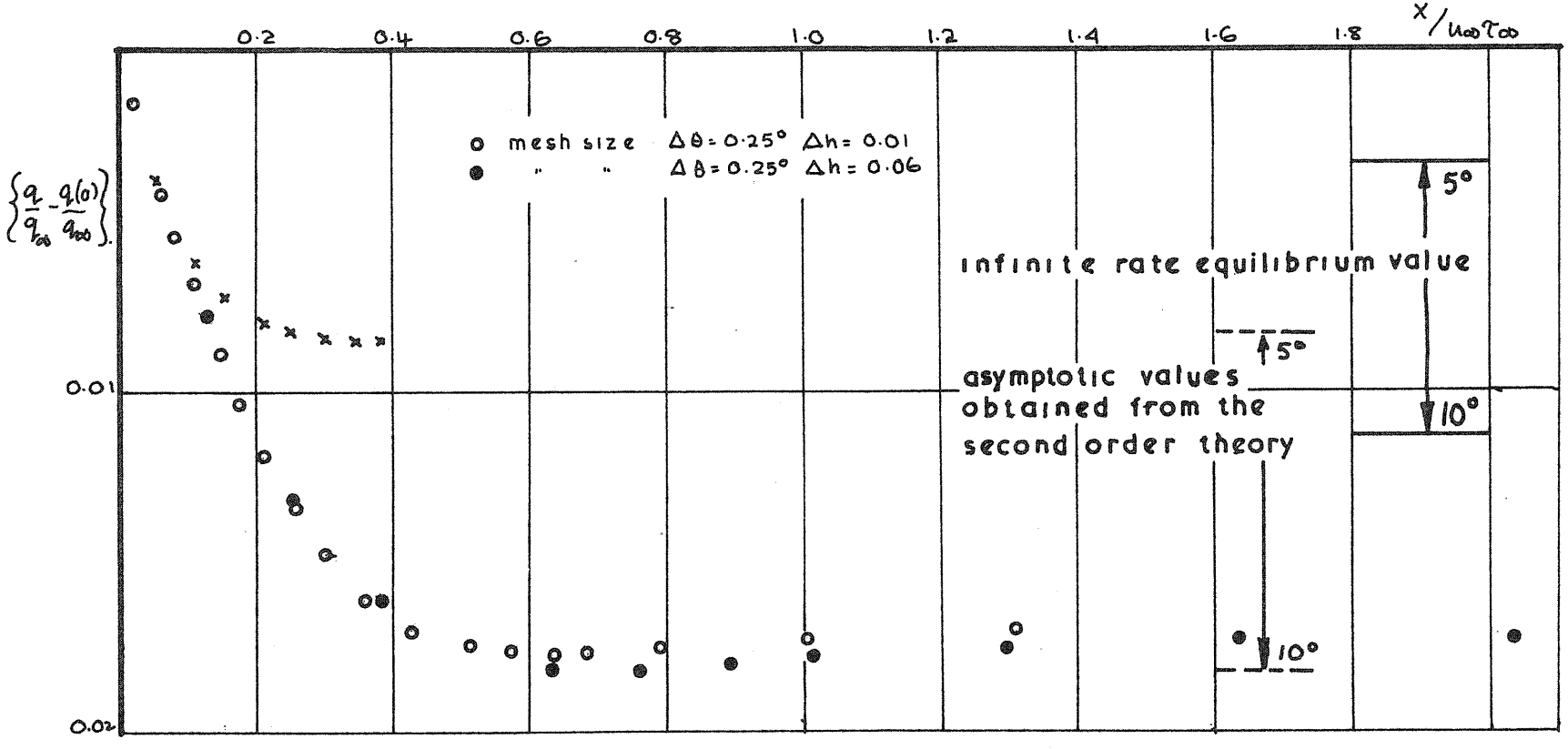

VELOCITY DISTRIBUTION ALONG THE WALL

FIG 2.3(2)

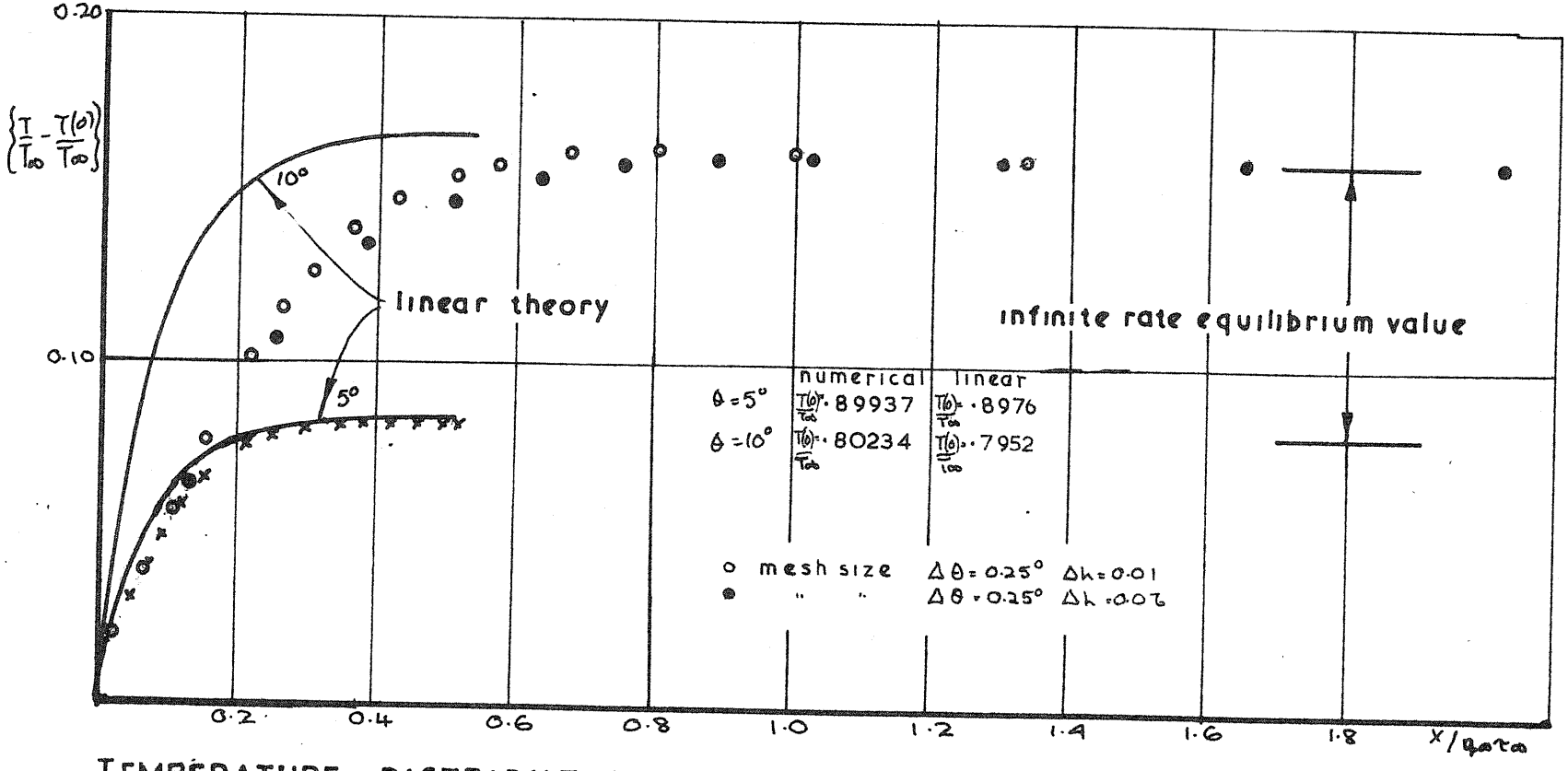

TEMPERATURE DISTRIBUTION ALONG THE WALL

FIG 2·3(3)

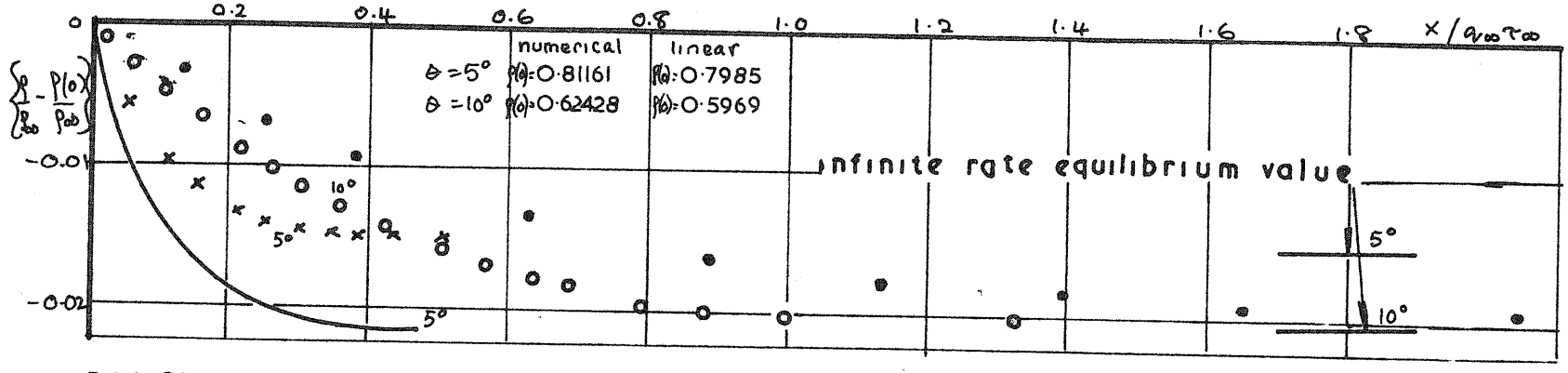

DENSITY DISTRIBUTION ALONG THE WALL

FIG. 2·3(4)

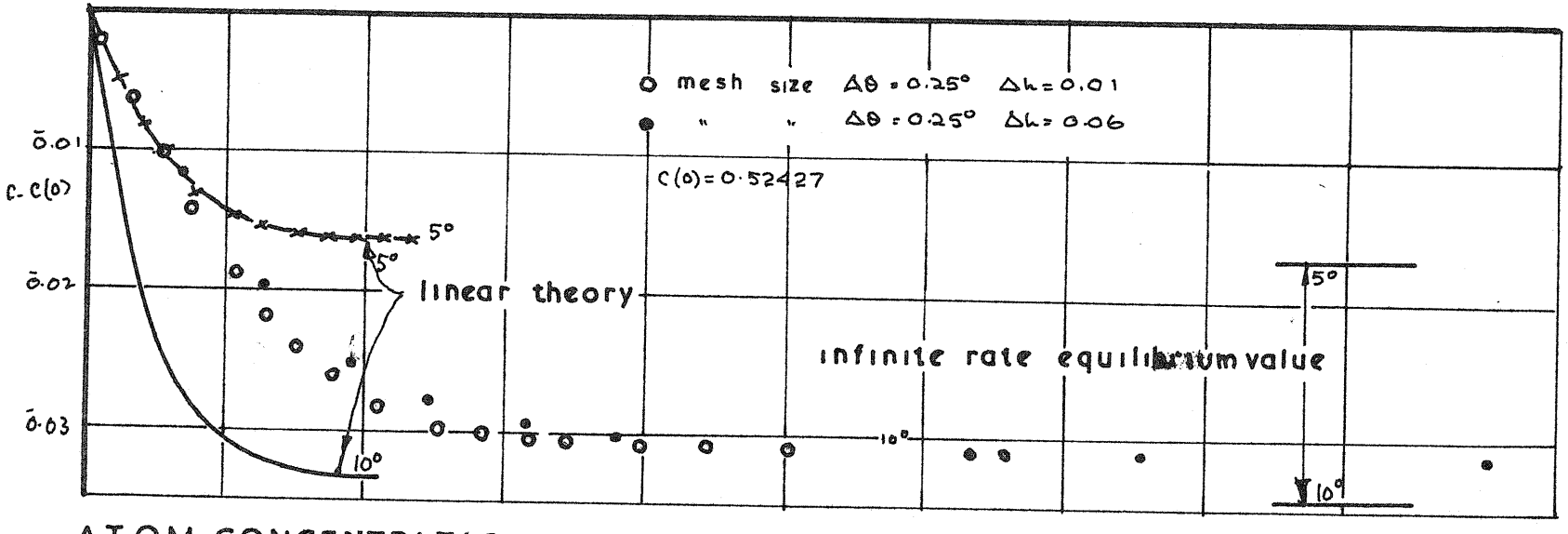

ATOM CONCENTRATION DISTRIBUTION ALONG THE WALL

FIG. 2·3(5)

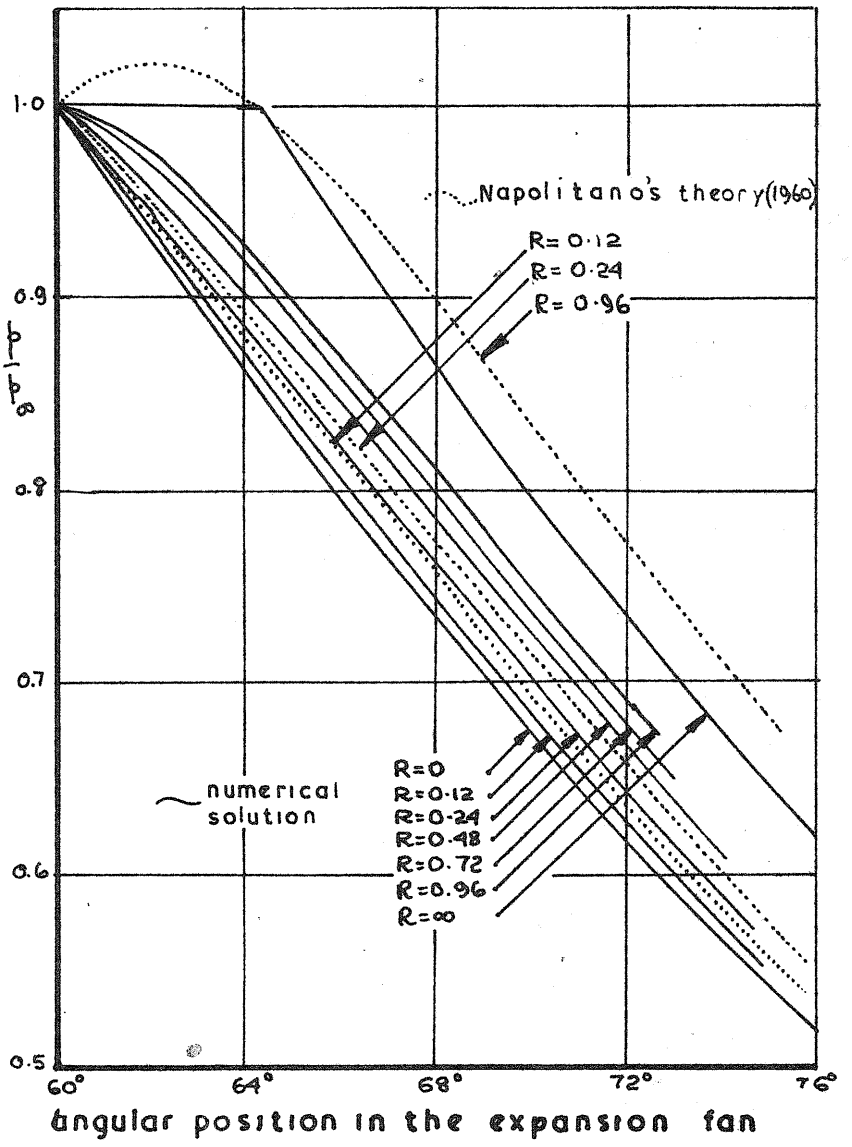

PRESSURE DISTRIBUTION IN THE EXPANSION

FIG. 2·3(6)

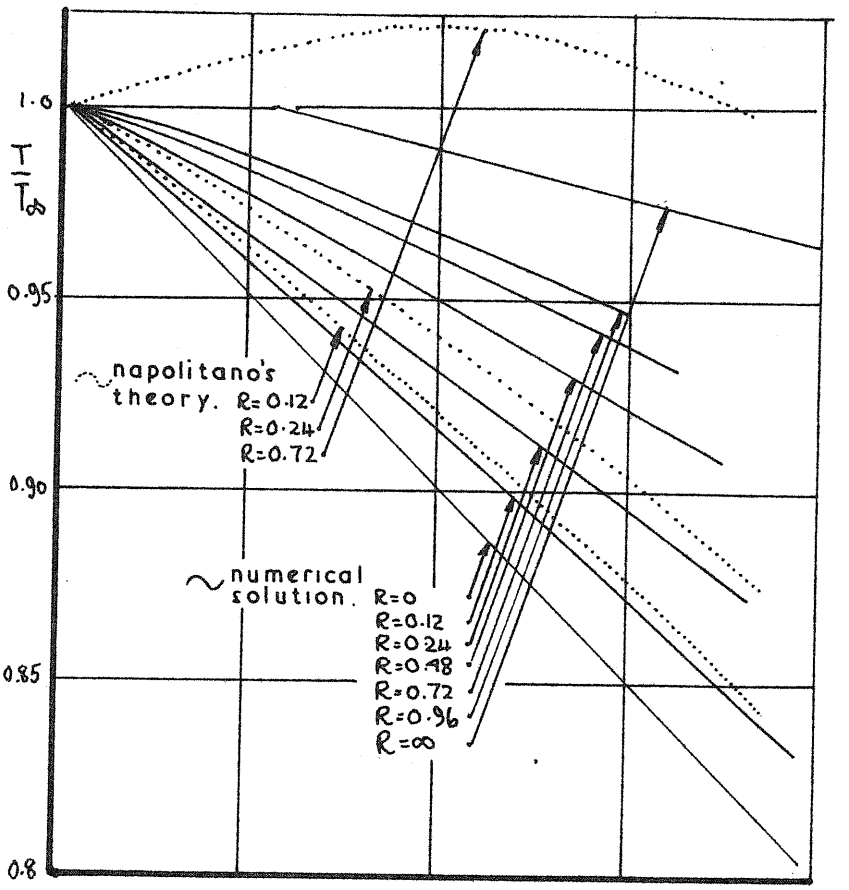

TEMPERATURE DISTRIBUTION IN THE EXPANSION. FIG.2·3(7)

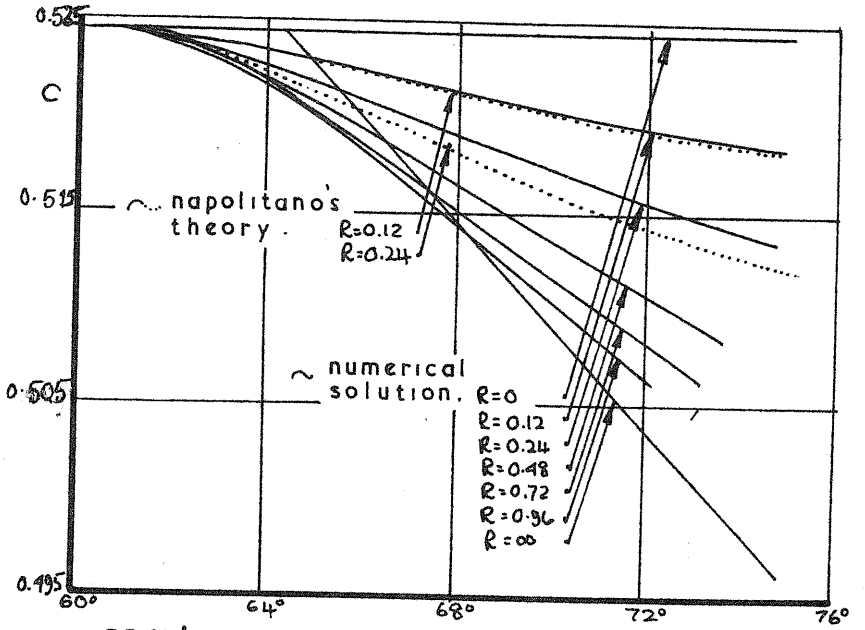

angular position in the expansion fan

ATOM CONCENTRATION IN THE EXPANSION FIG 2·3(8)

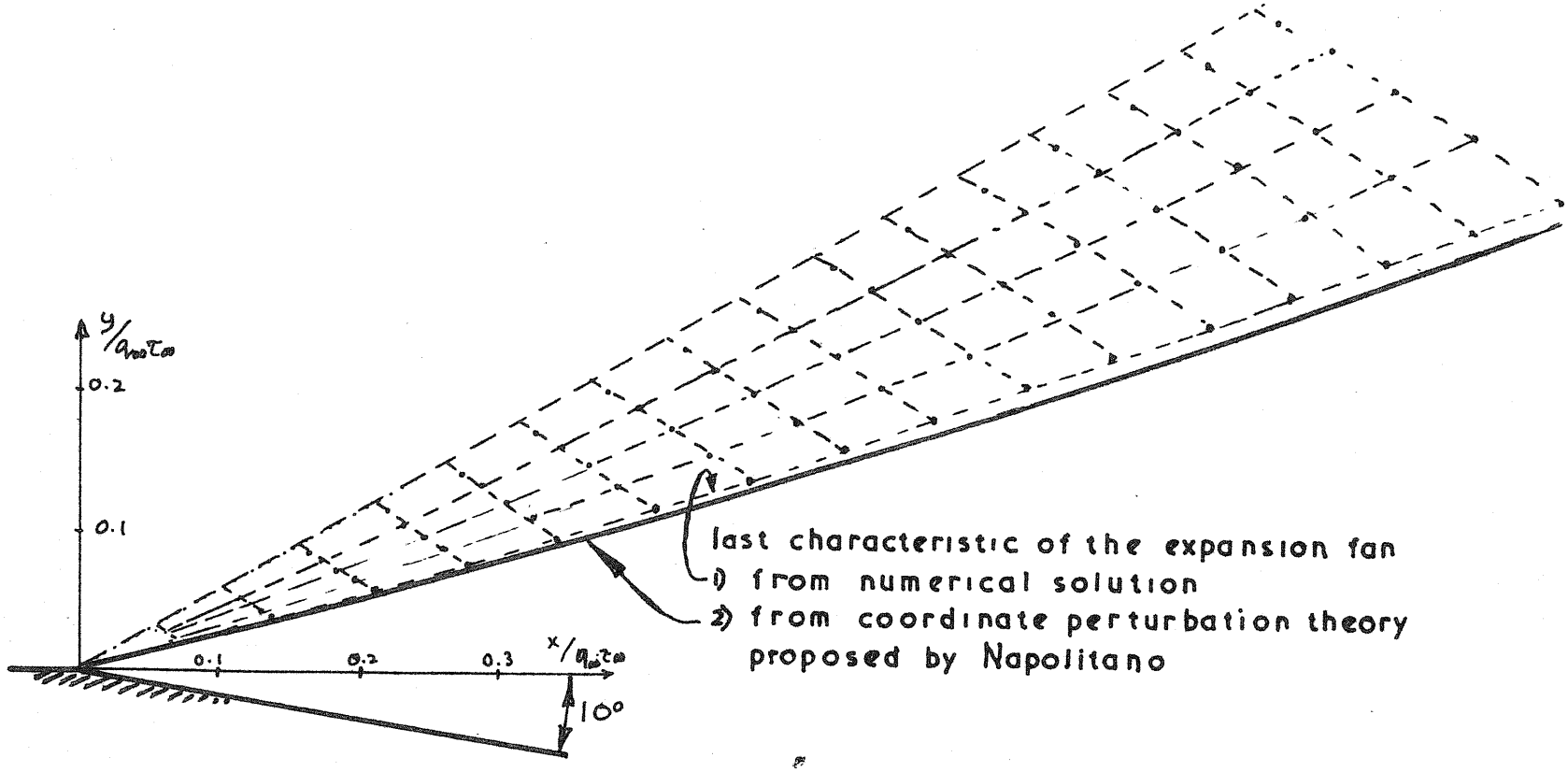

CHARACTERISTIC GRID WITHIN THE EXPANSION FAN FIG. 2·3(9)

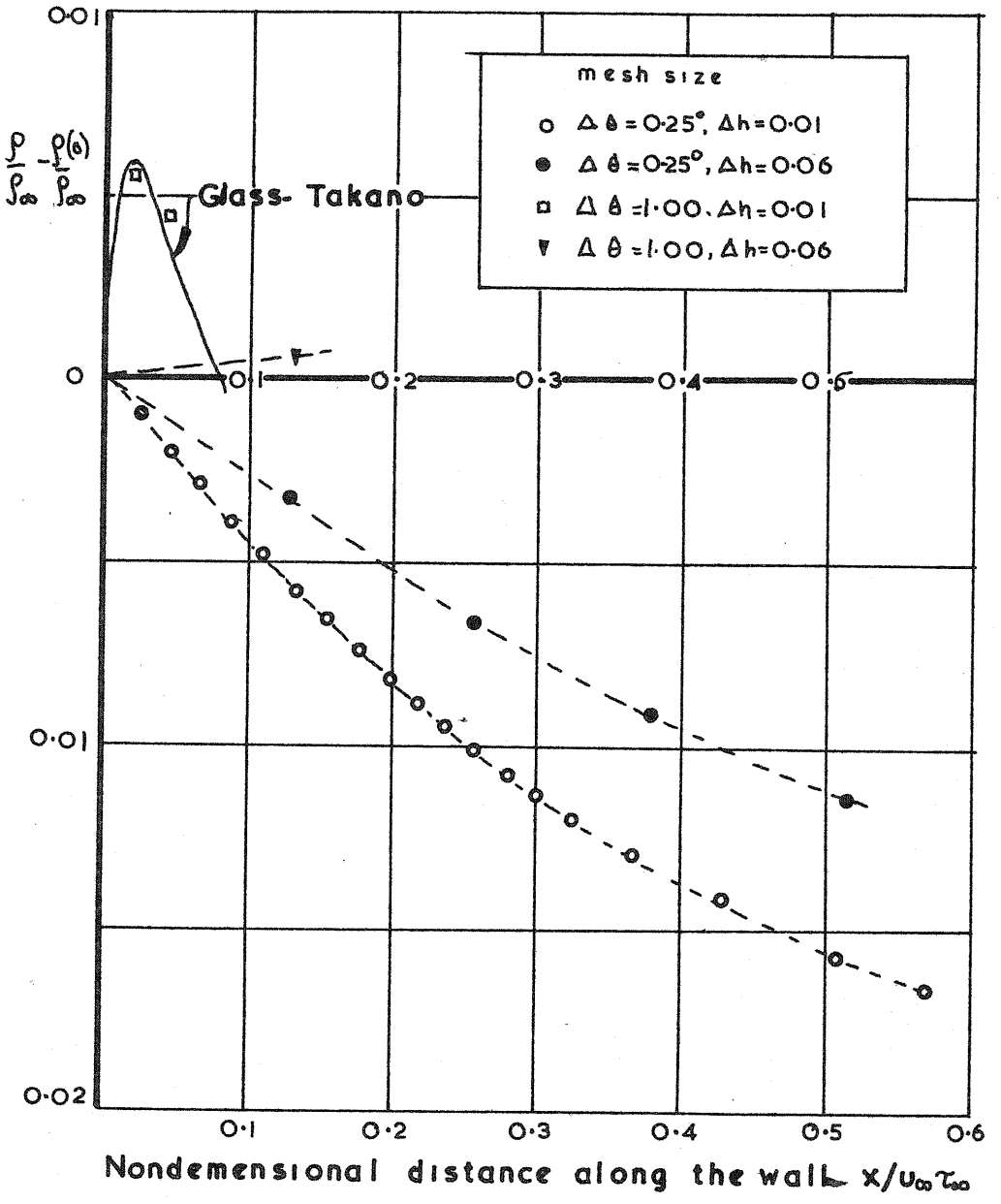

DENSITY VARIATION ALONG THE WALL FOR DIFFERENT MESH SIZES

FIG. 2·3 (10)

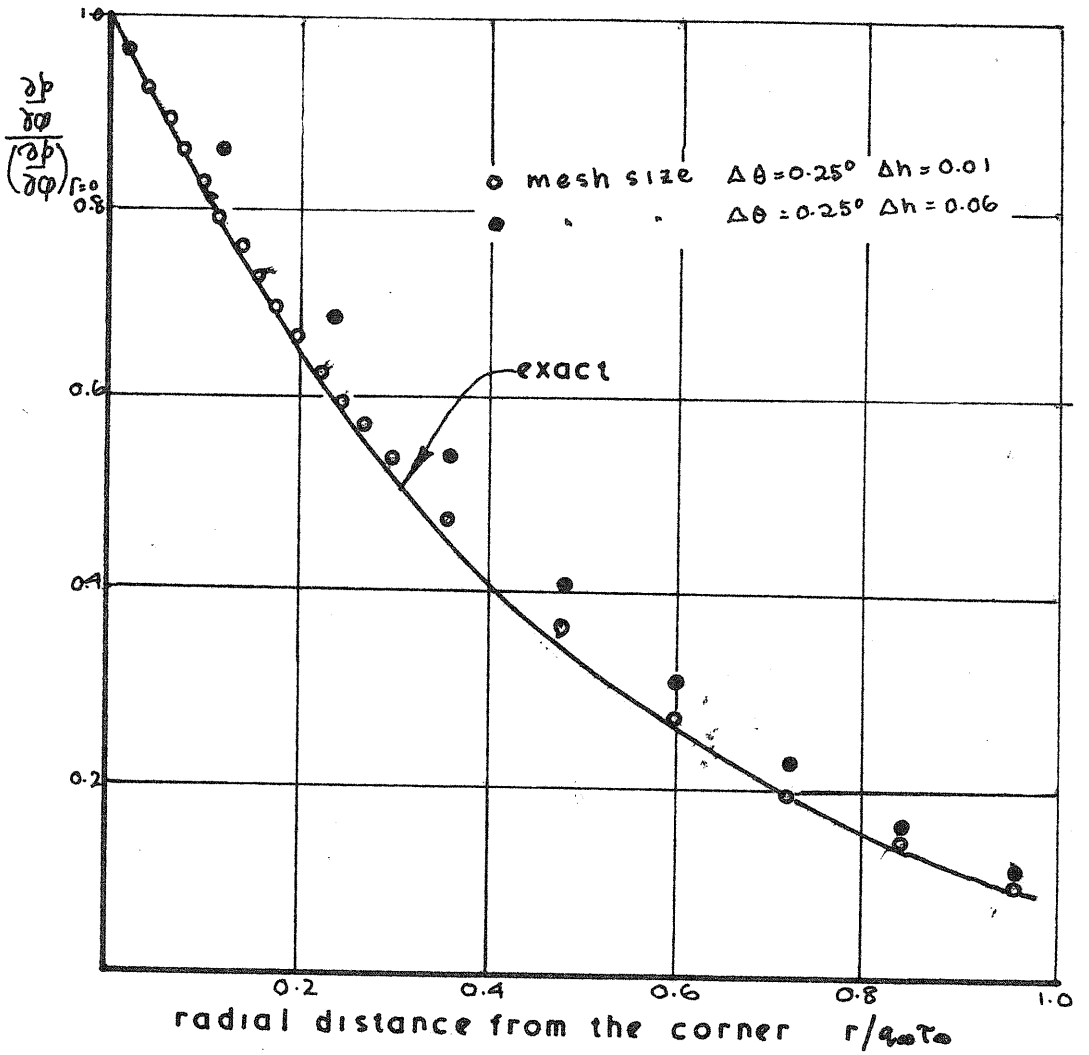

DECAY OF THE PPESSURE GRADIENT ALONG THE LEADING EDGE OF THE EXPANSION FAN.

FIG 2·3(11)

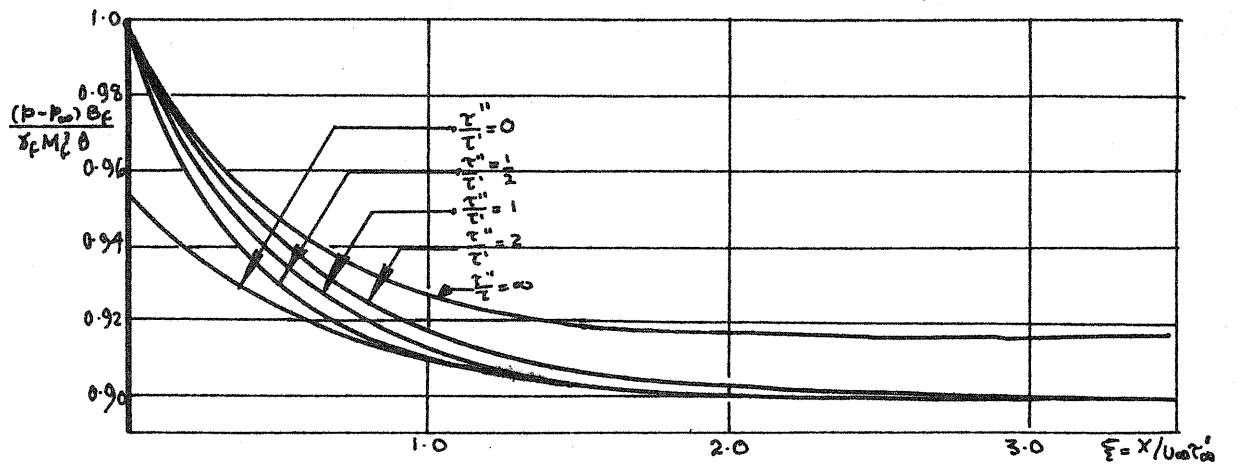

PRESSURE DISTRIBUTION ON THE WALL $\tau''' = \infty$ FIG. 24(1)

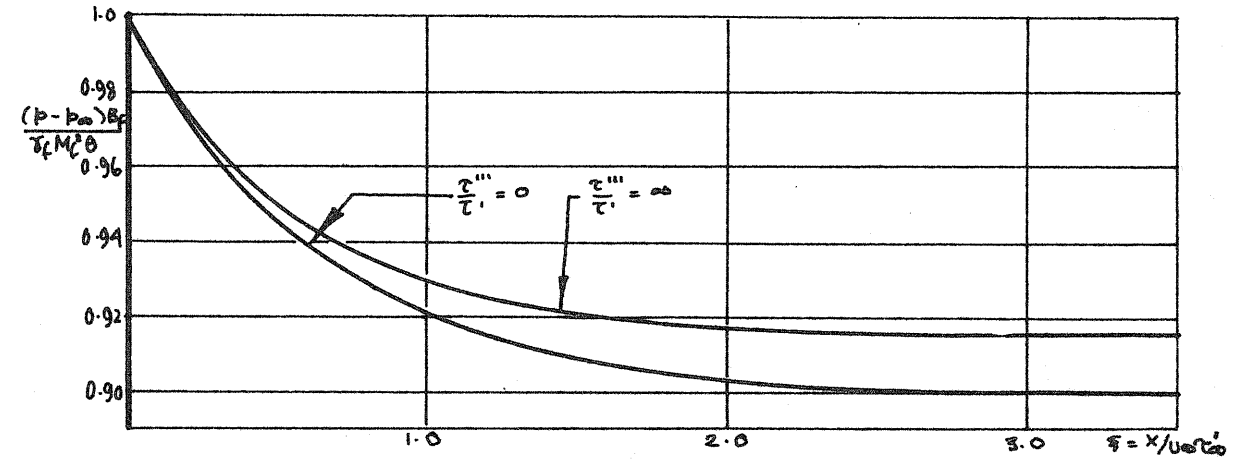

PRESSURE DISTRIBUTION ON THE WALL $\tau'' = \infty$ FIG 24(2)

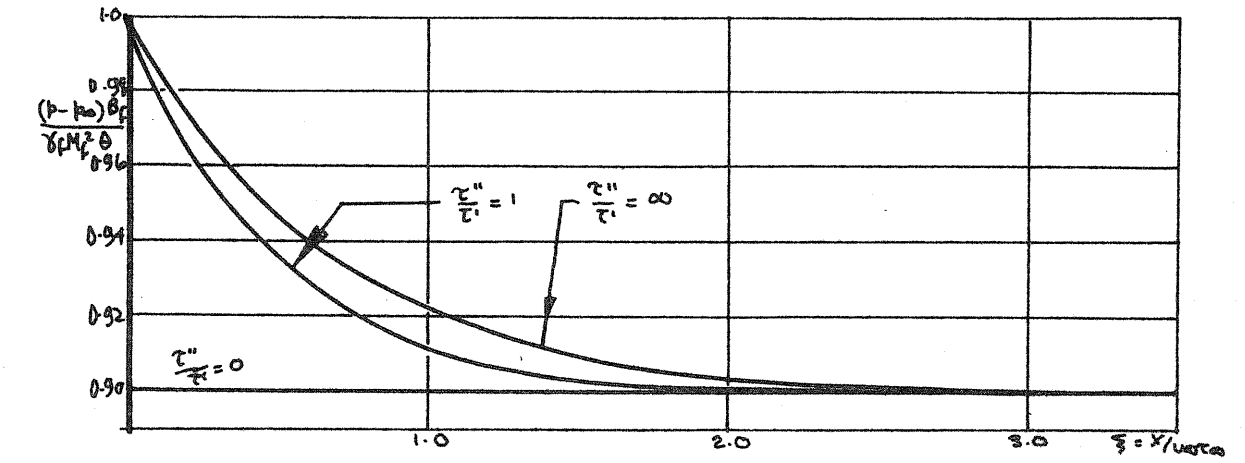

PRESSURE DISTRIBUTION ON THE WALL FIG. 24(3)

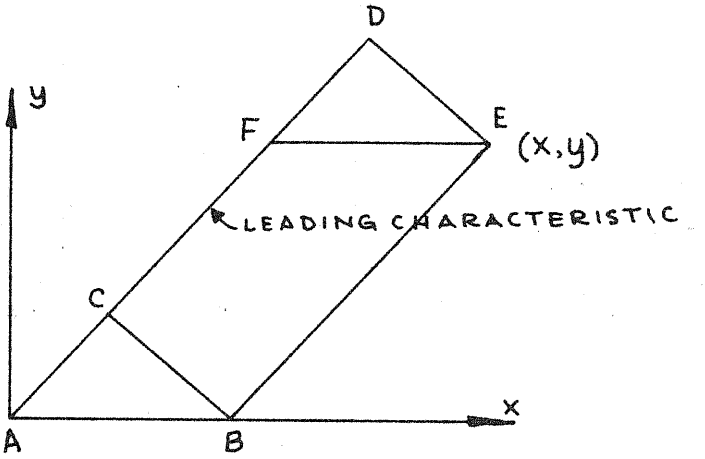

physical plane

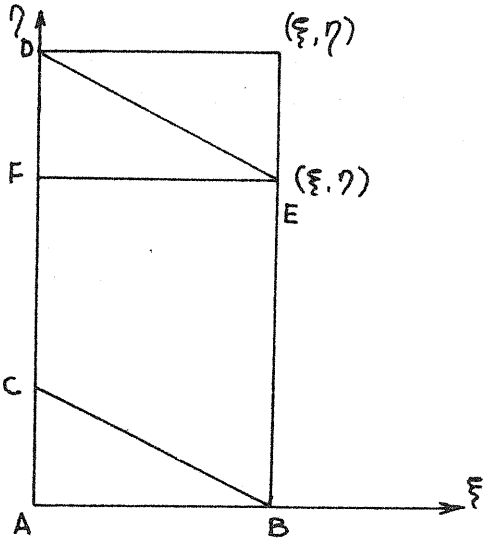

semi-characteristic coordinates

INTEGRATION REGIONS USED IN SECOND ORDER SOLUTION

FIG. 2·5(1)

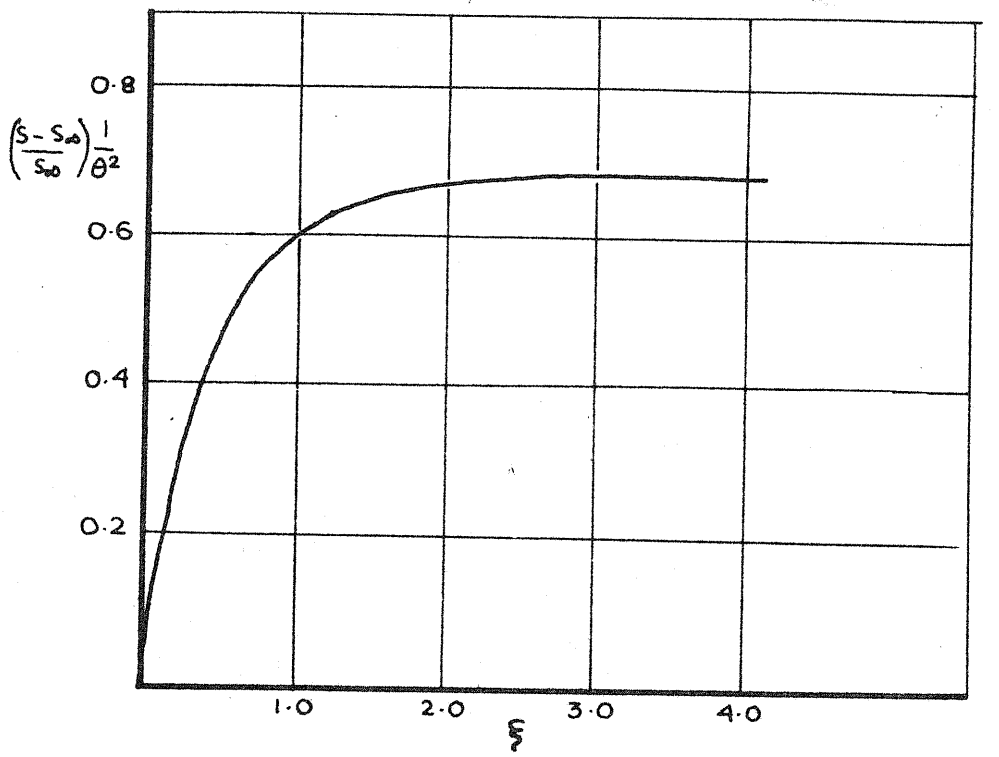

VARIATION OF THE ENTROPY ALONG THE WALL

FIG. 2·5(2)

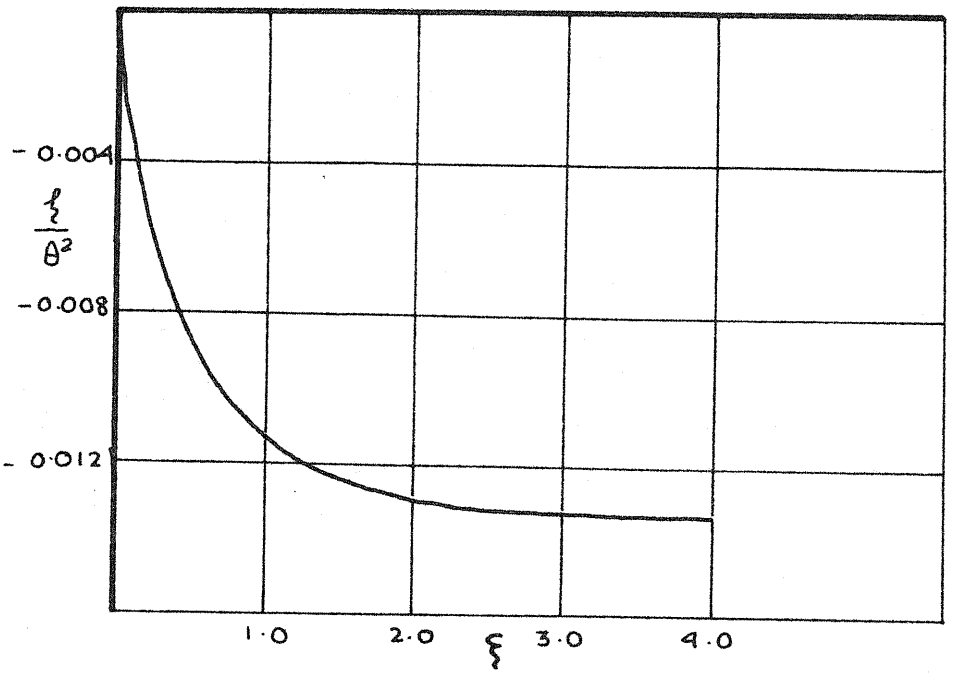

VARIATION OF THE VORTICITY ALONG THE WALL

FIG. 2·5(3)

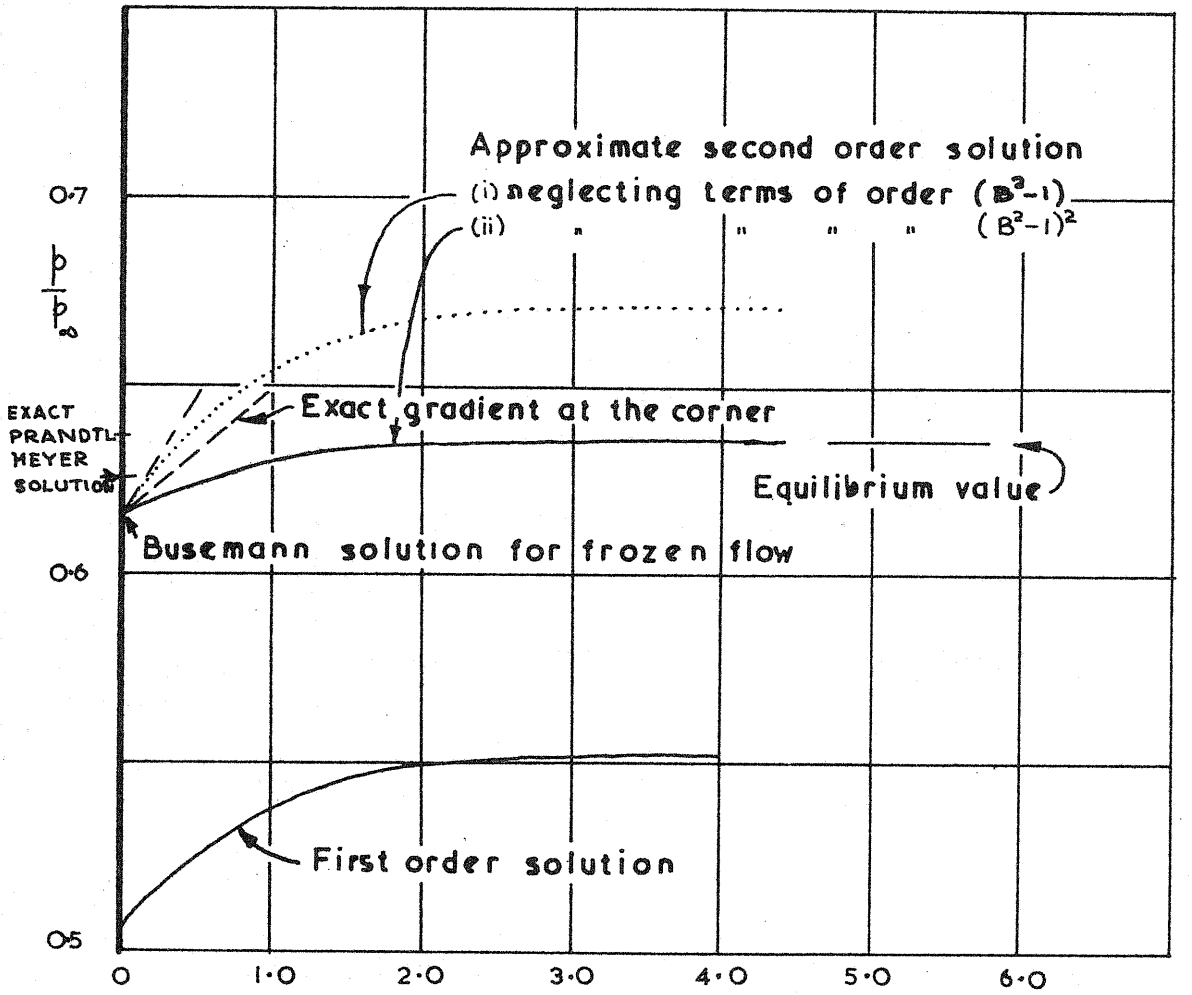

VARIATION OF THE PRESSURE ALONG THE WALL FOR A 10^0 EXPANSION IN CARBON DIOXIDE

FIG. 2·5(4)

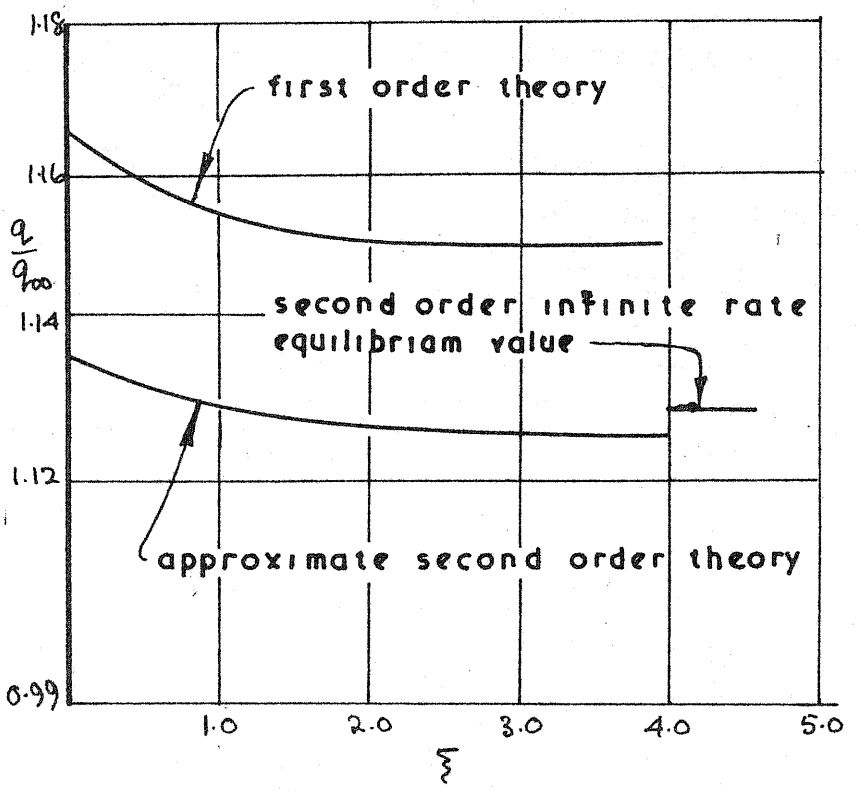

VARIATION OF THE VELOCITY ALONG THE WALL FOR A 10° EXPANSION IN CO_2.

FIG 2·5(5)

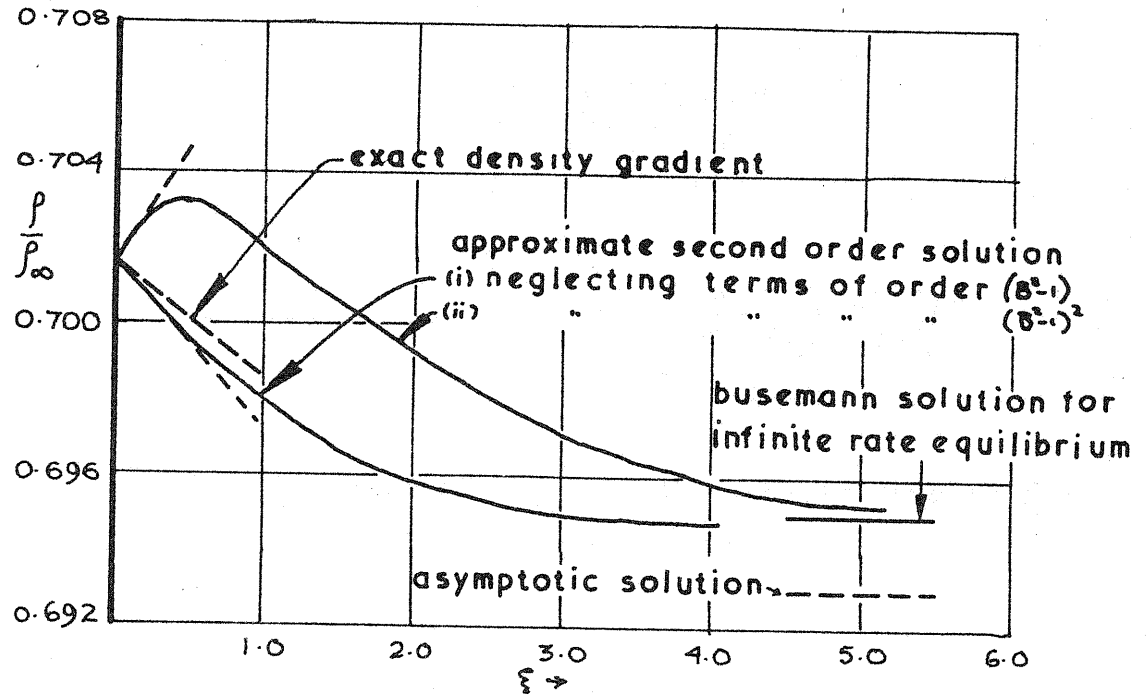

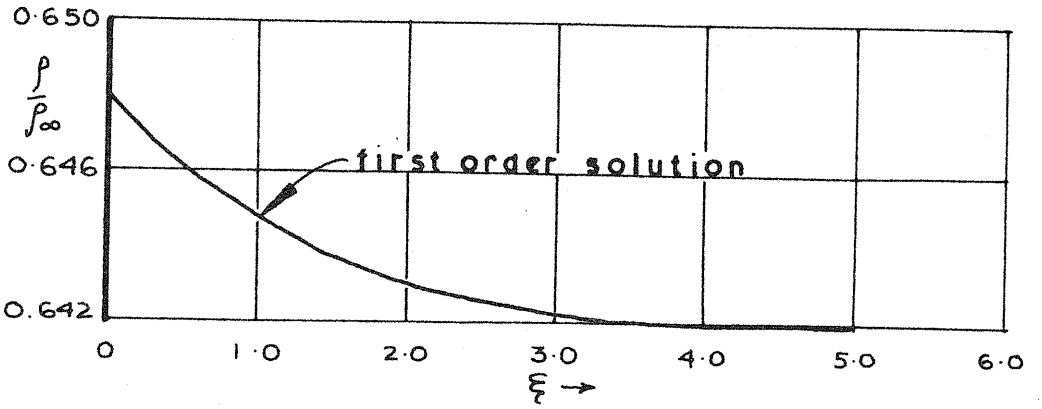

DENSITY VARIATION ALONG THE WALL FOR A 10° EXPANSION IN CARBON DIOXIDE.

FIG. 2.5(6)

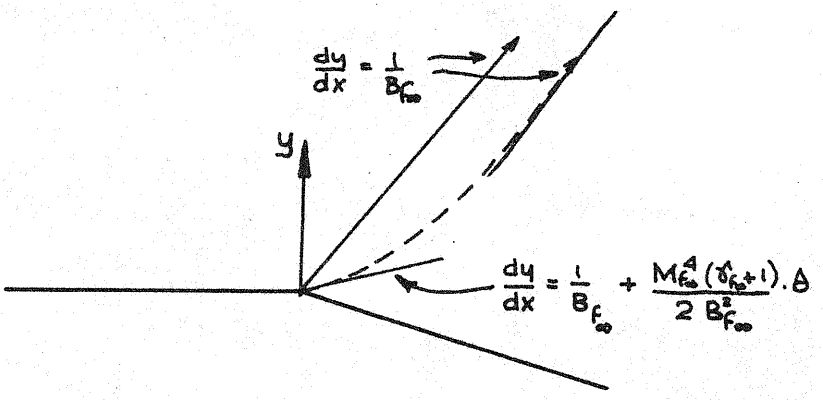

form of characteristics to second order

FIG. 2·5(7)

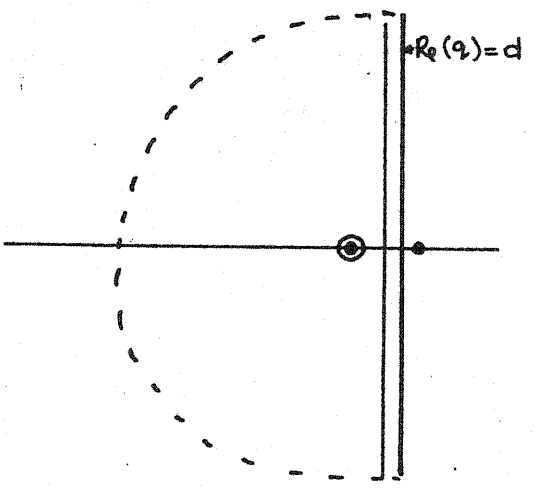

contour in the 'q' plane

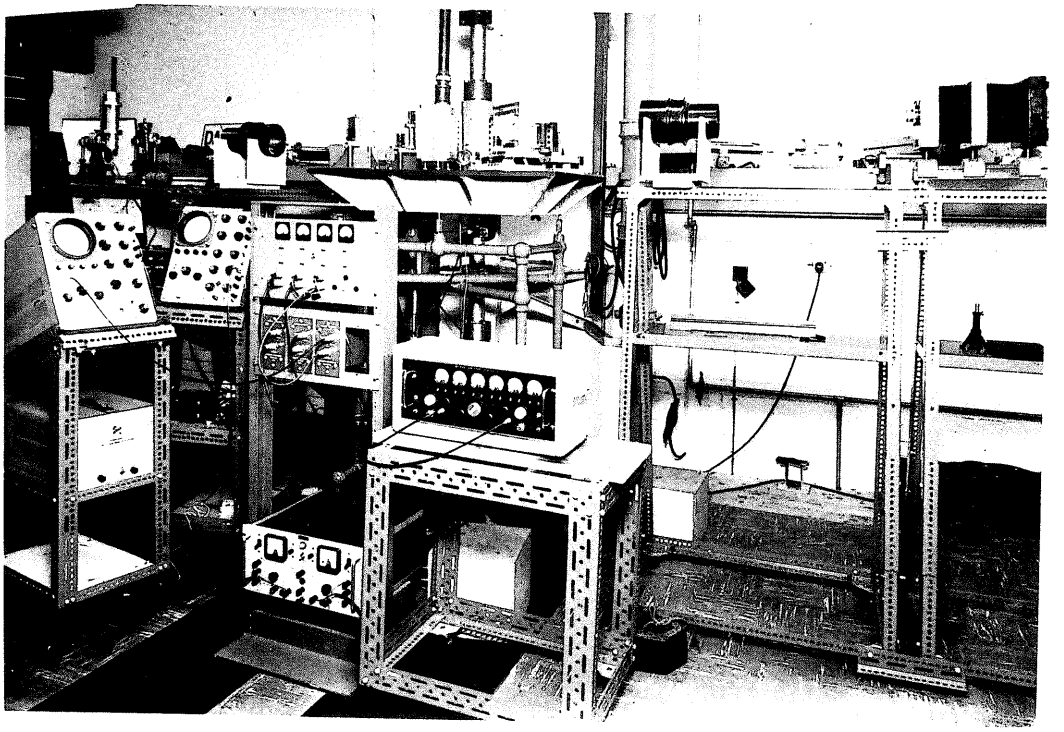

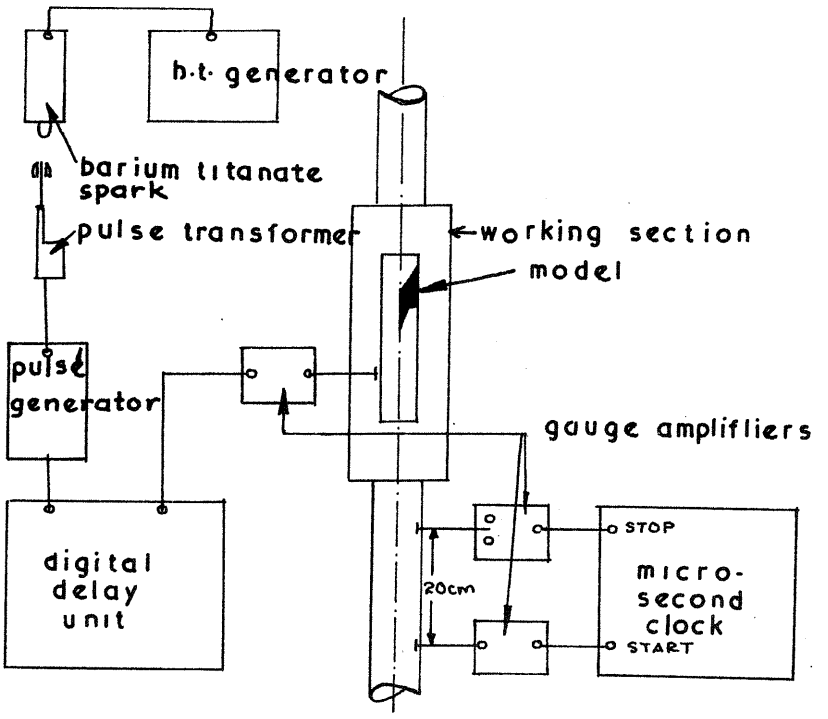

PHOTOGRAPH AND DIAGRAMMATIC LAYOUT OF THE INSTRUMENTATION

FIG. 3·3(1)

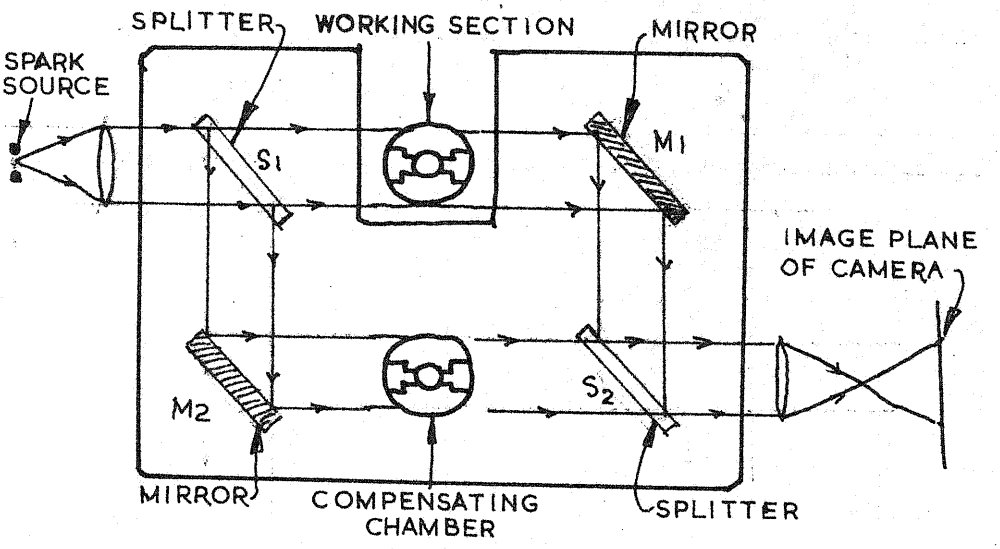

MACH-ZEHNDER INTERFEROMETER

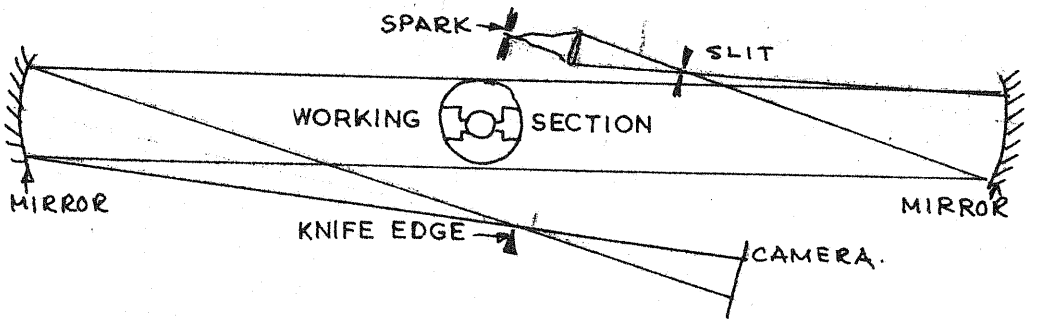

SCHLIEREN SYSTEM

DIAGRAMS OF SCHLIEREN AND INTERFEROMETER SYSTEMS

FIG 3·1(2)

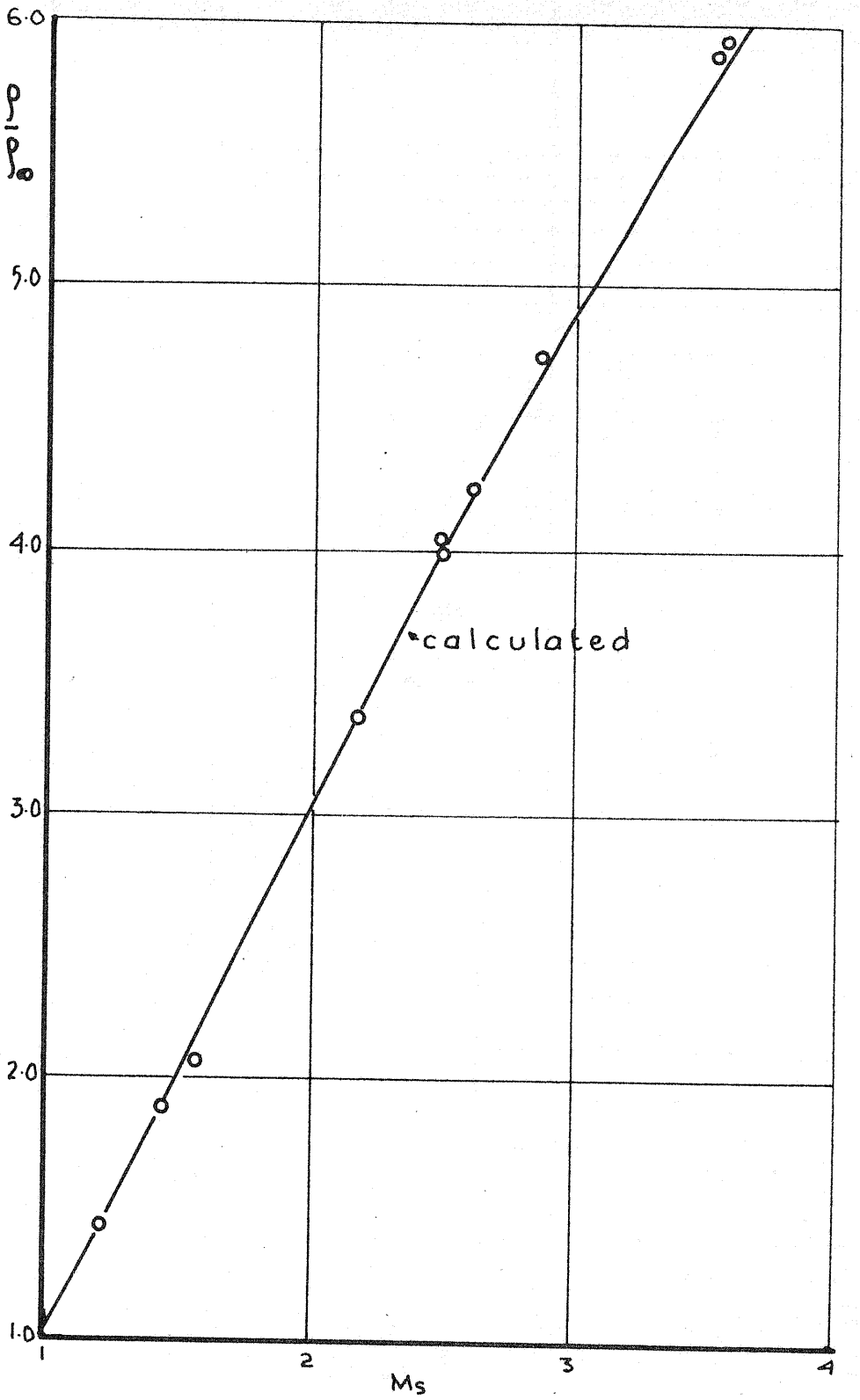

DENSITY RATIO ACROSS THE PRIMARY SHOCK

FIG. 3.2 (1)

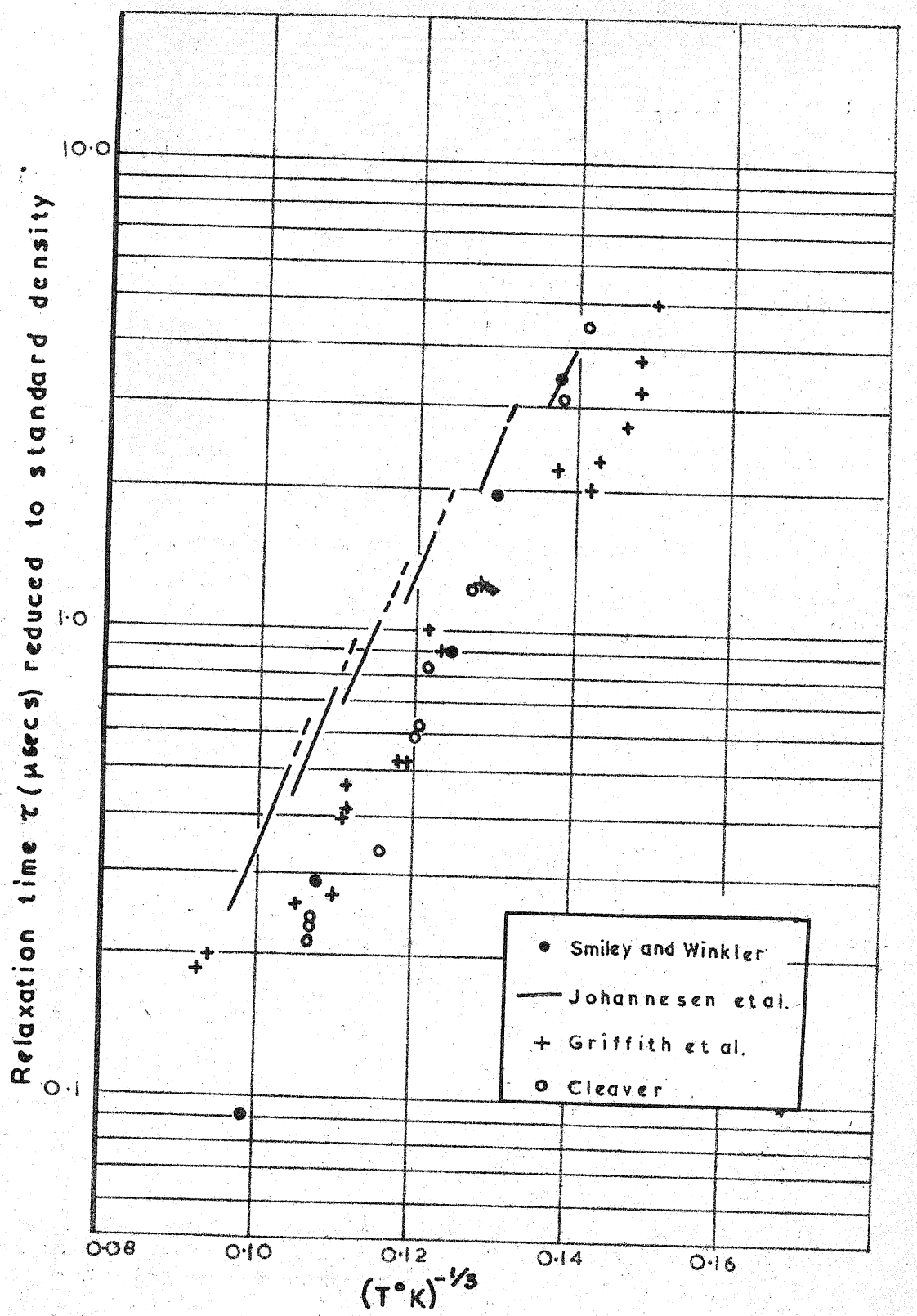

RELAXATION TIME FOR CO_2

FIG. 3·2(2)

undisturbed monochromatic fringes (4570 Å)

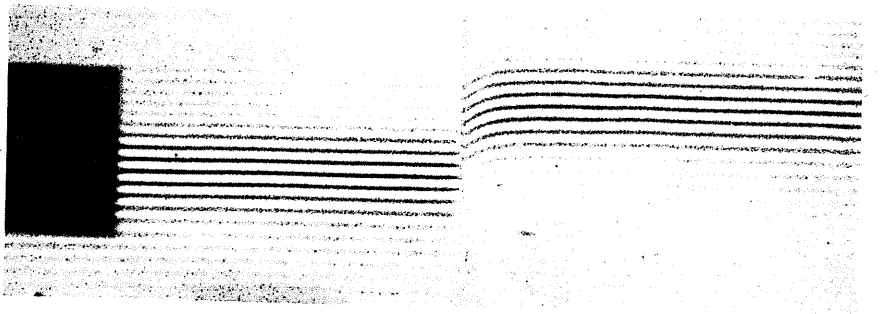

normal shock wave in carbon dioxide $M_S = 2{\cdot}85$, $p_1 = 23{\cdot}6$mm

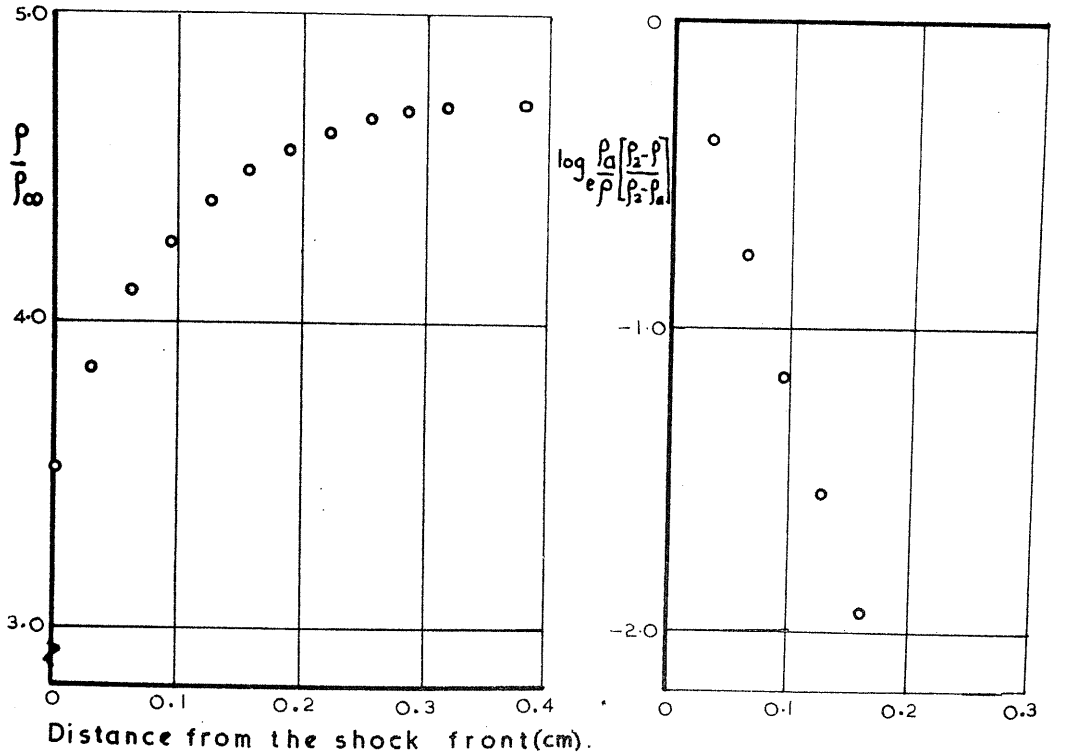

TYPICAL DENSITY PROFILES FOR SHOCK WAVES IN CO_2.

FIG. 3·2 (3)

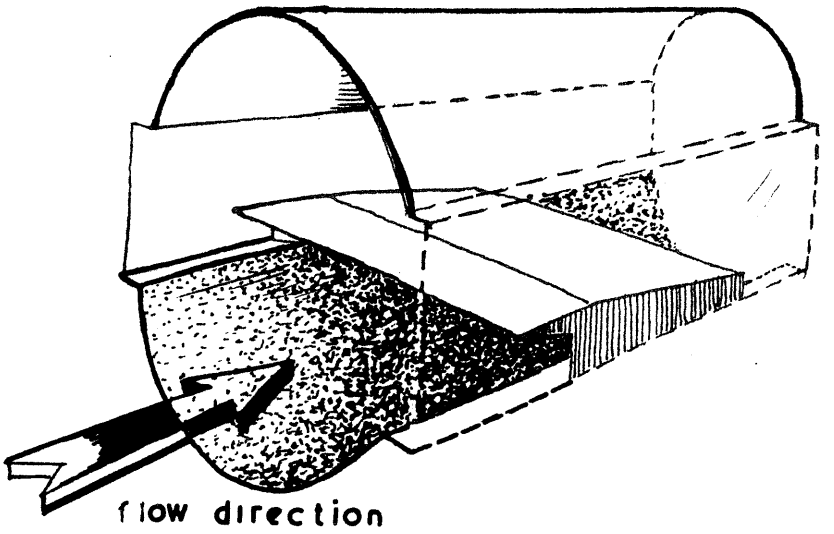

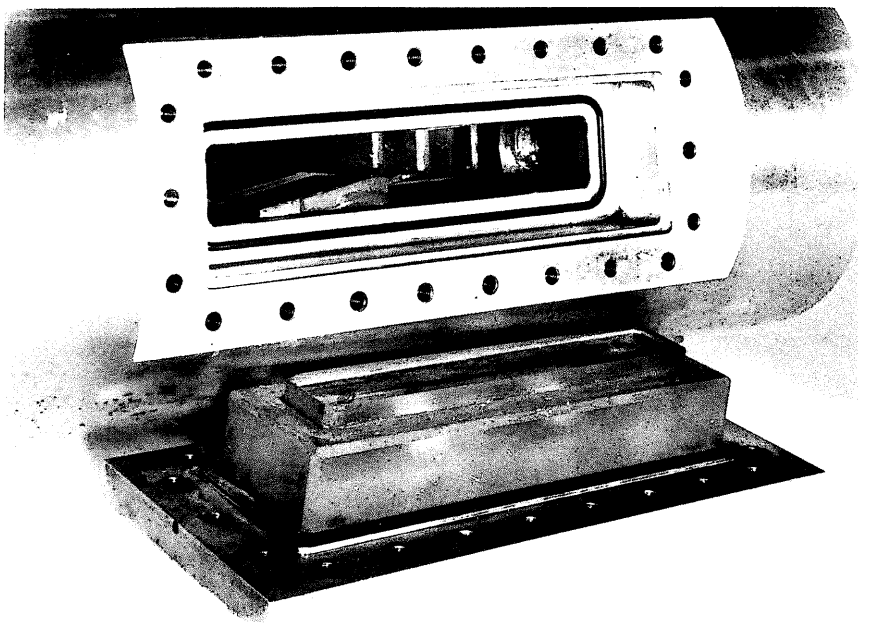

PHOTOGRAPH AND DIAGRAMMATIC SKETCH OF THE WEDGE MODEL MOUNTED IN THE WORKING SECTION

FIG. 3·3(I)

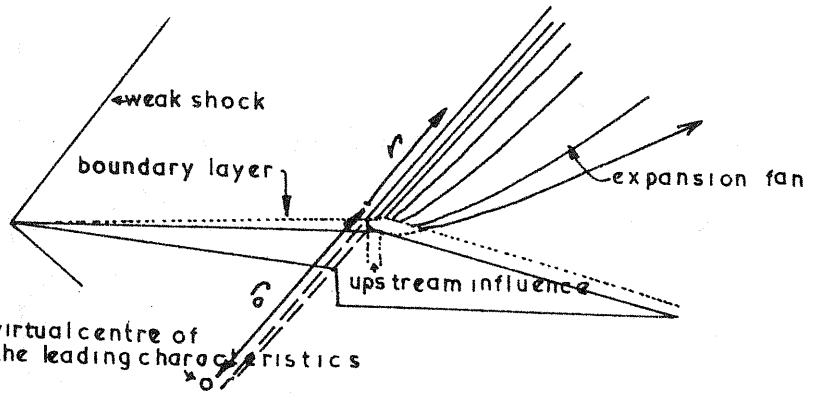

SCHEMATIC DIAGRAM OF THE FLOW OVER THE MODEL
FIG 3·3(2)

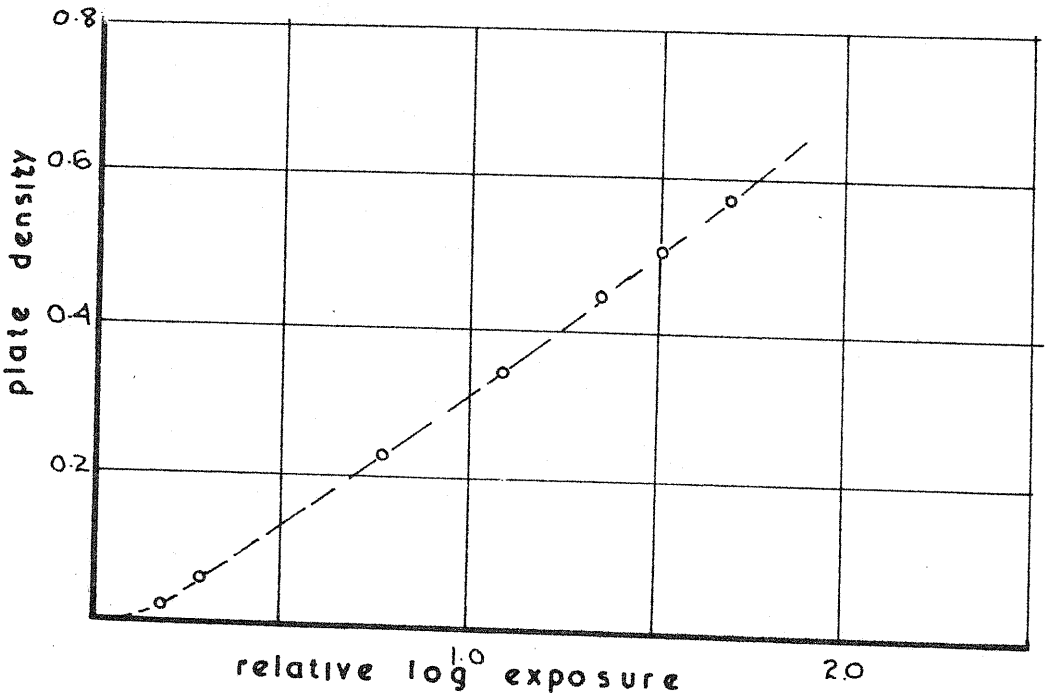

CHARACTERISTIC CURVE FOR ILFORD LN (BLUE SENSITIVE) PLATES EXPOSED TO A SPARK SOURCE.
FIG 3·3(3)

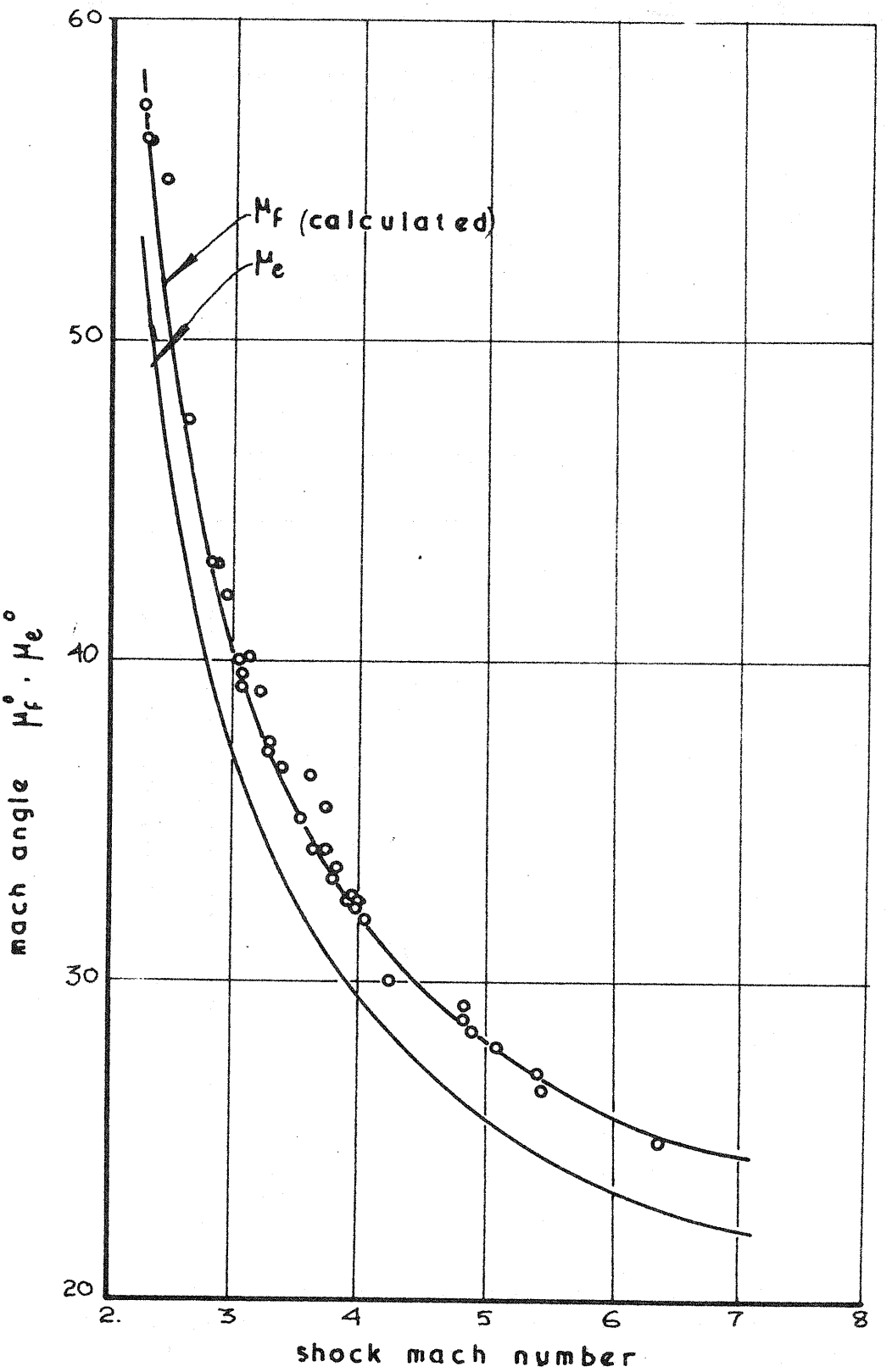

ANGLE OF MACH LINES PRODUCED BY SCRIBES ON THE SURFACE OF THE MODEL FIG 3-3(4)

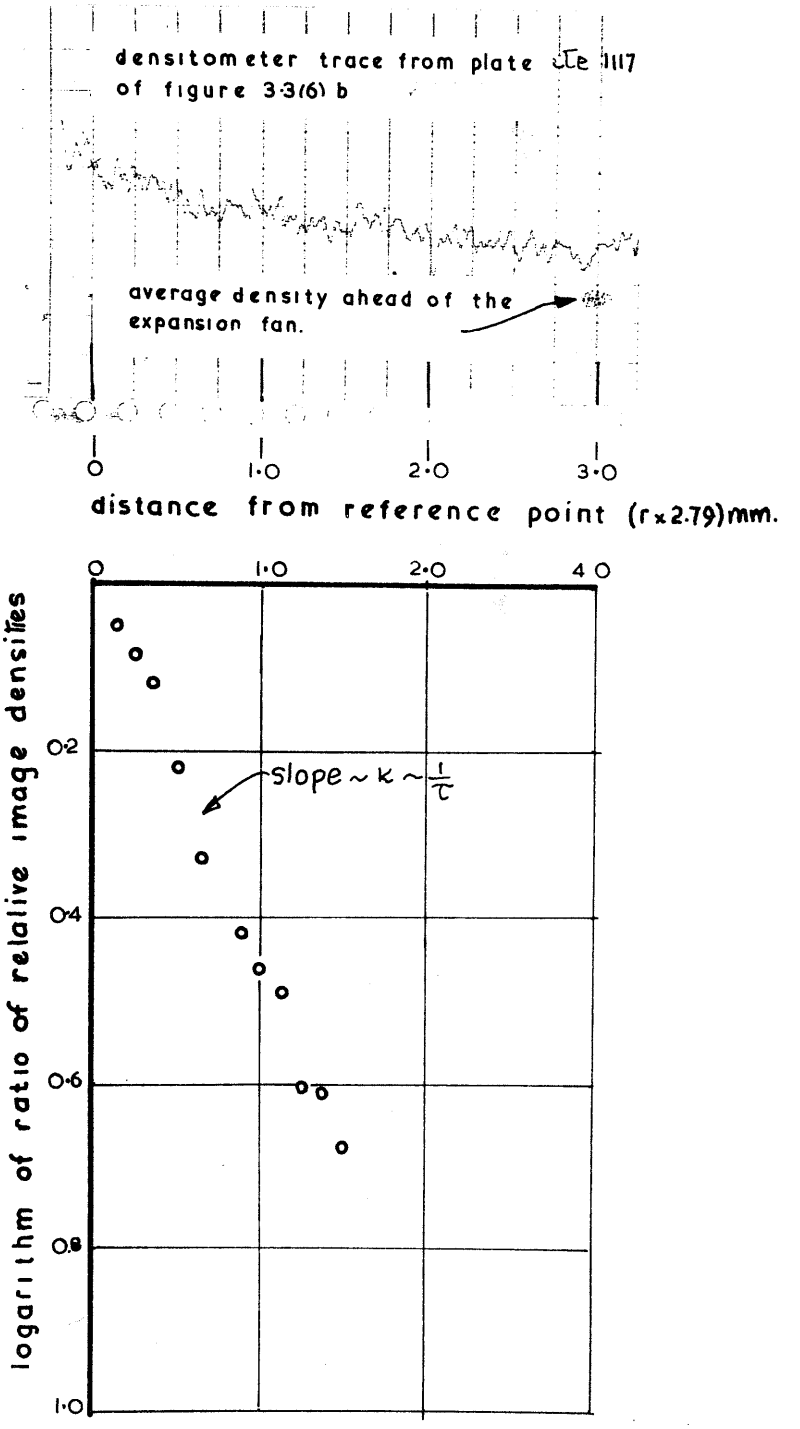

A TRACE FROM THE MICRODENSITOMETER SHOWING IMAGE DENSITY DISTRIBUTION ALONG THE LEADING EDGE OF THE EXPANSION RELATIVE TO THE AVERAGE DENSITY AHEAD OF THE EXPANSION.

FIG. 3·3(5)

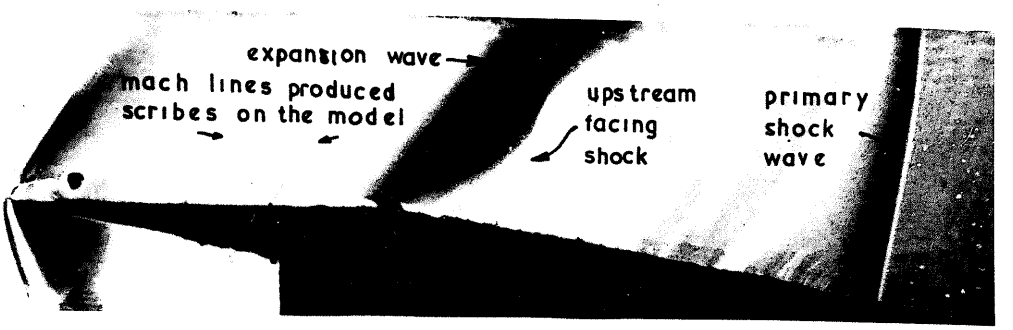

d). $M_s = 2{\cdot}28$ $p_1 = 177$ mm. hg.

b) $M_s = 3{\cdot}08$ $p_1 = 177$ mm. hg.

c) $M_s = 4{\cdot}26$ $p_1 = 41{\cdot}2$ mm.hg.

TYPICAL SET OF SCHLIEREN PHOTOGRAPHS FIG. 3·3(6)

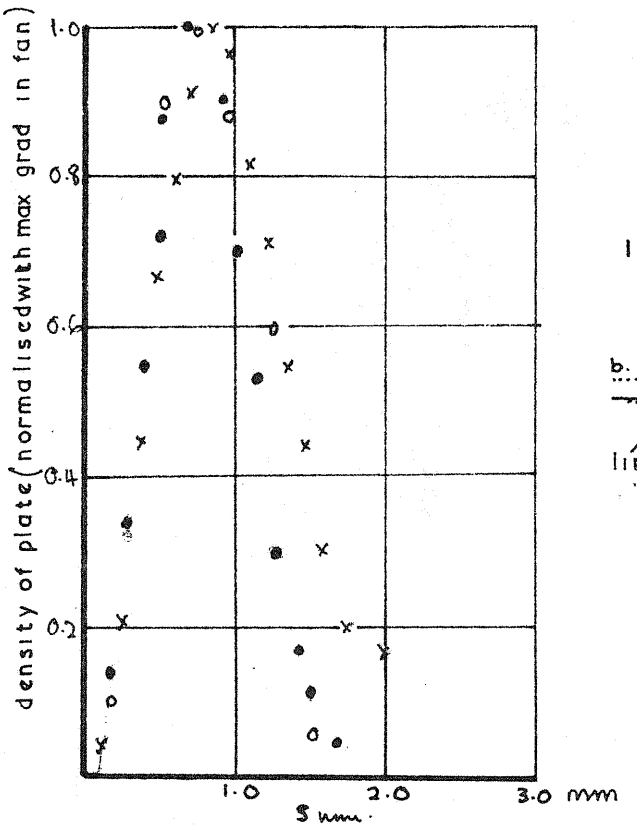

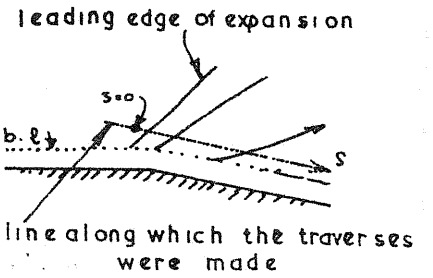

TYPICAL MICRO-DENSITOMETER READINGS THROUGH THE EXPANSION FAN JUST OUTSIDE THE BOUNDARY LAYER.

FIG. 3·3(7)

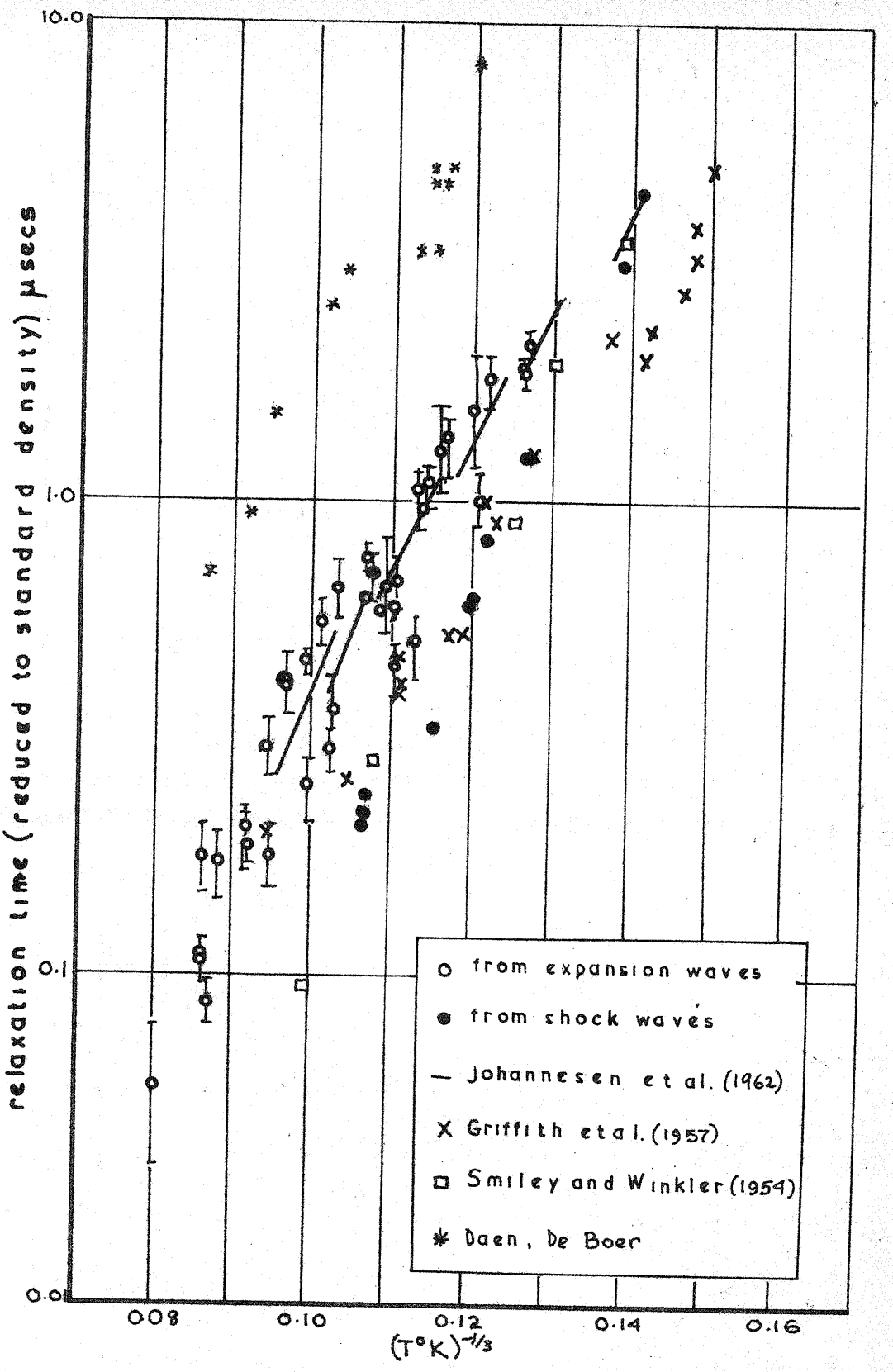

RELAXATION TIMES FOR CO_2 OBTAINED FROM EXPANSION WAVES.

FIG. 3·3(8)

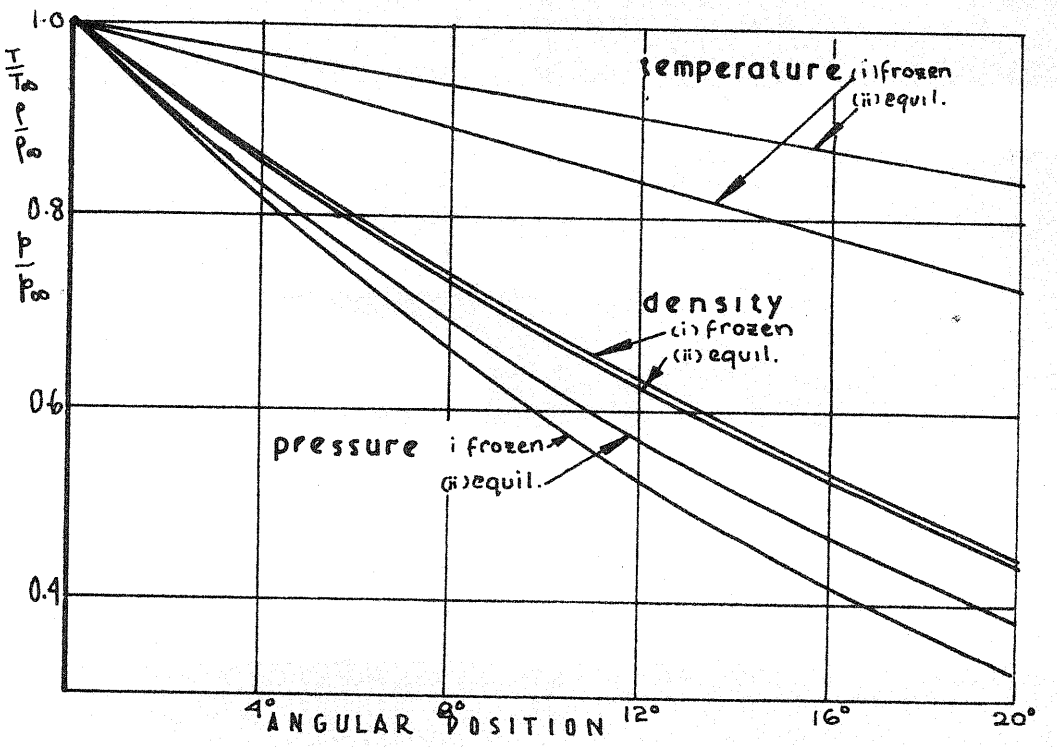

FROZEN AND EQUILIBRIUM VALUES OF THE PRESSURE, TEMPERATURE & DENSITY IN A PLANE EXPANSION. FOR CO_2.
FIG 3·4(1)

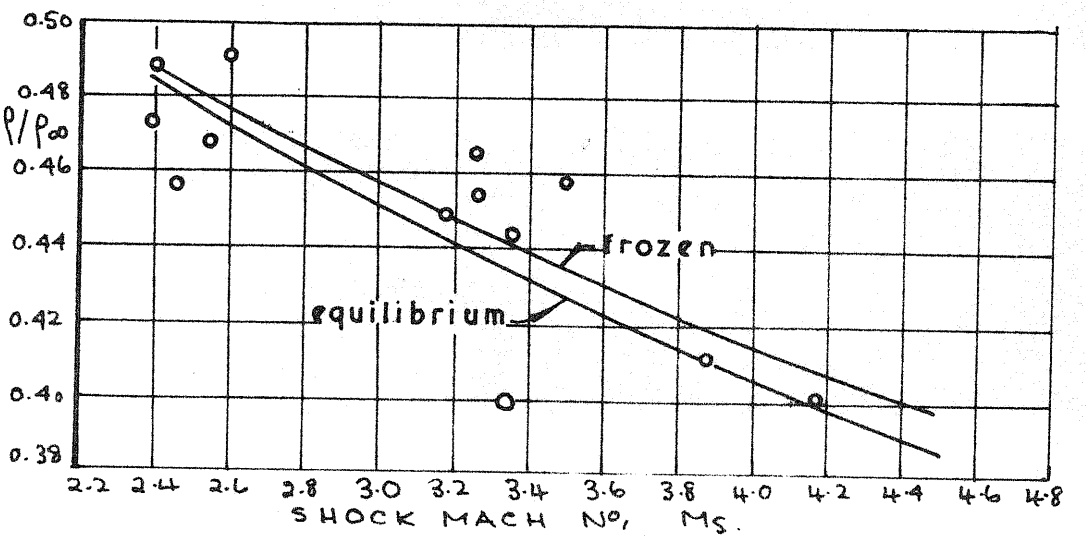

MEASURED DENSITY RATIO THROUGH A 20° EXPANSION
FIG. 3·4(3)

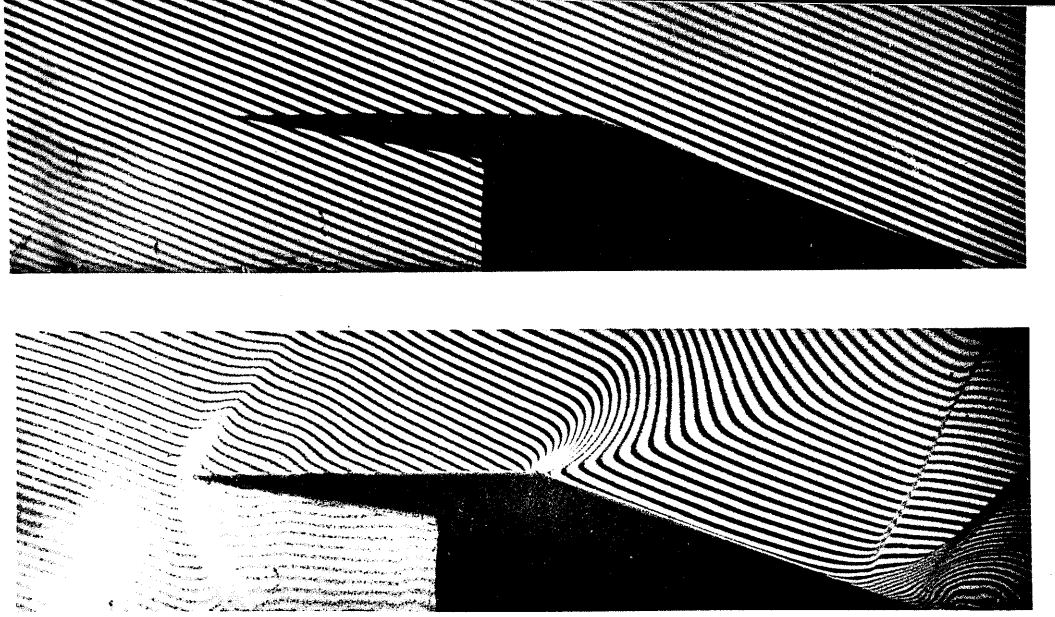

A) $M_S = 2.4$, $p_1 = 96.5$ mm Hg.

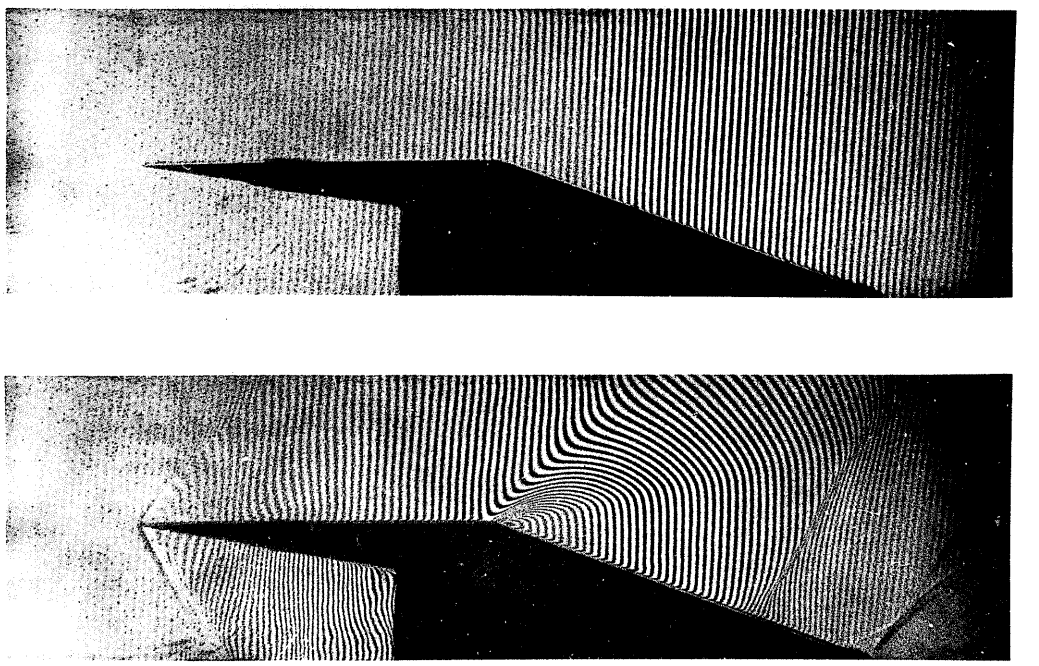

B) $M_S = 2.6$ $p_1 = 118$ mm Hg.

INTERFEROGRAMS OF THE FLOW OF CARBON DIOXIODE THROUGH A PLANE 20° EXPANSION

FIG. 3·4(2)